Title
Renal elimination mechanisms studies with p-aminohippuric acid and furosemide

Author
Gloff, Carol Ann

Publication Date
1984

Peer reviewed|Thesis/dissertation

Renal Elimination Mechanisms

Studies with p-Aminohippuric Acid and Furosemide

by

Carol Ann Gloff

B.S. Pharmacy, State University of New York at Buffalo

DISSERTATION

Submitted in partial satisfaction of the requirements for the degree of

DOCTOR OF PHILOSOPHY

in

Pharmaceutical Chemistry

in the

GRADUATE DIVISION

of the

UNIVERSITY OF CALIFORNIA

San Francisco

OK.
L. L. Benet

RENAL ELIMINATION MECHANISMS
STUDIES WITH p-AMINOHIPPURIC ACID AND FUROSEMIDE

Carol A. Gloff
Ph.D. in Pharmaceutical Chemistry

The objectives of this work were: 1) To determine if two organic anions could inhibit each other's transport by the carrier-mediated organic anion secretory pathway in the nephron, and 2) To determine if renal failure could affect the secretion of an organic anion. The compounds chosen to attain these objectives were p-aminohippuric acid (PAH) and furosemide for objective #1 and PAH for objective #2.

PAH is an organic anion which is 85-90% removed from plasma in one pass through the kidney. Its removal is mainly due to secretion. Because of this, the renal clearance of PAH (CL_{PAH}) is often used to measure renal plasma flow. PAH was therefore chosen as a prototype organic anion not only because of its renal elimination characteristics but also because of the possible diagnostic relevance of these studies.

Furosemide is also an organic anion which is secreted by the kidney. Furosemide, a diuretic, exerts its pharmacological effect from within the lumen of the nephron rather than from the plasma. Due to this location requirement for furosemide's effect, these studies were also of possible clinical interest.

Two types of experiments were used to study objective #1. Isolated basal-lateral membrane vesicles from proximal tubules of rabbit kidneys were used for one group of experiments. Basal-lateral membranes of proximal tubules are believed to contain a carrier (or carriers) for organic anion transport, making them a particularly appropriate experimental system to use in these studies. These results show that furosemide inhibited the transport of PAH by basal-lateral membranes. PAH inhibition of furosemide transport was less definite. The inability to measure significant inhibition of furosemide transport is most likely due to high furosemide nonspecific binding to the vesicle. This nonspecific binding masks changes in furosemide transport including those caused by competition for transport sites.

The second experimental system used to study objective #1 was the whole animal (rat) renal clearance model. Results from these studies demonstrated that PAH definitely inhibited furosemide renal clearance (CL_F). Changes in CL_{PAH} caused by furosemide were masked by a marked decrease in glomerular filtration rate (GFR), probably caused by the addition of the furosemide.

Objective #2 was studied by use of a well-known renal failure model-uranyl nitrate administration. These studies were designed to determine if uranyl nitrate toxicity could affect CL_{PAH} and/or the renal clearance of inulin (CL_{IN}). The experimental approach was again the rat renal clearance model. Results from these studies indicate that CL_{PAH} was always decreased in animals with renal failure, and it was decreased to a greater degree than was CL_{IN} in animals with the smallest degree of renal failure. These results may mean that CL_{PAH} is not a good measure of renal plasma flow (RPF) in certain types of renal failure.

The final conclusions from this work are that either the presence of another organic anion which is also secreted or the presence of renal failure may affect CL_{PAH} and thus its measure of RPF. Also, CL_F may be altered by the presence of another organic anion which also undergoes secretion. This change in CL_F may be of some clinical significance.

ACKNOWLEDGEMENTS

I owe a great debt to each of the following people:

Dr. Leslie Z. Benet for providing the project which has enabled me to write this dissertation, and for his intellectual and financial support during my graduate education;

Drs. Betty-ann Hoener and C. Anthony Hunt for their assistance with this dissertation as well as their advice and encouragement concerning post-graduate positions;

Dr. Emil Lin and Winnie Gee for their analytical assistance;

Dr. Richard Mamelok, Carolyn Bildstein and Dorothy Liu for the opportunity and assistance to complete the vesicle studies;

Alice Till, Linda Gustavson, Bobbe Ferraiolo, Bob Baughman, Mike McKinley, Jan McKinley, Linda Winkler, Sue Jordan, Donna Pierino, Sue Tsang, Phil Smith, Laurene Wang, Jeff Kurtock and countless others for making my years here more educational, interesting, enjoyable and sometimes just plain bearable.

TABLE OF CONTENTS

LIST OF TABLES

LIST OF FIGURES

GLOSSARY

CL_F	furosemide renal clearance
CL_{IN}	inulin renal clearance
CL_{PAH}	PAH renal clearance
d.d.	double-distilled
FUR	furosemide
GFR	glomerular filtration rate
HPLC	high performance liquid chromatography
PABA	para-aminobenzoic acid
PAH	para-aminohippuric acid
RPF	renal plasma flow
S.D.	standard deviation
TCA	trichloroacetic acid

STATEMENT OF PURPOSE

The objectives of this dissertation were two-fold:

1) To determine if two commonly-administered organic anions could inhibit each other's transport by the carrier-mediated transport system for organic anion secretion in the nephron, and

2) To determine if renal failure could affect the renal clearance of a secreted organic anion. Objective #2 also included an interest in determining whether or not such renal failure would follow the intact nephron hypothesis.

The compounds chosen to attain these objectives were p-aminohippuric acid (PAH) and furosemide for objective #1 and PAH for objective #2.

CHAPTER I

RENAL FUNCTION

BACKGROUND

A. Anatomy of the kidney and nephron

Each human kidney is composed of at least one million nephrons. The nephron serves as the functional unit of the kidney. Figure I-1 is a schematic representation of a nephron. The nephron begins with Bowman's capsule. This capsule surrounds the glomerulus. The glomerulus is a tuft of capillaries which supply Bowman's capsule with blood for exchange. Flow of fluid within the nephron proceeds from Bowman's capsule into the proximal tubule. The first part of the proximal tubule, the convoluted section (pars convoluta) is followed by a straight portion (pars recta). This straight portion then forms the thick descending limb of the loop of Henle. The loop of Henle is composed of this thick portion, followed by thin descending and ascending limbs, and finally the thick ascending limb. This last portion is also often referred to as the straight portion of the distal tubule. Following the straight portion of the distal tubule is the convoluted portion. Finally, a number of distal tubules combine to form a collecting duct. These ducts continue to join until the urine they carry is emptied into the papilla of the kidney. Blood supply to the nephron begins with delivery of blood by an afferent arteriole to the glomerulus. After the glomerulus is perfused the blood is drained by an efferent arteriole. Capillaries surrounding the rest of the tubule are supplied with blood by these efferent arterioles, making their blood

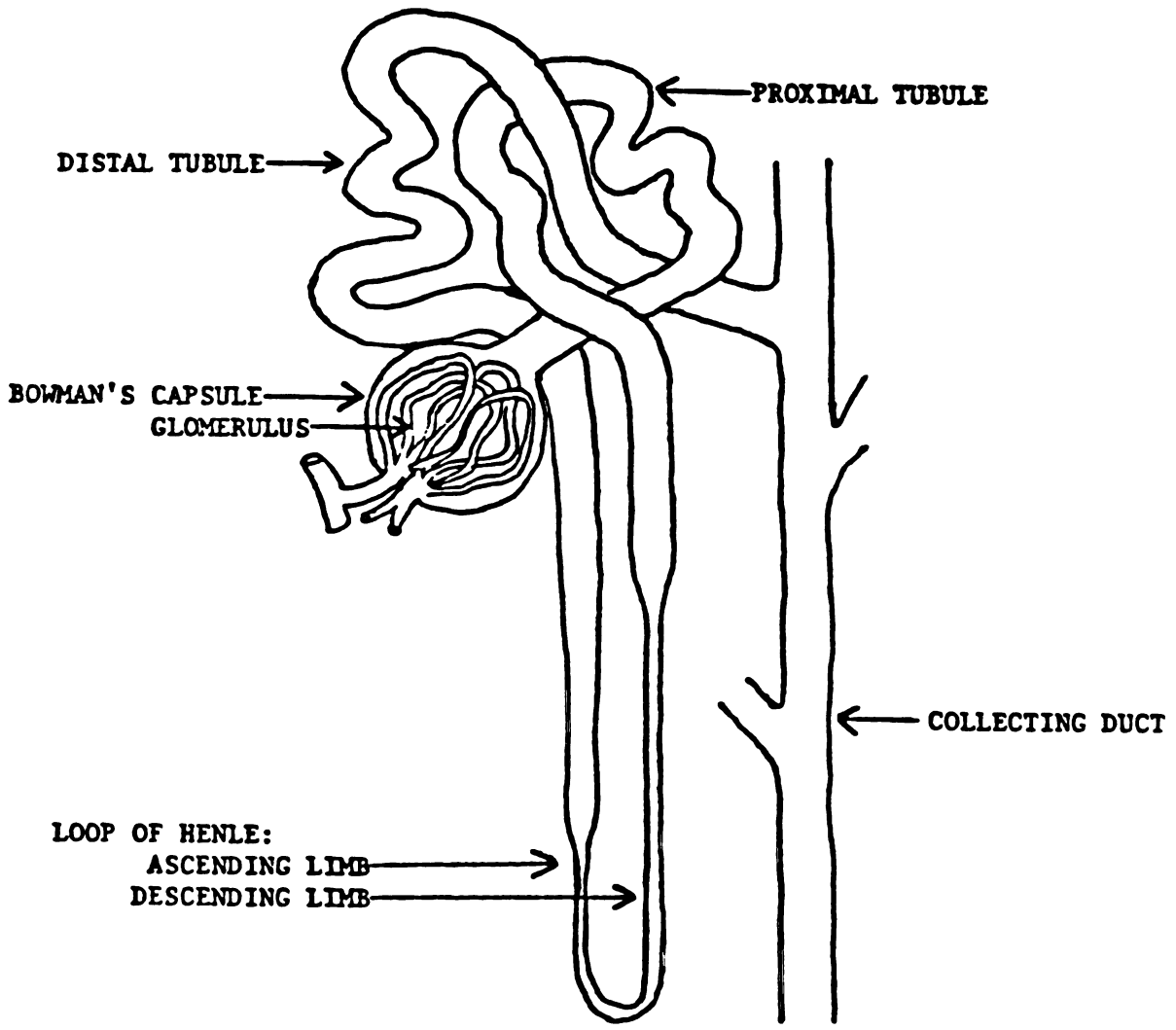

Figure I-1. The nephron.

supply a portal one (1-6).

The kidney as a whole has three major zones--the cortex, the medulla and the papilla. The papilla is the innermost area of the kidney. Urine from collecting ducts is drained into this region. The medulla overlays the papilla and may be divided into inner and outer zones. Some nephrons (juxtamedullary nephrons) have loops of Henle which extend into the inner zone of the medulla. Others (superficial cortical nephrons) only descend into the medullary outer zone. Covering the medulla and forming the outermost layer of the kidney is the cortex. Most of the glomeruli, proximal tubules and distal tubules are located in the cortex. Portions of the loop of Henle and collecting duct may also be located in the cortex, particularly in the case of the superficial cortical nephrons (2,3).

B. Renal excretion mechanisms

There are three major processes which take place in the kidney: filtration, reabsorption and secretion. These three processes govern the major controls on body fluid and electrolyte levels. They also serve to either enhance elimination or conservation of endogenous and exogenous compounds. Metabolism of compounds by the kidney also takes place, although it has not been well characterized (7). Renal metabolism will be briefly discussed in Section I.B.4.

1. Filtration

The first process performed by the nephron is filtration. Filtration takes place by the transfer of water and solutes from the plasma in the glomerulus to Bowman's capsule. Water, electrolytes, and most molecules of less than 75 Å diameter are freely filtered by the human kidney (2,3). One-fifth to one-third of renal plasma flow is filtered in mammals, with the fraction being one-fifth in humans (2,8).

Filtration is governed by such factors as the size of the capillary bed, permeability of the capsule, and hydrostatic and osmotic pressure gradients across the capillary wall (9). It has also been shown to be dependent on renal plasma flow (10). Protein binding will also affect filtration of a compound (2,3,9). Since most proteins are too large to be filtered, only a drug which is not protein-bound can undergo filtration. For example, if 10% of a compound's plasma concentration is free, that is, not bound to proteins, only 2% of that compound's total plasma concentration will be filtered. If it were not protein bound, 20% of it would pass into the filtrate. Changes in these factors cause generally predictable alterations in glomerular filtration rate (GFR).

Renal failure also affects GFR (2,11-16). It is commonly believed that renal failure affects all portions of a nephron equally. Bricker et al. (17) have presented this idea and refer to it as the intact nephron hypothesis. Consequently changes in GFR due to renal failure should be accompanied by changes in the other processes which take place in the tubule. Renal failure will be discussed in detail in Section I.F.

2. Reabsorption

Reabsorption is the process by which filtered or secreted material is removed from the tubular lumen and returned to the capillaries. Reabsorption may be via either passive diffusion or by a carrier-mediated process. Since protein is not generally present in the tubular lumen of a healthy nephron, protein binding is not a factor in reabsorption. In a damaged nephron, however, protein may enter the tubule with resultant protein binding of some molecules of a compound in the lumen. This might then affect reabsorption of that particular compound.

Reabsorption takes place in all segments of the nephron with the exception of Bowman's capsule. Water is passively reabsorbed in the proximal and distal tubule, as well as the descending limb of the loop of Henle and the collecting duct. Greater than 99% of filtered water is reabsorbed as it passes through the tubule (2,3,18). Sodium, chloride and bicarbonate ions are also reabsorbed by greater than 99%. These ions are at least to some extent reabsorbed by carrier-mediated processes. Most bicarbonate reabsorption takes place in the proximal tubule with a small percentage occurring in more distal portions of the nephron (3,19-23). Chloride and sodium are reabsorbed in the proximal tubule, loop of Henle, distal tubule and collecting duct (24-28). Potassium may be reabsorbed as required by the body in all segments of the nephron distal to Bowman's capsule (29-33). Potassium reabsorption also occurs by a carrier-mediated process.

Reabsorption of organic compounds may also be either passive or carrier-mediated. As a passive diffusion process such reabsorption may

be influenced by urine flow rate and by pH of the tubular fluid. As urine flow rate increases, passive reabsorption decreases. For example, the reabsorption of digitoxin in the rat kidney has been shown to be urine flow-dependent (34). For molecules where the net charge is dependent on the pH of the solution in which they are dissolved, passive reabsorption will be greater when the pH of the tubular fluid causes more of the molecules to be in the nonionized form. An example is salicylate, which is more extensively reabsorbed from the tubule when it is in an nonionized form (35,36).

Compounds which undergo carrier-mediated reabsorption include glucose and amino acids. Virtually 100% of filtered glucose and amino acids are reabsorbed in the proximal tubule by a co-transport system with sodium ions. Numerous studies (37-43) have shown that these transport systems are able to pump glucose and amino acids against a concentration gradient as long as a sodium ion concentration gradient is present. This is evidence that a carrier-mediated co-transport system is in use. The transport of glucose can also be inhibited with phlorizin (37-40), providing further evidence for a carrier-mediated transport system.

Other organic compounds may also be reabsorbed from the tubule by a carrier-mediated system. Cephapirin and cephaloridine have both been demonstrated to undergo carrier-mediated tubular reabsorption in man (44). Uric acid has also been shown to undergo carrier-mediated tubular reabsorption in the chicken (45) and in a number of mammalian species (46-50).

3. Secretion

Secretion involves the passage of molecules from blood to tubular lumen by either facilitated diffusion or by an active transport process. These two differ in that facilitated diffusion only involves a mechanism for increasing the rate at which a molecule can cross a membrane when it is moving with a concentration gradient. Active transport involves utilization of energy to move a compound across a membrane against a concentration gradient. Since it is difficult to absolutely separate these two processes, the term carrier-mediated transport will be utilized to cover both types.

Numerous molecules are known to be transported from blood to tubular lumen by a carrier-mediated process. Potassium (31,32,51,52) and hydrogen (53,54) ions both undergo secretion by the tubule. Organic anions such as para-aminohippurate (PAH) and urate are known to be secreted. The same holds true for organic cations such as N'-methylnicotinamide (NMN) and pseudoephedrine. Secretion of organic anions and cations will be discussed in greater detail in sections I.D.1. and I.D.2.

It has often been assumed that protein binding does not have a significant effect on secretion. This is due to the idea that once a molecule has attached to the carrier to be transported across the tubular membrane, a protein-bound molecule will be freed to maintain equilibrium between free and bound compound present in plasma. Assuming that this takes place rapidly enough, the molecules can be transported at a rate based on K_m and V_{max} for the carrier molecule and their total plasma concentration.

In actuality this is not always the case. The readjustment of equilibrium between free and bound may not take place rapidly enough. The rate at which the readjustment occurs depends upon the affinity of the molecule for the protein binding site as well as its affinity for the transport site (55). Thus, compounds which are highly protein-bound (i.e. phenol red (56) and furosemide (57)) are often secreted to a lesser extent than are compounds which are only somewhat protein-bound (PAH (2)).

4. Metabolism

A number of reviews have been published which discuss renal metabolism (58-60). This section is mainly concerned with the ability of the kidney to metabolize exogenous and endogenous compounds for purposes other than those involving maintenance of renal function and integrity.

This type of metabolism has been little studied and is poorly understood (7). It has been shown that the kidney contains mixed function oxidases (61). These enzymes are found mainly in smooth endoplasmic reticulum and are capable of performing numerous oxidative reactions. Reductive, hydrolytic and conjugation reactions (7) also take place in the kidney. Although the extent of this metabolism and its relationship to total body metabolism is not yet accurately quantified, Diamond and Quebbemann (62) have shown that over 20% of glucuronidation and sulfation of a specified p-nitrophenol dose in rats takes place in the kidney. Cimetidine has also been shown to be 10% metabolized by the chicken kidney (63). Based on these findings,

metabolism by the kidney may be more important than has often been thought.

C. Pharmacokinetic model of the kidney

Any model which is designed to explain the net effect of the kidney on the plasma concentration of any organic compound or electrolyte must consider the filtration, reabsorption and secretion processes of the kidney. Since metabolism is generally considered a minor pathway of elimination by the kidney, and is only known to come into play with a few compounds, it will not be included here. Øie and Benet (64) have described a pharmacokinetic model which addresses these three processes. This model states that:

$$CL_R = (CL_{RF} + CL_{RS})(1-FR)$$

where CL_R is renal clearance of the compound in question, CL_{RF} is its renal clearance due to filtration, CL_{RS} is its renal clearance due to secretion and FR is the fraction of the drug filtered and secreted which is reabsorbed.

Since filtration is strictly a passive, non-carrier-mediated process, the filtration clearance may be represented as :

$$CL_{RF} = f \cdot CL_{CR}$$

where f is the free (unbound) fraction of the drug in plasma and CL_{CR} is creatinine clearance, where creatinine clearance is assumed to be a

measure of GFR (3). Inulin clearance (CL_{IN}) may be substituted for CL_{CR} as a measure of filtration by the kidney.

Because secretion is a carrier-mediated transport process a more complex equation is needed to describe it. The rate of secretion of a molecule is dependent on a number of factors. These include the number of carriers available for transport of a particular molecule, the rate of presentation of the molecule to these carriers, the rate of transfer of the molecule-carrier complex across the membrane, the relative affinity of the molecule for the carrier versus its affinity for plasma proteins and the presence and amount of other types of molecules competing for the same carrier. The following equation describes this molecule-carrier interaction in the absence of competing molecules:

$$CL_{RS} = \frac{Q_K \cdot f \cdot CL^u_{int}}{Q_K + f \cdot CL^u_{int}}$$

where Q_K is blood flow to the transport site, f is the free fraction and CL^u_{int} is the intrinsic ability of the site to transport the unbound molecule across the tubular membrane.

Benet and Sheiner (65) state that $CL_{int} = V_{max}/(K_m + [S])$, where CL_{int} is equal to $f \cdot CL^u_{int}$, V_{max} is the maximum amount of compound which can be transported across a membrane per unit time, K_m is the concentration of compound at which one-half maximal transport rate is reached, and [S] is the concentration of the compound being studied. This equation is one version of the classical Michaelis-Menten process, in which a saturable system exists, allowing only a certain maximum transport rate or rate of reaction to take place.

In the presence of a second compound competing for the same transport carrier, the apparent value of CL_{int} will be decreased. A new CL_{int}, represented by CL'_{int}, is defined as:

$$CL'_{int} = \frac{V_{max}}{(K_m + [S])\ (1 + [I]/K_I)}$$

where [I] equals inhibitor concentration in plasma and K_I is the inhibitor concentration at which 50% of transport of the substrate is eliminated (at a given substrate concentration).

In the case of renal failure, CL_{int} will also be decreased. This decrease is due to changes in V_{max} and/or K_m which are caused by the renal failure. Yet another CL_{int}, represented by CL''_{int}, may be defined by the equation:

$$CL''_{int} = \frac{V'_{max}}{K'_m + [S]}$$

where V'_{max} is the value of V_{max} in renal failure and K'_m is the value for K_m in renal failure.

The expression for reabsorption presented by Øie and Benet (64) is represented only as the fraction reabsorbed. As mentioned previously, reabsorption may be either passive or facilitated. Passive reabsorption is dependent on the pH of the urine, urine flow rate, and the concentration of compound in the tubular fluid among other factors. Tang-Liu et al. (66) have described a complex relationship for passive reabsorption which takes into account these and other factors.

In the case of facilitated diffusional reabsorption, factors such as affinity of the molecule for the carrier and maximal rate at which the carrier can move across the membrane come into play. A Michaelis-

Menten type equation similar to that representing secretion might be used to describe this type of reabsorption.

D. Carrier-mediated transport of organic anions and cations

1. Organic anions

Organic anion transport by the renal tubule has been extensively studied (67,68). The proximal tubule is the site of organic anion transport and the majority of compounds which are transported show a net secretory component. Compounds for which secretion has been studied include p-aminohippurate (PAH) (69-74), urate (48,49,75,76), salicylate (36), phenolsulphthalein (77), cephaloridine (78), folic acid (79), methotrexate (79) and probenecid (80). Most of the work studying organic anion transport to date has used PAH as the prototype organic anion.

PAH is transported by a carrier-mediated process. This process exhibits a maximal transport rate (T_m or V_{max}) (69,71,74,81,82) and is competitively inhibitable by a number of other organic anions. The inhibitors of PAH transport include urate (83-86), probenecid (81-85,87,88), cinoxacin (89), bumetanide (90), salicylate (85,88), penicillin G (87), furosemide (84,85,87) and cephaloridine (91). This apparent competition for transport sites may indicate that other organic anions are transported by the same carrier system. The tubule is also able to pump PAH against a concentration gradient. This serves as further evidence that a carrier-mediated and perhaps active process is taking place in the transport of PAH, and perhaps other organic anions

as well.

Exactly where the carrier system(s) for organic anions is (are) located on the proximal tubule is of interest and importance. Figure I-2 is a cross-section of the proximal tubule. The proximal tubule is one cell wide. As the drawing suggests, the membranes on opposite sides of the proximal tubule cell are quite different. The brush border membrane has numerous microvilli whereas the basal-lateral membrane has larger infoldings which are fewer in number. The enzyme characteristics of the two membranes are very different as well. Sodium-potassium-ATPase is known to be located only on the basal-lateral membrane, whereas alkaline phosphatase and maltase are specific for the brush border membrane. The two membranes differ in their transport characteristics also. Brush border membranes contain specific carrier-mediated transport systems for the reabsorption of glucose and a number of amino acids (see Section I.B.2.). Basal-lateral membranes do not have analogous carriers for these compounds.

Whether or not there are carrier systems for organic anions (or organic cations) on one or both of these membranes is not definitely known. Either membrane, both or neither may contain a carrier system for each class of compounds. It is known that the proximal tubule can secrete these classes of compounds against a concentration gradient. The existence of an electrical potential or gradient may be useful to enhance their passage. As Figure I-2 indicates, the passage from capillary to inside the proximal tubule cell involves movement to a more electronegative environment. Conversely, movement from cell interior to lumen of the tubule involves a relatively electropositive change.

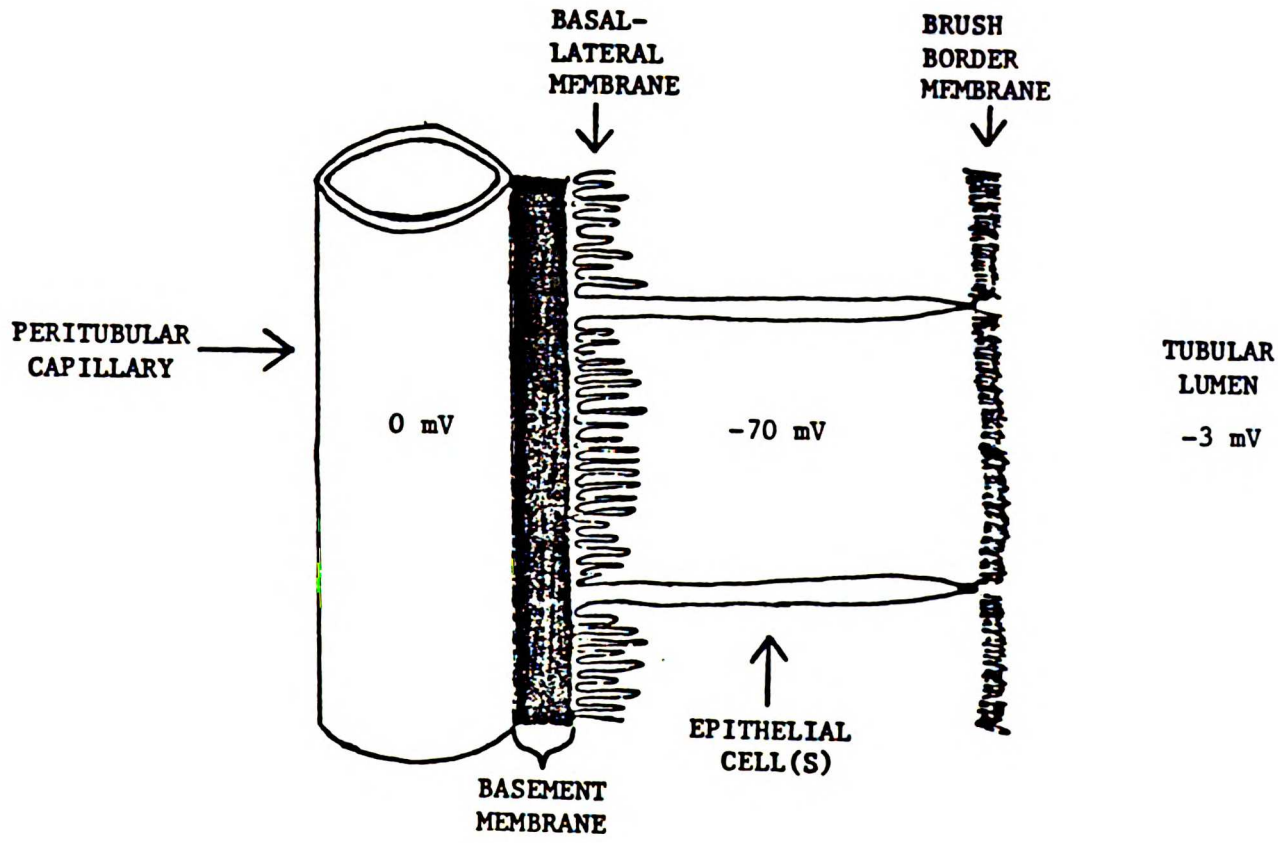

Figure I-2. Cross section of the proximal tubule.

In the case of an organic anion (i.e. PAH, urate), most of the molecules will be negatively charged at physiological pH in the blood. Passage of a negatively-charged molecule from blood to cell interior will not be favored due to the large electronegative potential. However, once the molecule is inside the cell, its passage into the lumen (a more electropositive region) will be favored. This difference may aid the proximal tubule in secreting organic anions. Based on this hypothesis, a carrier system is needed on the basal-lateral membrane in order to move an organic anion across the proximal tubule against a concentration gradient. However, a carrier system for these compounds on the brush border membrane may not be required--the molecules may be able to move against a concentration gradient by utilizing the electrical potential gradient.

One way in which the location of carrier-mediated transport systems may be studied is by the use of vesicles (for a discussion of vesicles, see Section I.E.2.). A number of researchers have examined the transport of PAH by one or both types of membranes using vesicles (61,81,82,84,85,91-98). Some of these reports (61,84,85,98) include data from brush border membrane studies only, while others (91-94,96) used only basal-lateral membranes. Only four reports include data from both types of membranes (81,82,95,97). Of these, Hori et al. (98) and Berner and Kinne (81) report carrier-mediated transport in rat basal-lateral membranes, but not in brush borders; Eveloff et al. (95) found carrier-mediated transport in brush border but not basal-lateral membranes of flounder kidney; and Kinsella et al. (82) demonstrated carrier-mediated transport in both membranes from dog kidney. However, the evidence of Kinsella et al. for carrier-mediated transport in brush

border membranes was much more tenuous than that in basal-lateral membranes. It is possible that the brush border carrier-mediated transport system found in Kinsella's studies is an artifact.

It is also possible that there are species differences. Eveloff et al. (95) utilized vesicles made from a member of the fish family, while the others used mammalian kidneys. This difference in evolutionary level may explain the difference in results. Based on the theory described and the results available in the literature, we believe that there is a carrier-mediated transport system for PAH on the basal-lateral membrane. Therefore basal-lateral membranes were used in the vesicle studies presented in this dissertation.

It has been speculated that the transport system(s) for organic anions may require a co- and/or countertransport molecule for most efficient transport. A number of researchers (92,99-104) have found that sodium ions stimulate PAH transport by serving as co-transport ions. Podevin and Boumendil-Podevin (104) have reported that potassium ions serve as countertransport ions to stimulate PAH transport. Still other researchers (105,106) have shown that inhibition of sodium-potassium-ATPase activity decreases PAH transport. This may indicate that sodium-potassium-ATPase activity is directly related to PAH transport. However, it is also possible that the enzyme only maintains appropriate sodium and/or potassium levels for efficient PAH transport.

Other researchers have shown a relationship between pH and PAH transport (107-110). Here PAH transport may be tied to either hydrogen ion or hydroxyl ion concentration. Which is the actual stimulatory ion has not been definitely proven. Still others (111-113) have shown that calcium ions stimulate transport of PAH.

Tse et al. (93) have examined mono-, di- and trivalent cations for their ability to stimulate PAH transport in rabbit renal basal-lateral membranes. The ions studied include sodium, potassium, calcium and magnesium. They have found that magnesium ion at a 5mM concentration stimulated PAH transport the most. It is possible that more than one type of cation is capable of combining with the carrier to enhance transport of PAH. From the results of Tse et al. however, it appears that magnesium is the most effective of these ions for stimulating PAH transport.

With reference to possible anion counter-transport ions, the most obvious choices are hydroxyl and chloride ions. As mentioned previously, a number of studies have been done which examined the effect of pH (107-110). Hydroxyl and hydrogen ion effects have not been separated however. Several researchers (110,114,115) have found that the absence of chloride ion decreases PAH transport.

In summary, these conflicting data indicate that there may be a co-transport and/or countertransport system for PAH transport. Since many researchers have limited themselves to studying the effect of only one possible ion the results are not truly comprehensive. More work of the type undertaken by Tse et al. (93) needs to be done in order to determine the true co- and/or counter-transport ions involved in organic anion transport.

The possibility exists that there is more than one carrier system on the basal-lateral membrane for organic anions. This is suggested by the results from some studies in which the effects of PAH and urate on each other's transport were examined. Weiner (48) has reviewed the disparities found in urate and PAH transport. Dantzler has used snake

tubules extensively and has found many differences in urate and PAH transport characteristics (74,75,83,116). The conclusion drawn from these studies is that snakes utilize two different systems for secreting PAH and uric acid. Studies in man and chimpanzee have also shown that PAH and urate are secreted by different mechanisms (48).

The presence of more than one organic anion renal transport system in other species is more speculative. Rabbits appear to have only one such transport system (48). Most of the data from rats and dogs also indicate the presence of only one system (48). It may be that there is true species variation in the transport of organic anions. However, it is also possible that the results published so far have not accurately characterized organic anion transport. If two organic anions utilize the same carrier system for secretion, their simultaneous presence in plasma may effectively decrease their renal clearances. This could cause increased levels of the compounds in the body leading to complications such as toxicity and/or inaccurate measurement of bodily functions. Consequently, the studies presented in this dissertation were designed to learn more about the transport characteristics of organic anions, particularly whether or not two commonly-used organic anions could affect each other's transport.

PAH was chosen as one of the organic anions to be studied for the following reasons. 1) PAH is the prototype compound for organic anion transport. There is a large data base available concerning its transport which could be useful in the quantitation of results. 2) Renal clearance of PAH is used to measure renal plasma flow (RPF). However, if another compound were present which could compete for the same transport sites, it could affect the accuracy of the RPF

measurement. We addressed this possibility.

The second organic anion chosen was furosemide. Furosemide was chosen for the following reasons: 1) Furosemide is an organic anion and is known to be secreted by the proximal tubule (57). There is a large data base available with regard to furosemide, as well as extensive on-going work in our laboratory. Again, this data base could be useful in quantifying our results. 2) Furosemide has been given in conjunction with compounds used to measure RPF (117). However, if furosemide competes with such compounds for transport sites, it may adversely affect the RPF measurement. The properties and uses of PAH and furosemide will be discussed in Chapter II.

The secretion of organic anions may also be affected by renal failure. Pitts (2) has reviewed the types of renal failure and discussed their effect on the renal clearance of PAH. He has also discussed the intact nephron hypothesis (17) and states that it does not always hold true. In conclusion, he reports that CL_{PAH} cannot always be used as a good measure of renal plasma flow. However, it is not clear how severe the renal failure must be before CL_{PAH} fails in this function. Most of the work mentioned by Pitts involved relatively extensive renal failure. The renal failure studies presented in this dissertation were designed to: 1) learn more about the severity of renal failure necessary to cause CL_{PAH} to give an inaccurate measure of RPF, and 2) determine if the intact nephron hypothesis holds true under a given set of conditions.

2. Organic cations

Organic cation transport by the nephron has also been studied, although not as extensively as organic anion transport. Rennick has written an excellent review of this process and the studies pertaining to it (118). Endogenous organic cations known to be transported include acetylcholine, epinephrine, N'-methylnicotinamide (NMN) and thiamine. Drugs which are organic cations and are transported by the proximal tubule include meperidine, atropine, procaine, quinine and pseudoephedrine (118,119). Most work on organic cation renal transport to date has utilized NMN as the prototype compound.

Carrier-mediated transport of organic cations also takes place in the proximal tubule. Based on the model involving electrical potential which was discussed in the previous section, it would be expected that an organic cation transport system must be located on the brush-border membrane but not necessarily on the basal-lateral membrane. This theory is supported by the results of Kinsella et al. (82). They have found that transport by the brush-border membrane is a carrier-mediated process whereas basal-lateral membrane transport behaves more like a gated diffusion process.

Only limited work has been done concerning possible co- and/or countertransport molecules for organic cation transport. Kinsella et al. (82) report that sodium ion has no effect on NMN transport. Holohan and Ross (120) have shown that there is a hydrogen ion countertransport system for NMN transport. These studies have all been done using dog kidneys. Further studies utilizing other species are necessary to determine if these results are species-specific.

The question of one or more transport systems on the brush-border membrane for organic cations also arises. Holohan and Ross (121) have demonstrated countertransport stimulation of NMN transport with a number of organic cations. They conclude that at least all of the tested organic cations utilize the same carrier system. Again, further work is necessary.

E. Methods for studying renal excretion

Both in vivo and in vitro models have been developed for the study of how the kidney handles various compounds. These methods include whole animal renal clearance, isolated perfused kidney, isolated perfused tubule, stop-flow, micropuncture and isolated cell membrane (vesicle) techniques. In vivo renal clearance and in vitro isolated cell membrane models have been used for the studies to be presented here. Use of these two obviously disparate techniques affords the opportunity to study the individual transport characteristics of a particular membrane as well as net renal clearance in the whole animal. Effects of changes in the experimental procedure could be viewed from both a sub-cellular and a whole animal vantage point. These two methods will be discussed more specifically in the next sections.

1. In vivo renal clearance studies

In vivo renal clearance studies involve administration of the compound(s) to be studied to the subject, followed by collection and analysis of plasma and urine samples. The subject may be in either a

conscious or anesthetized state, and bodily functions, including renal function, are considered to be normal. Numerous researchers (57,119,122,123) have utilized some version of in vivo renal clearance techniques. This type of study is one of the few which can be done not only in animals but also in humans as it does not require removal or destruction of the kidney.

The in vivo renal clearance studies included in the present work were done in rats. For this work, the use of the in vivo renal clearance technique has allowed us to determine how the animal and its renal function react to the changes induced by the experiment. In one set of experiments, the renal clearance of an organic anion was measured before and after the addition of a second organic anion. This second anion may compete for the same transport site and thus decrease the renal clearance of the compound in question. In another set of experiments, renal failure was induced prior to administration of the organic anion. By comparison with controls, changes in renal function could be measured. The qualitative and quantitative changes seen in these studies may be extrapolatable to similar human situations.

2. In vitro isolated cell membrane (vesicle) studies

Vesicle studies might properly be thought of as at almost the opposite end of a spectrum from in vivo renal clearance studies. Vesicle studies involve the isolation of a particular type of cell membrane. This is done by disrupting the cell. The cell contents are released and most pieces of membrane spontaneously form closed sacs called vesicles. With cell and organelle components removed, the

researcher is able to study the transport characteristics of the specific membrane.

A potential disadvantage of this technique is that procedures for isolating cell membranes may well affect the "normal" renal function characteristics of the membrane. Also, an isolated cell membrane under artificial conditions is far removed from its true physiological state within the animal. Results from isolated cell membrane studies are therefore not readily extrapolated to real-life situations. This technique does, however, allow the researcher to break down the elimination or conservation of compounds by the kidney into the three elementary functions.

The use of vesicles to study the transport characteristics of membranes has a long history. Red cell ghosts, which are the membranes of red blood cells, have been used for many years to learn about some of the characteristics of these cells (124). Vesicles have more recently been prepared from intestinal cells (125), renal tubule cells (126), and cells of the choroid plexus (127). Although similar methods may be used to isolate the cell membranes from different organs, this dissertation will only present methods utilized in preparing vesicles from renal tubule membranes (See Chapter III).

As has been discussed, organic anions are secreted by the proximal tubule. In order to study the transport of these compounds using vesicles, it is necessary to isolate cell membranes from this portion of the tubule. Since proximal tubules are located in the cortex of the kidney, selective processing of the cortices only will enrich a preparation in proximal tubule membranes. Other organelle membranes and components such as those of glomeruli and distal tubules, which are also

located in the cortex, may be separated from proximal tubule membrane vesicles by centrifugation. The two types of proximal tubule membrane vesicles may then be separated from each other by a variety of techniques. Some of the methods for preparing renal proximal tubule membranes will be presented in Chapter III.

As previously mentioned (Section I.D.1.), basal-lateral and brush border membranes have very different characteristics. They are distinct from each other in physical appearance as well as enzyme and transport characteristics. The differences in enzyme components are routinely used to determine the purity of a particular cell membrane preparation (see Section III.A.).

Two other pieces of information which are important to know when utilizing vesicles for transport studies are the percent of cell membranes which are actually in closed vesicle form and the orientation of the membrane in its vesicle form (right-side-out versus inside-out). Kinsella et al. (128) have found that 90% of basal-lateral membranes form vesicles. Although they did not calculate a similar vaule for brush-border membranes, no open "sheets" of brush border membranes were visible upon electron microscopic examination. The authors therefore feel that no significant percentage of brush border membranes occur as open membrane pieces. They also report that 76% of basal-lateral membranes and 86% of brush border membranes form vesicles that are right-side-out—that is the side of the membrane which was oriented toward the cell interior is now oriented toward the vesicle interior.

Vesicles can serve as a useful tool for studying transport characteristics of particular cell membranes. However, it is important

to recognize their limitations. As long as these are kept in mind, the use of vesicles may be continued and expanded. The studies presented in this dissertation involve the use of vesicles to examine the effect of the presence of one organic anion on another's transport. Using isolated cell membrane vesicles enables us to have a clearer view of the isolated transport processes.

F. Renal failure

1. General

There are numerous types and causes of renal failure. Renal failure may be acute or chronic, stable, progressive or reversible. It may be caused by ischemia, trauma to the kidney or interaction of the kidney with various toxins (2). Because of the importance to life of maintaining adequate renal function, models for studying renal failure have been devised. A number of methods are currently used in order to induce renal failure in animal models. They may be used to study the effects of the renal failure on the animal's well-being and to devise methods in an attempt to alleviate the renal failure.

It is also possible to utilize varying degrees of renal failure in order to study their effects on the kidney and its processes. As discussed earlier, Bricker's intact nephron hypothesis (17) states that all portions of the nephron are affected equally by a decrease in function of any one segment. Although Pitts (2) states that this theory does not always hold true, little work has been done which might prove or disprove this theory. We chose to perform some experiments which

might provide more information about the suitability of the intact nephron hypothesis. In doing these experiments we chose to utilize PAH, a compound whose utility as a measure of RPF depends upon the kidney's ability to clear it from plasma. The choice of this compound enabled us to gain not only more information about the suitability of the intact nephron hypothesis, but also information about the clearance of PAH and how it is affected by varying degrees of renal failure.

2. Methods of induction

Renal failure may be induced by any of the following means: 1) Ischemia, caused by narrowing and/or total occlusion of the renal artery; 2) Five-sixths nephrectomy, in which two-thirds of one kidney is ligated and the other is removed completely; 3) Ureteral ligation which causes urine to collect in the kidney and results in renal failure; 4) Administration of nephrotoxins. A number of compounds cause renal damage. These include glycerol, mercury-containing compounds, uranium-containing coumpounds and a variety of drugs commonly used to treat other conditions (i.e., aminoglycosides, phenacetin (129)). Each class of nephrotoxins works in its own peculiar way.

Uranyl nitrate, a nephrotoxin, was chosen as the means of inducing renal failure in these studies. It was chosen because uranium compounds appear to affect all segments of the nephron, yet have a more significant effect on the proximal tubule (130). Because these studies were particularly concerned with the ability of the proximal tubule to secrete PAH, we wanted a toxin which was likely to cause an adverse change in PAH clearance. Uranyl nitrate appeared to be a good choice.

Uranyl nitrate mediates its effect on renal function by binding with lipid bilayers as well as penetrating these same bilayers (131). Histopathological and morphological studies of tubules after uranyl nitrate administration show diffuse brush border loss and increased vacuolization, with eventual desquamation, shrinkage of glomerular network and rupture of blood vessels (132,133).

Uranyl nitrate-induced renal failure has been shown to affect GFR and RPF (11-16,130,134-138). These studies have generally used high (>5mg/kg) uranyl nitrate doses. Since PAH clearance is used as a measure of RPF, we were interested in determining whether or not a low dose of uranyl nitrate would change the measure of RPF obtained from PAH clearance. We were also interested in the suitability of the intact nephron hypothesis (17) under conditions of only limited renal failure. The studies presented in this dissertation were designed to answer these questions.

G. Project objectives

The objectives of this project were two-fold:

1) To determine if two organic anions could inhibit each other's transport by the carrier-mediated transport system for organic anions in the nephron.

2) To determine if renal failure could affect a measure of RPF which is dependent on tubular function, and to determine if such renal failure follows the intact nephron hypothesis.

CHAPTER II

para-AMINOHIPPURIC ACID AND FUROSEMIDE

BACKGROUND

A. para-Aminohippuric acid

1. Chemistry

p-Aminohippuric acid (PAH), N-(4-aminobenzoyl)glycine, $C_9H_{10}N_2O_3$ is shown in Figure II-1. Its molecular weight is 194.19. PAH is an organic acid with a pK_a of 4.0. It has a melting point of 198-199°C and forms needles from hot water. PAH is soluble in alcohol, chloroform, benzene and acetone, but is practically insoluble in water, ether and carbon tetrachloride. Aqueous solutions of the sodium salt are alkaline and must be buffered with citric acid to pH 7.0-7.6 for intravenous administration (139,140).

2. Diagnostic use

PAH does not exert any pharmacological effect at commonly-used doses. Moreover, ninety percent of PAH in plasma is cleared in one pass through a healthy human kidney (141). Because of these characteristics, PAH renal clearance (CL_{PAH}) commonly been used to measure renal plasma flow (RPF). This technique involves infusion of PAH at a rate that will result in a steady, low plasma concentration which will not saturate the renal transport mechanism. Once steady-state levels have been reached, the PAH concentration in plasma and urine, as well as the urine flow

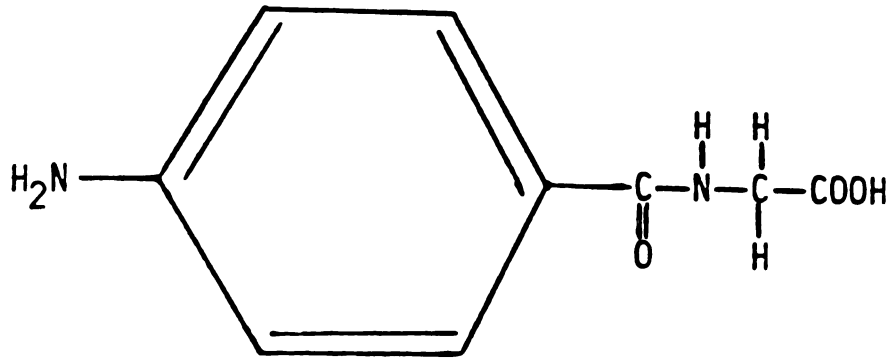

Figure II-1. para-Aminohippuric Acid (PAH)

rate, are measured. These data can be used to calculate CL_{PAH} according to the following equation:

$$CL_{PAH} = \frac{C_u \cdot V_u/t}{C_p}$$

where C_u = PAH urine concentration, V_u/t = urine flow rate and C_p = PAH plasma concentration (3).

Schnurr et al. (142) have developed a method for measuring CL_{PAH} which does not require urine collection. It assumes that true steady state has been reached and thus replaces urine concentration and flow rate with PAH concentration in the infusion fluid and rate of fluid infusion. This technique gives comparable results to those obtained from urine data.

Favre (143) has tested a bolus dose technique in which the decay of plasma levels is tracked and used to calculate total PAH clearance. He obtained satisfactory results although the clearance values tended to be higher than those found with the steady-state technique.

PAH has commonly been used to measure RPF because it has no pharmacological effect, it is not toxic, its plasma and urine concentrations can be readily measured (see Section V.A.1.) and its renal elimination has generally been considered consistent from subject to subject for a given RPF under various conditions. The studies undertaken for this dissertation examine the validity of the last reason/assumption--i.e., consistent elimination under various conditions.

3. Pharmacokinetics

a. Renal elimination

The renal clearance and extraction ratio of PAH are the parameters which have generally been measured when PAH is used. Volume of distribution and half-life are of little or no interest and are therefore not calculated. As stated before, approximately 90% of plasma is cleared of PAH as it passes through the kidney. This represents an extraction ratio of 0.9. This statement only holds true at relatively low PAH plasma concentrations. At higher plasma concentrations, the carrier-mediated transport system becomes saturated and the extraction ratio decreases (141). It is not clear why the extraction ratio of PAH is 0.9 rather 1.0. Some of the possible reasons are covered in the following paragraph.

Ten to twenty percent of PAH in plasma is bound to proteins (72,144-146). This protein binding may cause the extraction of PAH to be less than 100%. However, PAH does not partition into red blood cells (144). Therefore partitioning is not a factor in determining the extraction ratio. The extraction ratio may also deviate from 1.0 because of intrarenal blood flow. This is a factor in that not all blood perfuses the cortex as it passes through the kidney. Blood which passes through the medullary portion of the kidney does not flow past proximal tubules and is therefore not available to undergo PAH extraction (147). Consequently, the extraction ratio of 0.9 for PAH may be caused by this.

Rats and rabbits have frequently been used as models to study the renal clearance of PAH (68,69,80,81,83,86,145,148-154). Their ability to clear PAH is similar to that of man. Because of the large data base and the similarities in renal function, these species were utilized in the studies included in this dissertation.

b. Metabolism

Although the vast majority of PAH has been shown to be cleared unchanged by the kidney, the compound can be metabolized. Rats and mice have been shown to N-acetylate PAH in the kidney (155-157). Rats have also been shown to renally metabolize PAH to p-aminobenzoic acid (155). This metabolism was not observed, however, in the studies presented here. Overall, PAH metabolism is generally considered to be inconsequential.

c. Effect of competition for transport sites

Some work has been done which demonstrates an effect of competition for transport sites on PAH transport. Pitts (2) states that competition takes place and can decrease PAH transport. Compounds which have been shown to decrease PAH renal transport include probenecid (88), indomethacin (158), acetylsalicylic acid (87), bumetanide (90), cinoxacin (89), uric acid (86), cephaloridine (91), penicillin G (87) and furosemide (87). Most, and perhaps all of these compounds appear to inhibit PAH transport by competition for the transport sites. However, the mechanism by which this happens, where on the cell it happens, and

what, if any, clinical significance it may have, have not been well-studied. Consequently, the studies in this dissertation were designed to further examine the effect of one particular organic anion drug, namely furosemide, on the transport of PAH. The intent was to determine if the co-administration of PAH and furosemide might have a significant effect on the renal clearance of PAH.

d. Effect of renal failure

The effect of renal failure on the kidney's ability to excrete PAH has not been extensively studied. Pitts (2) states that renal failure does decrease CL_{PAH}. However, it is not clear how extensive the renal failure must be to see a significant decrease in CL_{PAH}. Only one study has been done in rabbits, concerning the effect of uranium-induced renal failure on CL_{PAH} (130). This study was done two days after administration of the uranium. Since the peak effect of uranium-induced failure is known to take place five days after injection (12), we chose to do studies with low doses of uranyl nitrate and examine their peak effects, five days after dosing.

Also, little work has been done which separates renal failure effects on clearance of compounds which are only filtered (i.e., inulin) from effects on clearance of secreted compounds (i.e., PAH). Bricker's intact nephron hypothesis (17) states that as one function of a nephron is decreased, so will other functions be decreased to the same extent. Althought Pitts (2) states that this does not always hold true, only limited work has been done which closely examines this. The renal failure work included in this dissertation was designed 1) to determine

if low levels of renal failure could affect CL_{PAH} and thus its measure of RPF and 2) to determine if Bricker's intact nephron hypothesis holds true in this particular situation.

B. Furosemide

1. Chemistry

Furosemide, 4-chloro-N-furfuryl-5-sulfamoylanthranilic acid, is shown in Figure II-2. Furosemide has a composition of $C_{12}H_{11}ClN_2O_5S$ and a molecular weight of 330.77. It has a pK_a of 4.7 for the carboxyl group which serves to make furosemide an organic anion at physiologic pH. Furosemide forms crystals from aqueous ethanol. These crystals melt at 206°C. The compound is only slightly soluble in water or chloroform. However, it is soluble in acetone, methanol, dimethylformamide and aqueous solutions above pH 8.0. It is somewhat less soluble in ethanol. Furosemide is incompatible in solution with a number of other compounds, including calcium gluconate, ascorbic acid, tetracyclines, urea and epinephrine (139,159).

2. Therapeutics

Furosemide is a potent diuretic. It is similar in structure to the thiazides, although its mechanism of action is different (see Section II.B.3.). Furosemide has been used in the treatment of hypertension, congestive heart failure, and the edema resulting from hepatic and renal dysfunctions (160-162). It is also able to promote diuresis at

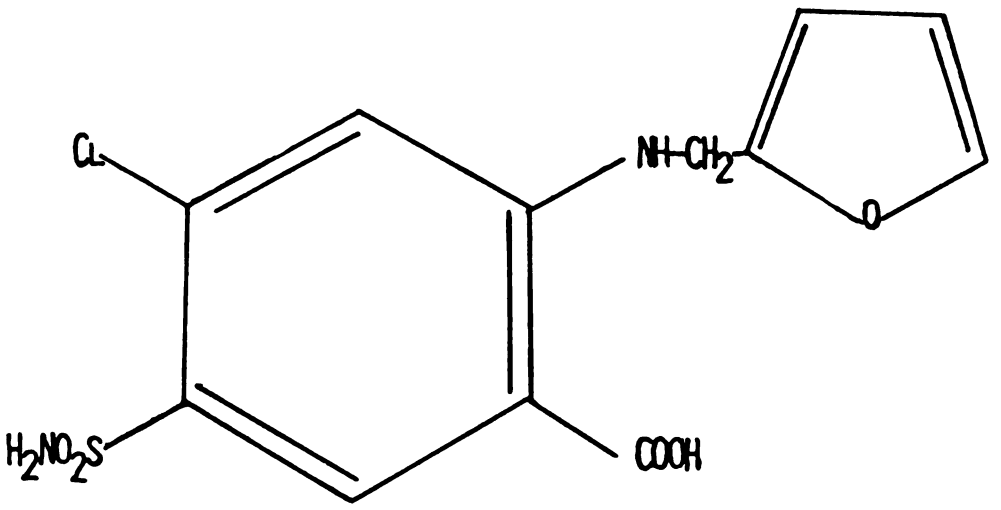

Figure II-2. Furosemide.

extremely low GFR (163,164). Since most other diuretics do not have this capability, furosemide is a diuretic of choice in renal failure. Furosemide has a rapid onset of action and a relatively short half-life (160). It may be administered either IV or orally. Its pharmacokinetics will be discussed in Section II.4.

3. Mechanism of action

Furosemide is believed to exert its diuretic effect at the luminal surface of the nephron (57,165). Its main effect is to inhibit the active reabsorption of chloride which takes place in the ascending limb of the loop of Henle. This inhibition of chloride transport is probably mediated through prostaglandins, which have been shown to inhibit chloride reabsorption and cause diuresis (166). It has been shown that furosemide inhibits enzymes which degrade prostaglandins (167,168). Furosemide also increases free arachidonic acid levels (169), which can then be converted to prostaglandins. As a result, furosemide causes increased prostaglandin levels which in turn cause increased diuresis.

4. Pharmacokinetics

a. Renal elimination

Benet (170) has written a comprehensive review of the pharmacokinetics of furosemide. He reports that a number of researchers have found furosemide renal clearance values of 75 to 149 ml/min in humans. These values fall in the general range of GFR. However,

furosemide is 98.8% bound to proteins in plasma of normals (171). It must therefore be cleared not only by filtration but also by secretion, most likely via the organic anion pathway.

Bowman (172) has shown that changes in protein binding affect renal secretion of furosemide by the rat kidney. Hammerlund and Paalzow (173) also found an effect of protein binding on furosemide renal excretion in the rat. Their results showed that 0.92% of furosemide in plasma is free at an 11 µg/ml total concentration. This free percentage increased to 9.1 at a total furosemide plasma concentration of 425 µg/ml. These data indicate that even though furosemide undergoes secretion, the transport process is not able to clear all of the compound which is protein-bound.

In humans, from 34 to 92% of furosemide has been shown to be excreted unchanged (170). It is probable that this variability is due to problems with assay methodolgy, i.e., treatment of samples and/or inaccuracy in measuring metabolites.

b. Metabolism

The metabolism of furosemide has not been studied extensively. A number of researchers have reported that 2-amino-4-chloro-5-sulfamoylanthranilic acid (CSA) is a metabolite of furosemide (170). However, Smith et al. (171) have found that CSA is an artifact of the assay methods used by others and is not a true metabolite of furosemide.

Smith et al. (171) have also found that approximately 14% of the available dose of furosemide is excreted as the glucuronide metabolite. There appear to be one or more other metabolites as well.

The glucuronide is, however, the only metabolite that has been positively identified to date.

c. Effect of competition for transport sites

The diuretic effect of furosemide in the kidney has been shown to be inhibited by a few compounds. These include probenecid (174-178), acetylsalicylic acid (179-182) and indomethacin (183-188). Although it is not clear whether or not the cause of this decreased diuretic effect is inhibition of furosemide transport, it is likely that this is the case. Because of this data, some of the studies included here were done to determine if PAH could affect furosemide transport and thus perhaps alter its diuretic effect.

CHAPTER III

RENAL PROXIMAL TUBULE VESICLES

METHODS OF PREPARATION, CHARACTERIZATION AND UTILIZATION

A. Introduction

Renal transport of organic anions such as PAH and furosemide may be studied by the use of renal proximal tubule vesicles. As discussed in Chapter I, vesicles are isolated cell membranes which are formed by disruption of the membranes and loss of the cell contents. After disruption, most pieces of the cell membrane spontaneously form closed sacs, which are called vesicles.

Several methods have been developed for the isolation of renal proximal tubule membrane vesicles. A mixture of basal-lateral and brush border membranes may be separated from debris by a series of centrifugations (126,128,189-192). Separation of these two types of membranes from each other may be accomplished in a number of ways. The simplest, most straightforward method for separating brush border membranes from basal-lateral membranes is by use of divalent cation precipitation and differential centrifugation (84,85,94,95,98,128,193-196). Addition of a divalent cation, such as Mg^{2+} or Ca^{2+}, to a homogenized cell mixture will cause basal-lateral membranes and unwanted material to pellet upon slow speed centrifugation, leaving brush border membranes in the supernatant. Basal-lateral and brush border membranes may also be separated by free flow electrophoresis, as demonstrated by Heidrich et al. (126) and Reynolds et al. (191). Differences in membrane surface charge, and corresponding attraction to or repulsion

from external charges are the reasons why free flow electrophoresis works to separate these membranes. A number of researchers (94,128,190,197,198) have utilized discontinuous sucrose density gradients for purification of these membranes. Success of these techniques is dependent upon the different densities of the two types of membranes. Other methods include the use of modified colloidal silica (Percoll) self-forming gradients (189,192,199) or use of sorbitol gradients (98) for separation of basal-lateral and brush border membranes. Again, these methods depend upon the different densities of the two types of membrane. The method used in the work to be described here involves the use of a step sucrose density gradient for preparation of basal-lateral membranes as described by Mamelok et al. (94).

It is important to identify which fractions from a membrane separation procedure contain basal-lateral membranes and which contain brush border membranes. The accepted way of doing this is to make use of enzyme markers. As stated in Chapter I, Na^+-K^+-ATPase is an enzyme known to be located on the basal-lateral membrane but not on the brush border membrane. Alkaline phosphatase is, conversely, located on the brush border but not basal-lateral membrane. If each fraction is assayed for these two enzymes, the results will indicate whether or not the membrane types have been separated and where the desired membranes are located. If each fraction's protein concentration is determined, and this data is combined with enzyme activity information, we obtain knowledge about the relative enrichment of each type of membrane in each fraction. Consequently, this chapter will describe methods for determining Na^+-K^+-ATPase activity, alkaline phosphatase activity, and protein concentration in these samples.

Once renal proximal tubule membrane vesicles have been isolated, they can be used to study the transport characteristics of that particular membrane type. In order to do this, a method of measuring transport by these vesicles must be available. Generally, a radiolabelled form of the transport compound is used, allowing the researcher to measure transport by radioactive decay. This chapter will describe the general transport method used in these experiments, as well as a method for measuring nonspecific binding to vesicles and a method for pre-loading vesicles with a potential counter-transport compound.

B. Preparation of vesicles

Purification of basal-lateral membrane vesicles using a step sucrose density gradient

The method to be described here was developed by Mamelok et al. (94).

1. Chemicals and instrumentation

Mannitol, Tris, Leupeptin, Magnesium chloride ($MgCl_2 \cdot 6H_2O$), HEPES (Sigma Chemical Company, St. Louis, Missouri); EDTA, Hydrochloric acid, Sucrose, crystalline (J.T. Baker Chemical Company, Phillipsburg, New Jersey); Sorvall Omnimixer, GSA rotor, Sorvall RC-5B Refrigerated Superspeed Centrifuge, SS34 rotor (Dupont Instruments-Sorvall, Wilmington, Delaware); 6ml polycarbonate centrifuge tubes (Dupont Company, Newtown, Connecticut); Polycarbonate centrifuge tubes, 50 ml (American Scientific Products, McGaw Park, Illinois); Teflon PE tissue

grinder, size C (Thomas Scientific, Philadelphia, Pennsylvania); Ti-15 zonal rotor, Seal assembly unit for Ti-15 zonal rotor, L5-50B ultracentrifuge, Beckman Model 35 UV/visible spectrophotometer (Beckman Instruments, Fullerton, California); LKB Multiperplex Pump, Ultrorac II fraction collector (LKB, Gaithersburg, Maryland); refractometer (Bausch & Lomb, Rochester, New York).

2. Preparation of reagents

All of the following buffers were prepared in advance and stored at 4°C. All water used was double distilled. 1) Buffer #1, containing 50mM mannitol, 2mM Tris, 0.5mM EDTA, and 3.8mM leupeptin, was prepared by dissolving 9.11 gm mannitol, 244 mg Tris, 146 mg EDTA, and 1.807 gm leupeptin in 990 ml water. The pH was adjusted to 7.0 using HCl, and the volume brought to 1000 ml with water. 2) Buffer #2 contained 50mM mannitol, 2mM Tris, 12mM $MgCl_2$, and 0.5mM EDTA. Mannitol, 9.11 gm, 244 mg Tris, 146 mg EDTA, and 1.02 gm $MgCl_2$ were dissolved in 990 ml water, the pH was adjusted to 7.0 with HCl, and the volume brought to 1000 ml with water. 3) Buffer #3, containing 50mM mannitol, 2mM Tris, and 5mM EDTA, was prepared by dissolving 9.11 gm mannitol, 244 mg Tris, and 1.461 gm EDTA in 990 ml water. The pH and volume were adjusted as for Buffer #1. 4) Buffer #4 contained 50mM mannitol, 2mM HEPES, and 2mM EDTA. This was prepared by dissolving 9.11 gm mannitol, 476.6 mg HEPES, and 292 mg EDTA in 990 ml water. Volume and pH were adjusted as with Buffer #1. 5) Buffer #5, containing 50mM mannitol and 6.9mM HEPES, was prepared by dissolving 9.11 gm mannitol and 1.644 gm HEPES in 990 ml water, then continuing as before. 6) Ninety gm of sucrose was dissolved

in water to make a final volume of 1000 ml, and a resultant 9% sucrose solution. Solutions of 14%, 25%, 50%, and 60% sucrose in water were prepared in similar ways.

3. Preparation of vesicles

Female New Zealand White rabbits, weighing approximately 2.3 kg each, were decapitated and their abdomens opened using surgical scissors. Kidneys were located and perfused with thirty ml each of ice-cold Buffer #1. Kidneys were dissected using a tissue slicer blade, forceps and scissors, and the cortices were removed and weighed. The cortices were placed in a volume of ice-cold Buffer #1 equal to ten times their weight. Cortices were then homogenized in an Omnimixer at #10 setting for ten minutes. The homogenate remained on ice during this procedure to prevent temperature increases during mixing.

The volume of homogenate was measured and solid $MgCl_2$ was added to make a final concentration of 12mM Mg^{2+}. This mixture was stirred magnetically on ice for twenty minutes.

These steps were followed by a series of centrifugations. Figure III-1 shows the scheme for the centrifugation spins. The first was done at 8,000 rpm for 15 minutes in a GSA rotor in a Sorvall centrifuge. The supernatant (S_1) was removed, and the pellet (P_1) was resuspended in Buffer #2, using ten strokes with a Teflon PE homogenizer for each tube. The total volume of buffer used for this step was equal to ten times the original weight of the cortices. The resulting mixture was spun at 3,500 rpm for fifteen minutes, after which the supernatant (S_A) was removed. The pellet (P_A) was resuspended in ten times volume Buffer

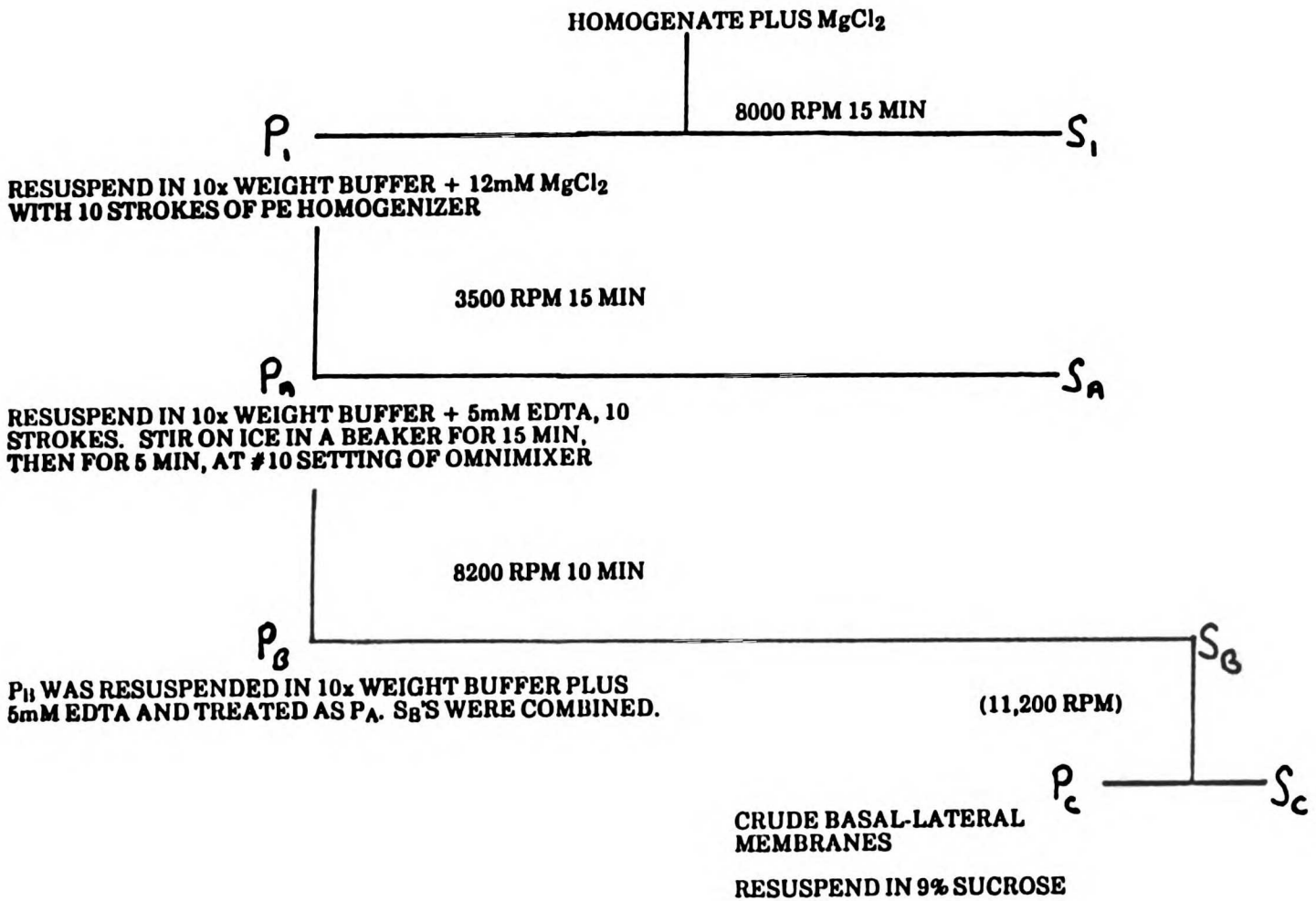

Figure III-1. Centrifugation steps to obtain crude basal-lateral membranes.

#3 in order to complex the Mg^{2+} ion. Each pellet was resuspended by ten strokes with a Teflon PE homogenizer. After resuspension, the contents of all tubes were combined and stirred magnetically on ice for fifteen minutes. This was followed by stirring for an additional five minutes at #10 setting in the Omnimixer.

Following this step, the mixture underwent centrifugation at 8200 rpm for ten minutes, the supernatant (S_B) was removed and saved, and the pellet (P_B) was treated exactly as the previous pellet had been treated. Centrifugation at 8,200 rpm for ten minutes again took place, after which the resulting supernatant (S_B) plus the previously-saved S_B were combined. This suspension was spun at 11,200 rpm for thirty minutes. The supernatant was removed and discarded, and the pellet (P_C) resuspended in thirty ml of 9% sucrose. This resuspension contained the crude basal-lateral membrane vesicles.

At this point a biuret protein assay was performed to determine the protein concentration and yield from the day's preparation. The biuret protein assay is described in Section III.C.3.

In order to further purify the basal-lateral membranes, a step sucrose gradient was used. This was done in a Ti-15 zonal rotor, which is a large, open bucket rotor, in a L5-50B ultracentrifuge. The rotor contained a cross piece which separated the interior into quadrants, and allowed loading and unloading of the rotor from either its center or its outer edge. In order to load or unload material, the rotor needed to be spinning at 2000 rpm. Otherwise, the gradient was disturbed during the loading or unloading procedure.

To prepare the step sucrose gradient, the following solutions were first loaded from the edge:

14% sucrose--400 ml

25% sucrose--150 ml

50% sucrose--approx. 1200 ml

An LKB Multiperplex Pump, with 1:10 gear ratio, was used to load all liquids. The #5 setting was used to load the 25% sucrose and the first 250ml of 50% sucrose. The rest was loaded at #8 setting. The volume of 50% sucrose is listed as approximately 1200 ml because it was used to completely fill the rotor. Its loading was discontinued only when sucrose solution began appearing from the outlet.

Once the rotor was full, the filling assembly was changed to permit loading of solution through the center. First 100 ml of 9% sucrose was loaded, followed by the crude basal-lateral membrane vesicles in 9% sucrose. Finally another 125 ml of 9% sucrose was loaded. All of these additions were made at #5 setting on the Multiperplex pump. The outlet was now at the edge of the rotor, so some of the most dense (50%) sucrose solution was forced out. The purpose of totally filling the rotor previously was to be certain that no large air pockets were inside. If present, air could seriously disturb the gradient and ruin the separation.

After the rotor was loaded, it was spun at 29,000 rpm (55,000xg) for sixty minutes. At the end of this time, the speed was decreased to 2000 rpm and the gradient unloaded. This was done by pumping 60% sucrose into the rotor from the edge. This forced out the contents of the rotor through the center so that the least dense material came out first. This removal was done at #6 setting on the Multiperplex pump.

Twenty ml fractions (equivalent to one minute of unloading time) were collected using a LKB fraction collector.

As fractions were collected, both sucrose and protein concentrations were determined. Sucrose concentration was read as a function of refractive index using a Bausch & Lomb refractometer. Protein concentration was roughly determined by reading the absorbance of each sample at 280 nm on a Beckman UV/visible spectrophotometer. Figure III-2 shows a representative plot of both sucrose concentration and protein concentration versus fraction number. Knowledge of the relationship between Na^+-K^+-ATPase peak location (the enzyme marker for basal-lateral membranes), alkaline phosphatase peak location (brush border membrane enzyme marker) and the sucrose and protein readings was utilized to select those fractions (generally six) which contained the highest concentrations of the most pure basal-lateral membranes. Figure III-2 indicates where the basal-lateral membranes were found. These fractions were combined, and diluted with three times their volume of Buffer #4. This mixture was spun at 11,200 rpm for thirty minutes in a GSA rotor. The supernatant was removed and discarded, and the pellets resuspended, using a disposable pipet, in approximately twelve ml of Buffer #5. The suspension was placed in 1cm x 10cm tubes and stored overnight at 4^oC. The last centrifugation step was at 13,000 rpm for thirty minutes in an SS34 rotor. Upon completion of this spin, the supernatant was removed and the pellet resuspended using a 27 gauge needle and a one ml syringe. No buffer was added for resuspension. Finally, a Bradford protein determination was done. This procedure is described in Section III.C.4.

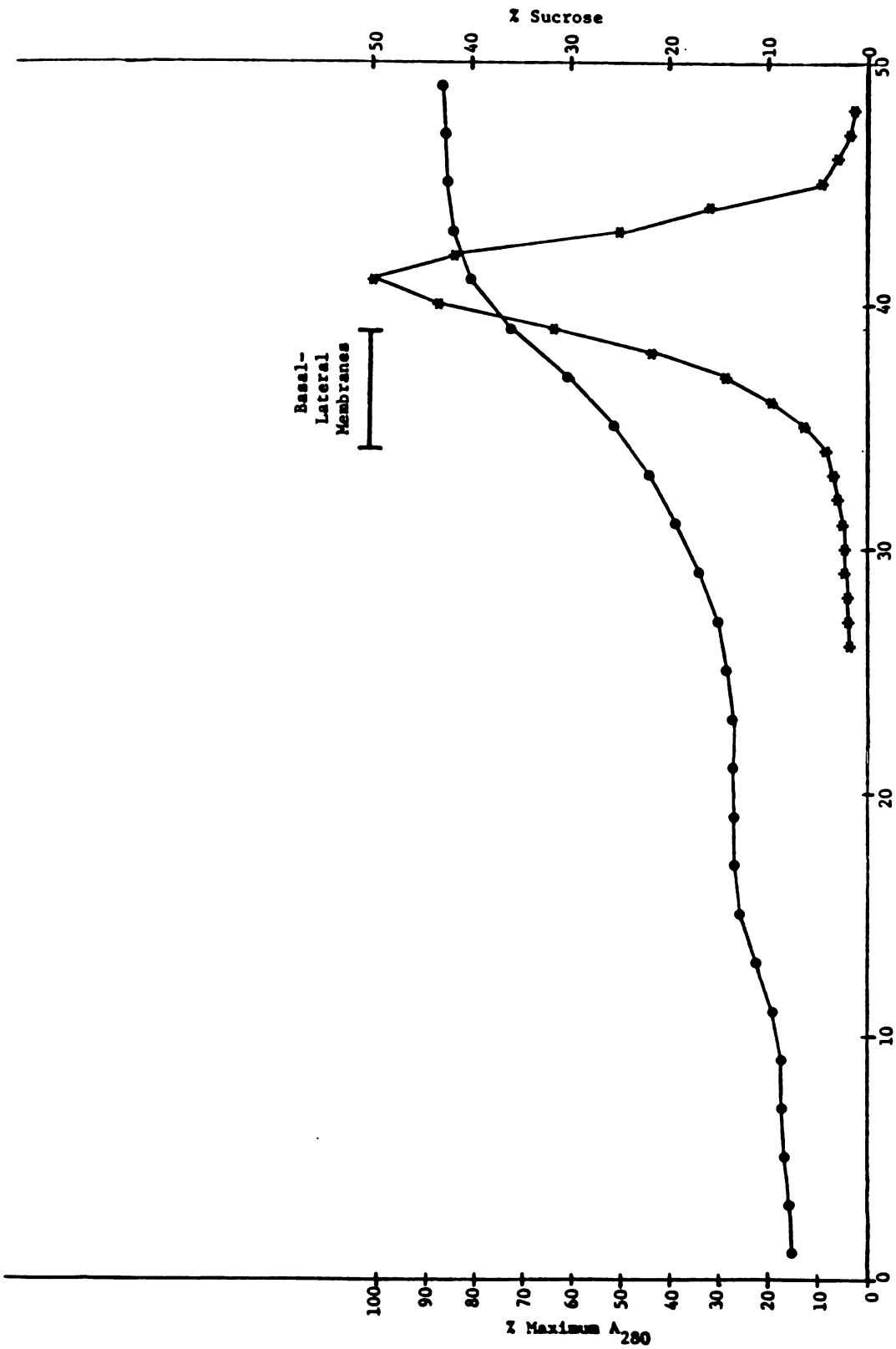

Figure III-2. Plot of % Sucrose and % Maximum A_{280} versus Fraction #.
●—● represents % Sucrose.
— represents % Maximum A_{280}.
Basal-lateral membranes are located in fractions 34-39.

C. Enzyme and protein assays

1. Alkaline phosphatase assay

Alkaline phosphatase is a marker enzyme for brush border membranes. Therefore, this assay was used to determine the presence of brush border membranes in the preparation. The method followed for this assay has been described by Kirk and Prusiner (127).

a. Chemicals and instrumentation

Magnesium chloride, Sodium hydroxide (Mallinckrodt Inc., St. Louis, Missouri); Tris (BDH, Gallard-Schlesinger Chemical Manufacturing Corporation, Carle Place, New York); para-Nitrophenylphosphate (Sigma Chemical Company, St. Louis, Missouri); Hydrochloric acid (Mallinckrodt, Inc., Paris, Kentucky); Neslab water bath (Neslab Instruments, Portsmouth, New Hampshire); GLC-2 centrifuge (Dupont Instruments-Sorvall, Wilmington, Delaware); Gilford sampler (Gilford Instrument Laboratories, Oberlin, Ohio); Beckman UV/visible spectrophotometer (Beckman Instruments, Fullerton, California).

b. Preparation of reagents

Double-distilled water was used for all solutions. 1) A 1M Tris stock solution was prepared by dissolving 122 gm Tris in water to make 1000 ml. 2) A 500mM $MgCl_2$ stock solution was prepared by dissolving 47.5 gm $MgCl_2$ in water to make 1000 ml. 3) A solution of 100mM NaOH was

prepared by dissolving 4 gm NaOH in water to make 1000 ml. Solutions 1-3 were prepared in advance and stored at room temperature. 4) Reaction Solution, containing 100mM Tris, 2.22mM $MgCl_2$, and 10mM p-nitrophenylphosphate, was prepared fresh for each day's use. This solution was prepared by combining 412 mg p-nitrophenylphosphate, 10 ml of 1M Tris stock solution, and 444 µl of 500mM $MgCl_2$ stock solution with 85 ml of water. The pH was adjusted to 9.5, using HCl, and the volume brought to 100 ml using water.

c. Assay procedure

Vesicle samples were diluted from 1/5 to 1/160, using Buffer #5 (See Section III.B.2.). A 0.1 ml diluted vesicle sample was added to 0.9 ml Reaction Solution. Blanks were prepared by adding 2 ml of 100mM NaOH to the Reaction Solution prior to addition of the vesicle sample. Samples and blanks were then incubated at 37°C for 10 minutes in a Neslab water bath. At the end of the incubation, the reaction was stopped by addition of 2 ml of 100mM NaOH to each sample. If a precipitate was present, samples were spun at 2500 rpm for 10 minutes. Absorbance of the supernatant was read at 410nm.

d. Calculations

The alkaline phosphatase activity present in each sample was calculated using Beer's Law:

$$A=abc$$

where A=absorbance (at 410nm in this case)

a=extinction coefficient

b=cell path length

c=concentration of solution

We wished to calculate "c" for each sample. For this instrumentation, b=1. For p-nitrophenol, a=16.2/mM. It was necessary to calculate net absorbance, A, for each sample. Then, c=A/ab.

Net absorbance was calculated by taking the difference between the A_{410} for each sample and the A_{410} for each corresponding blank. Then:

$$\Delta A_{410} \text{ X } 1/\text{dilution of vesicles} = \text{corrected } \Delta A_{410}$$

The reaction was allowed to proceed for ten minutes. Since the total sample volume was 3 ml and 0.1 ml of vesicles were used, the following equation was used to convert corrected ΔA_{410} to µmoles phosphate produced/ml vesicle suspension/min;

$$\text{Corrected } \Delta A_{410} \text{ X } 0.186 = \underline{z} \text{ µmoles phosphate produced/ml vesicle suspension/min}$$

2. Sodium-potassium-ATPase assay

Sodium-potassium-ATPase is the generally-accepted marker for basal-lateral membranes. Measurement of sodium-potassium-ATPase thus provides a measure of the presence of basal-lateral membranes. The method described here has been utilized by Mamelok et al. (200).

a. Chemicals and instrumentation

Sodium chloride, Potassium chloride, Magnesium chloride, Sodium hydroxide, Trichloroacetic acid, Potassium phosphate, monobasic (Mallinckrodt Inc., St. Louis, Missouri); EGTA, Ouabain octahydrate, Ascorbic acid (Sigma Chemical Company, St. Louis, Missouri); Sodium azide (NaN_3), Sulfuric acid (Fisher Scientific, Pittsburgh, Pennsylvania); Tris (BDH, Gallard-Schlesinger Chemical Manufacturing Corporation, Carle Place, New York); Hydrochloric acid (Mallinckrodt Inc., Paris, Kentucky); ATP (CalBiochem-Behring, San Diego, California); Ammonium molybdate (J.T. Baker Chemical Company, Phillipsburg, New Jersey); Neslab waterbath (Neslab Instruments, Portsmouth, New Hampshire); GLC-2 centrifuge (Dupont Instruments-Sorvall, Wilmington, Delaware); Thermolyne Dri-Bath (Sybron/Thermolyne, Dubuque, Iowa); Gilford sampler (Gilford Instrument Laboratories, Oberlin, Ohio); Beckman UV/visible spectrophotometer (Beckman Instruments, Fullerton, California).

b. Preparation of reagents

Stock solutions 1 through 7 were prepared in advance and stored at 4°C. Double-distilled water was used for all solutions. 1) NaCl 1M was prepared by dissolving 58.45 gm of NaCl in water to make 1000 ml. 2) KCl 500mM was prepared by dissolving 37.275 gm KCl in water to make 1000 ml. 3) $MgCl_2$ 500mM was prepared by dissolving 47.5 gm $MgCl_2$ in water to make 1000 ml. 4) EGTA 50mM was prepared by dissolving 19.02 gm EGTA in water to make 1000 ml. 5) NaN_3 100mM was prepared by dissolving 6.502 gm NaN_3 in water to make 1000 ml. 6) Tris 1M was prepared by dissolving 122 gm Tris in water to make 1000 ml. 7) Double-strength assay buffer, in which the compounds were two times their final desired concentrations, contained 112mM NaCl, 16mM KCl, 4.4mM $MgCl_2$, 2.4mM EGTA, and 16mM TRIS. This buffer was prepared by combining 28.0 ml NaCl 1M stock solution, 8.0 ml KCl 500mM stock solution, 2.2 ml $MgCl_2$ 500mM stock solution, 12.0 ml EGTA 50mM stock solution, 5.0 ml NaN_3 100mM stock solution, and 4.0 ml Tris 1M stock solution. The volume was brought to 250 ml with water, and the pH adjusted to 7.4 with HCl. 8) Reaction mix without ouabain contained 10mM ATP in single-strength assay buffer. This was prepared by dissolving 60.52 mg ATP in 5 ml double-strength assay buffer and 4.0 ml water. The pH was adjusted to 7.4, using NaOH, and the volume brought to 10.0 ml, using water. 9) Reaction mix with ouabain contained 10mM ATP and 5mM ouabain in single-strength assay buffer. This was prepared by dissolving 60.52 mg ATP and 36.5 mg ouabain in 5 ml double-strength assay buffer and 4.0 ml water. The pH was adjusted to 7.4, using NaOH, and the volume brought to 10.0 ml with water. Solutions 8 and 9 were made fresh each day. 10) 10% ascorbic

acid, prepared by dissolving 10 gm ascorbic acid in water to make 100 ml, was prepared fresh each day. 11) Ammonium molybdate 0.42% in 1N H_2SO_4 was prepared by dissolving 2.1 gm ammonium molybdate in 14 ml of concentrated sulfuric acid and enough water to bring the volume to 500 ml. This solution was prepared in advance and stored at room temperature. 12) Ames Reagent was required and was prepared by combining 1 part solution 10 with 6 parts solution 11. This was prepared fresh each day. 13) A 10% TCA solution was also required for this assay and was prepared by dissolving 100 gm TCA in water to make 1000 ml. This was prepared ahead of time and stored at room temperature. 14) A standard solution of 0.64μM K_3PO_4 was prepared by dissolving 136 μg K_3PO_4 in water to make 1000 ml. Serial dilutions provided solutions of 0.32, 0.16, 0.08, and 0.04 μM K_3PO_4 for standard curves. These solutions were prepared in advance and stored at 4°C.

c. Assay procedure

Vesicle samples were diluted from 1/100 to 1/1600 with Buffer #5 (see Section III.B.2.). Three hundred μl of appropriately-diluted vesicles was combined with 200 μl of reaction mix with ouabain, and another 300 μl of the same vesicle dilution was combined with 200 μl of reaction mix without ouabain. Each sample was processed both with and without ouabain in order to separate sodium-potassium ATPase activity from other types of ATPase activity.

Samples were vortexed and incubated at 37°C for ten minutes in a water bath. The reaction was stopped by adding 500 μl of ice-cold 10% TCA solution and then placing the tube on ice for at least fifteen

minutes. Samples were next spun at 3000 rpm for fifteen minutes at 4°C.

Next, 800 µl of sample supernatant was combined with 1,600 µl Ames Reagent. These samples were incubated at 45°C for five minutes using a Thermolyne Dri-Bath. The reaction was stopped by placing the tubes on ice. Once the samples had cooled to room temperature, the A_{660} was read for each.

A standard curve was prepared for each experiment by combining either 200 µl standard K_3PO_4 solution or 200 µl d.d. water with 100 µl assay buffer (single strength), 200 µl of either reaction mix, and 500 µl ice-cold 10% TCA solution. Eight hundred µl of the resulting mixture was combined with 1,600 µl Ames Reagent. Standards were incubated for five minutes at 45°C, then placed on ice. A_{660} was read for each sample.

d. Calculations

For each standard, the difference between its A_{660} and the A_{660} obtained for water was determined. The difference was the standard's ΔA_{660}. The nmoles of phosphate present in each standard was determined by multiplying the concentration of K_3PO_4 in the standard solution by the volume used for assay (200 µl). Next, ΔA_{660} was plotted as a function of nmoles phosphate present.

For each vesicle sample ΔA_{660} was determined. This is the difference between the A_{660} for the tube not containing ouabain and the A_{660} for the tube which did contain ouabain. Using the standard curve, the amount of phosphate present in each sample was determined. This was the amount of phosphate (in nmoles) produced by the sodium-potassium-

ATPase in the sample over ten minutes.

A 0.3 ml vesicle sample was used for each assay, so the amount of phosphate produced was divided by 0.3 to obtain the amount of phosphate per ml of sample. Correction for dilution of the vesicle sample was done by dividing the nmoles phosphate produced by the dilution factor (i.e., divide by 1/100). Next, this value was divided by ten minutes to obtain the answer in units of nmoles phosphate produced/ml vesicle sample/minute. In summary,

nmoles phosphate produced / 3 / dilution factor =

z nmoles phosphate produced/ml vesicle preparation/min.

3. Biuret protein assay

This protein assay was used for protein determinations prior to loading the sucrose gradient. The method utilized for this assay has been described by Gornall et al. (201).

a. Chemicals and instrumentation

Bovine serum albumin (BSA, Fraction V) (Pentex Biochemicals, Kankakee, Illinois); Copper sulfate (Mallinckrodt Inc., St. Louis, Missouri); Sodium potassium tartrate (J.T. Baker Chemical Company, Phillipsburg, New Jersey); Sodium hydroxide (Mallinckrodt Inc., Paris, Kentucky); Gilford sampler (Gilford Instrument Laboratories, Inc., Oberlin, Ohio); Beckman UV/visible spectrophotometer (Beckman Instruments, Fullerton, California).

b. Preparation of reagents

Double-distilled water was used for all solutions. 1) BSA stock solution, 1.0 mg/ml in water, was prepared by dissolving 25 mg BSA in water to make 25 ml. This solution was prepared in advance and stored at -20°C. 2) A 10% sodium hydroxide solution was prepared in advance, by dissolving 100 gm NaOH in water to make 100 ml, and stored at room temperature. 3) Biuret Reagent was prepared by weighing 1.50 gm copper sulfate and 6.00 gm sodium potassium tartrate. These solids were dissolved in 500 ml water. Three hundred ml of 10% sodium hydroxide solution was added with constant swirling. The volume was brought to 1,000 ml with water, and the solution was mixed. This reagent may be stored indefinitely at room temperature. It should be dark blue in color.

c. Assay procedure

A standard curve was prepared by placing 0, 0.5, 0.75, 1.0, 1.25, and 1.5 ml of BSA stock solution into six respective test tubes. The volume in each tube was brought to 1.5 ml using d.d. water. Sample test tubes were prepared containing 20 µl of vesicle preparation and d.d. water to make a final volume of 1.5 ml. All vesicle preparation assays were run in duplicate. 1.5 ml of Biuret Reagent was added to each tube, and the tubes were placed in boiling water for twenty seconds. Tubes were placed on ice at the end of the incubation in order to stop the reaction. A_{540} was read for each sample.

d. Calculations

For each standard curve sample, ΔA_{540} was determined by subtracting A_{540} for the water sample from A_{540} for the BSA standard sample. The amount of BSA present was calculated as the original BSA concentration times the volume of BSA standard solution used. A plot of ΔA_{540} versus amount protein present was prepared. ΔA_{540} for each vesicle sample was also calculated (A_{540} for vesicle sample minus A_{540} for water sample), and the standard curve was used to determine the amount of protein in each vesicle sample. Each sample contained a 20 µl vesicle sample. Therefore:

protein/sample / 0.020 ml = protein/ml of vesicle preparation.

4. Bradford protein assay

The Bradford protein assay has been described by Bradford (202). It is a more accurate protein assay than the biuret assay. However, it takes longer, and therefore was only used for protein determinations of the final basal-lateral preparation from the sucrose density gradient.

a. Chemicals and instrumentation

Coomassie Brilliant Blue G-250, Bovine serum albumin (BSA, Fraction V) (Sigma Chemical Company, St. Louis, Missouri); Ethanol (95%) (Gold Shield Chemical Company, Hayward, California); Phosphoric acid (85%) (J.T. Baker Chemical Company, Phillipsburg, New Jersey); Whatman Number

1 filter paper (Whatman Inc., Clifton, New Jersey); instrumentation as previously described.

b. Preparation of reagents

1) BSA stock solution (1 mg/ml) was prepared by dissolving 25 mg BSA in d.d. water to make 25 ml. This solution was prepared in advance and stored at -20°C. 2) Bradford Protein Dye Reagent was prepared by completely dissolving 100 mg Coomassie Brilliant Blue G-250 in 50 ml of 95% ethanol. To this solution, 100 ml of 85% (w/v) phosphoric acid was added. The solution's volume was brought to 1 liter using d.d. water, giving a final concentration of 0.01% (w/v) Coomassie Brilliant Blue G-250, 4.7% (w/v) ethanol, and 8.5% (w/v) phosphoric acid. The solution was filtered twice using Whatman Number 1 filter paper, and stored at room temperature.

c. Assay procedure

A standard curve was prepared by placing 0, 10, 20, 30, 40, and 50 µl of BSA (1mg/ml) stock solution in six respective test tubes. The volume in each tube was brought to 0.1 ml using d.d. water. For vesicle samples, 10 µl of sample was diluted to 100 µl with d.d. water. Ten µl of this dilution was then combined with 90 µl d.d. water to provide a sample for assay. Each dilution was assayed in duplicate.

To each standard and sample, five ml of Bradford Protein Dye Reagent was added and the mixture was vortexed. Samples were allowed to stand at room temperature for at least two minutes, but not more than

one hour, prior to reading A_{595}.

d. Calculations

For each standard curve sample, ΔA_{595} was determined by subtracting A_{595} for the blank (water) sample from A_{595} for each standard. The amount of protein present was calculated by multiplying the concentration of BSA stock solution by the volume of stock solution used. A standard curve of ΔA_{595} as a function of amount of protein present was prepared.

For each vesicle sample, ΔA_{595} was determined by subtracting A_{595} for the blank sample from A_{595} for the vesicle sample. Using the standard curve, the corresponding protein content was determined for each ΔA_{595}. The dilution factor used was 1/10, and 10 µl of our diluted vesicle sample was used for each assay, so that 1 µl of undiluted vesicle preparation was assayed in each sample. Therefore:

protein/sample X 1000 = protein/ml vesicle preparation

D. Methods of transport studies

This transport study method has been described in the literature by Tse et al. (93). The general method will be described first, followed by modifications for several types of experiments.

1. General method

a. Chemicals and instrumentation

Mannitol, Tris, PAH, Furosemide, Probenecid (Sigma Chemical Company, St. Louis, Missouri); Hydrochloric acid (J.T. Baker Chemical Company, Phillipsburg, New Jersey); ^{3}H-PAH, ACS (aqueous counting scintillant) (Amersham Corporation, Arlington, Illinois); ^{3}H-Furosemide (New England Nuclear, Boston, Massachusetts); Thelco waterbath, Model 86 (Precision Scientific, Chicago, Illinois); Gelman glass fiber filters, Type A/E (Gelman Sciences, Ann Arbor, Michigan); Hoefer vacuum filtration assembly (Hoefer Scientific Instruments, San Francisco, California).

b. Preparation of reagents

All water used was double-distilled. All reagents were prepared in advance and stored at 4^{o}C unless otherwise stated. 1) Tris was prepared as a 1M solution by dissolving 122 gm Tris in water to make 1000 ml. This solution was made in advance and stored at room temperature. 2) Solution #1, which contained 50mM mannitol and 6.9mM Tris, was prepared by dissolving 9.11 gm mannitol and 841.8 mg Tris in 990 ml water. The pH was adjusted to 7.0 using HCl and the volume brought to 1000 ml with water. 3) Buffer containing 50mM mannitol and 150mM Tris was prepared by dissolving 9.11 gm mannitol and 18.3 gm Tris in 990 ml water, adjusting the pH to 7.0 using HCl, and bringing the volume to 1000 ml with water. 4) Stop Mix, containing 50mM mannitol and 2mM Tris, was

prepared by dissolving 9.11 gm mannitol and 244 mg Tris in 990 ml water, adjusting the pH to 7.0 with HCl and adjusting the volume to 1000 ml with water. 5) Probenecid, 50mM in 50mM mannitol and 69mM Tris, was prepared by dissolving 142.68 mg probenecid, 91.1 mg mannitol, and 84.2 mg Tris in 9 ml water. The pH was adjusted to 7.0 using HCl and the volume brought to 10 ml with water. 6) Furosemide, 6mM, was prepared by dissolving 99.23 mg furosemide in 45 ml of Solution #1. Additional Tris was required for this dissolution, so Tris, as a 1M stock solution, was added, bringing the final Tris concentration to 16mM. The pH was adjusted to 7.0, using HCl, and the volume brought to 50 ml, using Solution #1. This solution was prepared up to several weeks in advance and stored at $4^{o}C$. 7) Furosemide, 1.2mM, was prepared by diluting 1 ml of Furosemide 6mM Solution with 4 ml of Solution #1. This dilution was generally done on the day of the experiment. 8). PAH, 14.56 mg, was dissolved in 9 ml of Solution #1 to make a 7.5mM PAH solution. The pH was adjusted to 7.0 with HCl, and the volume brought to 10 ml with Solution #1. 9) PAH, 6mM and 1.2mM in Solution #1 were prepared by diluting 4 ml of PAH 7.5mM in Solution #1 with 1 ml of Solution #1 to make the 6mM solution. This was further diluted to 1.2mM by combining 1 ml of PAH 6mM solution with 4 ml of Solution #1. These solutions were generally prepared on the day of use. 10) ^{3}H-Furosemide was purified as described in Section V.C. It was never purified more than nine days in advance of an experiment, and was kept in a dried form at $4^{o}C$ after purification and prior to use. 11) ^{3}H-PAH was purchased in powdered form from Amersham. It was dissolved in Solution #1 to make a 1mM PAH concentration. The specific activity of the radiolabelled PAH was generally around 250 mCi/mmole. This solution was prepared up to one

month in advance and stored at 4°C. 12) Magnesium chloride, 100mM in Solution #1, was prepared by dissolving 476 mg $MgCl_2$ in 50 ml Solution #1. 13) ^{3}H-PAH solution, containing 0.75mM PAH in Solution #1, contained both tritiated and "cold" PAH, and was prepared fresh for each day's experiment. The volume of 0.75mM PAH solution required (at 8 µl/sample) was determined for a particular experiment. From this, the molar quantity of PAH needed was calculated, and either 1/6 or 1/4 of this amount was contributed in the form of ^{3}H-PAH, as the 1mM solution. The rest of the PAH required was added as the 7.5mM "cold" solution. The volumes contributed by the addition of "cold" and tritiated PAH were determined and subtracted from the total volume of 0.75mM PAH solution needed. Solution #1 was used to bring the ^{3}H-PAH solution to volume. A volume of 100mM $MgCl_2$ in Solution #1, equal to 3 µl/sample, was added to the ^{3}H-PAH solution. This brought the volume to 11 µl/sample, and provided a PAH concentration of 0.55mM. 14) To prepare ^{3}H-furosemide solution for an experiment, the amount of ^{3}H-furosemide (in powder form) available for that day's experiment was determined. Five µl aliquots of purified ^{3}H-furosemide solution had been counted prior to drying. By correcting for quenching and using the total volume present before evaporation of the purified ^{3}H-furosemide solution, the amount of ^{3}H-furosemide available was calculated. The total amount of furosemide needed for that day's samples was calculated (0.75mM furosemide solution, 8 µl/sample), and consequently the amount of "cold" furosemide necessary was determined. This was added as 6.0mM Furosemide Solution. The volume was brought to 8 µl/sample, using Solution #1. Excess Tris present from purification of ^{3}H-furosemide and solubilization of 6mM furosemide in Solution #1 was determined to

increase the Tris present by a maximum of 2.2% over the usual concentration. This was considered an insignificant increase and consequently no change was made in the components of the buffers used in these experiments. A volume of 100mM $MgCl_2$ in Solution #1, equal to 3 µl/sample, was added to the ^{3}H-furosemide solution, giving a final volume of 11 µl/sample and a 0.55mM furosemide concentration.

c. Experimental procedures

For each experiment, the protein concentration in the vesicle preparation was determined using a Bradford protein assay. Vesicles were then diluted to between 8 and 13 mg protein/ml, using Solution #1.

Each sample was prepared by combining different volumes of some of the solutions described above. Tables III-1 and III-2 show the solutions and volumes combined for each type of sample in the ^{3}H-PAH (Table III-1) and ^{3}H-furosemide (Table III-2) experiments. Each type of sample was prepared in quadruplicate for each time point. Fractions 1, 2, 3, and 6 were always preincubated for thirty minutes in a 37°C waterbath. Fractions 4 and 5 were sometimes included in this preincubation. In other experiments, these fractions were not included in the preincubation (see Sections VI.B.2. and VI.C.3.)

At t = 0 for each sample, 11 µl of Fraction 7 was added to the test tube. The sample was mixed rapidly on a vortex mixer, and replaced in the 37°C waterbath. Samples were incubated for times ranging from 5 seconds to 1 hour. For samples allowed to incubate only 5 seconds, the tube was not placed in the waterbath again; rather, it was held for the several seconds after mixing. At the end of the incubation time for

TABLE III-1. COMPONENTS OF SAMPLES FOR ^{3}H-PAH UPTAKE STUDIES.

Fraction # (Solutions to be combined)	Volume (µl) per Sample				
	Types of Samples				
	^{3}H-PAH 0.1mM alone	^{3}H-PAH + Probenecid 6.67mM	^{3}H-PAH + Furosemide 0.1mM	^{3}H-PAH + Furosemide 0.5mM	^{3}H-PAH + Furosemide 1.0mM
#1 (50mM mannitol, 6.9mM Tris, pH 7.0)	20	16	15	15	10
#2 (50mM mannitol, 150mM Tris, pH 7.0)	20	16	20	20	20
#3 (Probenecid 50mM in 50mM mannitol, 69mM Tris, pH 7.0)	—	8	—	—	—
#4 (Furosemide 1.2mM in Solution #1)	—	—	5	—	—
#5 (Furosemide 6.0mM in Solution #1)	—	—	—	5	10
#6 (Vesicles 8-13mg/ml in Solution #1)	9	9	9	9	9
#7 (^{3}H-PAH 0.55mM and $MgCl_2$ 27.3mM in Solution #1)	11	11	11	11	11
Total volume per sample (µl)	60	60	60	60	60

TABLE III-2. COMPONENTS OF SAMPLES FOR ^{3}H-FUROSEMIDE UPTAKE STUDIES.

Fraction # (Solutions to be Combined)	Volume (µl) per Sample — Types of Samples				
	^{3}H-Furosemide 0.1mM alone	^{3}H-Furosemide + Probenecid 6.67mM	^{3}H-Furosemide + PAH 0.1mM	^{3}H-Furosemide + PAH 0.5mM	^{3}H-Furosemide + PAH 1.0mM
#1 (50mM mannitol, 6.9mM Tris, pH 7.0)	20	16	15	15	10
#2 (50mM mannitol, 150mM Tris, pH 7.0)	20	16	20	20	20
#3 (Probenecid 6.67mM in 50mM mannitol, 69 mM Tris, pH 7.0)	—	8	—	—	—
#4 (PAH 1.2mM in Solution #1)	—	—	5	—	—
#5 (PAH 6mM in Solution #1)	—	—	—	5	10
#6 (Vesicles 8-13mg/ml in Solution #1)	9	9	9	9	9
#7 (^{3}H-furosemide 0.55mM + $MgCl_2$ 27.3mM in Solution #1)	11	11	11	11	11
Total Volume per sample (µl)	60	60	60	60	60

each sample three ml of ice-cold Stop Mix was added. The sample was then removed from the test tube, using a disposable pipet, and filtered on a Gelman glass fiber filter, positioned on a Hoefer vacuum filtration assembly. The filter was washed twice with three ml of Stop Mix, after which the filter was removed and placed in 10ml of ACS for scintillation counting. After removal of a used filter, the filter support was washed with d.d. water prior to the placement of a fresh filter.

d. Calculations

The first step in converting cpm into uptake of PAH (or furosemide) was to determine what portion of the PAH was associated with the filter, and was not actually associated with the vesicles. The cpm values obtained from samples containing no vesicles were averaged, and this average value was subtracted from the cpm value for each sample containing vesicles, giving a Δcpm value for each sample.

Due to quenching, cpm values did not equal dpm values. However, because quenching was quite constant from sample to sample, cpm were not converted to dpm.

Next, the specific activity of the ^{3}H-PAH solution was determined. By measuring the cpm value for each of the two or more aliquots of ^{3}H-PAH solution (x), and knowing the total PAH concentration (z) in the solution and the volume per aliquot (y), the specific activity (a), in cpm/pmoles PAH, was calculated as follows:

$$\underline{x} \text{ cpm} / \underline{y} \text{ µl} / \underline{z} \text{ mM PAH} / 1000 = \underline{a} \text{ cpm/pmole PAH}$$

The protein content (d) of each sample was also determined. The volume of vesicle suspension (b) added to each sample was multiplied by the protein concentration of the vesicle suspension (c) as follows:

$$\underline{b}\ \mu l \times \underline{c}\ \text{mg protein/1000 } \mu l \text{ vesicles} = \underline{d}\ \text{mg protein/sample}$$

Finally:

$$\Delta\text{cpm/sample} / \underline{a}\ \text{cpm/pmole PAH} / \underline{d}\ \text{mg protein/sample} = \underline{e}\ \text{pmole PAH/mg protein}$$

A plot of pmole PAH/mg protein versus incubation time was prepared utilizing these results. This same series of calculations was used to determine furosemide uptake.

2. Modifications for binding experiments

a. Chemicals and instrumentation

Sucrose (J.T. Baker Chemical Company, Phillipsburg, New Jersey); Sulfisoxazole (Sigma Chemical Company, St. Louis, Missouri); others as previously detailed.

b. Preparation of reagents

All solutions were prepared in advance and stored at $4^{o}C$ unless otherwise described. 1) Sucrose 2M in Solution #1 was prepared by

dissolving 34.23 gm sucrose in 50 ml Solution #1. 2) Sulfisoxazole, 6mM in Solution #1 was prepared by dissolving 48.1 mg sulfisoxazole in 30 ml Solution #1. This buffer was diluted to 0.1mM sulfisoxazole by combining 1 part 6mM sulfisoxazole in Solution #1 with 59 parts Solution #1. 3) Buffer containing 50mM mannitol and 69mM Tris was prepared by dissolving 9.11 gm mannitol and 8.42 gm Tris in 990 ml water. The pH was adjusted to 7.0 using HCl, and the volume brought to 1000 ml using water. Other solutions were prepared as previously described.

c. Experimental procedures

For these studies, samples were needed with concentrations of sucrose ranging from 0 to 1.06M. Table III-3 shows the buffer components and volumes added to prepare each type of sample. Vesicles were diluted to 8-13 mg protein/ml, as before. The first five sample components were combined and incubated for at least 15 minutes at 37°C. The ^{3}H-furosemide was then added, samples were incubated for either 15 seconds or 1 hour, and transport was stopped and measured in the usual manner.

In some experiments, a portion of the vesicles was incubated in the 0.1mM sulfisoxazole in Solution #1 overnight, at 4°C, prior to the last centrifugation step. The rest of the vesicles were left in Buffer #5 (see Section III.B.2.) at 4°C. Both vesicle fractions were then pelleted and used in the usual manner for these experiments.

TABLE III-3. COMPONENTS OF SAMPLES FOR ^{3}H-FUROSEMIDE BINDING EXPERIMENTS.

Sample Type	Solutions to be Combined (µl per sample)					
	Solution #1 (Mannitol 50mM Tris 6.9mM pH 7.0)	Sucrose 2M in Solution #1	Mannitol 50mM Tris 69mM pH 7.0	Probenecid in Mannitol 50mM, Tris 69mM, pH 7.0	Vesicles 8-13mg/ml in Solution #1	^{3}H-Furosemide 0.55mM + $MgCl_2$ 27.3mM in Solution #1
No Sucrose	32	—	8	—	9	11
No Sucrose + Probenecid	32	—	—	8	9	11
Sucrose 0.05M	29	3[a]	8	—	9	11
Sucrose 0.05M + Probenecid	29	3[a]	—	8	9	11
Sucrose 0.1M	26	6[a]	8	—	9	11
Sucrose 0.1M + Probenecid	26	6[a]	—	8	9	11
Sucrose 0.2M	26	6	8	—	9	11
Sucrose 0.2M + Probenecid	26	6	—	8	9	11
Sucrose 0.3M	23	9	8	—	9	11
Sucrose 0.3M + Probenecid	23	9	—	8	9	11
Sucrose 0.5M	17	15	8	—	9	11
Sucrose 0.5M + Probenecid	17	15	—	8	9	11
Sucrose 0.7M	11	21	8	—	9	11
Sucrose 0.7M + Probenecid	11	21	—	8	9	11
Sucrose 1.06M	—	32	8	—	9	11
Sucrose 1.06M + Probenecid	—	32	—	8	9	11

[a]Sucrose 2M was diluted to Sucrose 1M with Solution #1 for addition to these samples.

d. Calculations

There were no changes in the calculations used to determine uptake of ^{3}H-furosemide in these experiments. Total osmolarity of each sample was determined by summing the moles of components present per sample, and dividing by the sample volume. Plots of pmole furosemide/ mg protein versus 1/total osmolarity of the sample were prepared from these experimental results.

3. Modifications for counter-transport studies

a. Chemicals and instrumentation

Chemicals and instrumentation used were previously described in Section III.A.1.

b. Preparation of reagents

1) Furosemide 0.1mM in Solution #1 was prepared by diluting 1 part 6mM furosemide in Solution #1 with 59 parts Solution #1. This was prepared not more than two weeks prior to its use and stored at 4^{o}C. 2) PAH 0.1mM in Solution #1 was prepared by diluting 1 part 7.5mM PAH in Solution #1 with 74 parts Solution #1. This was prepared not more than two weeks prior to use and stored at 4^{o}C. Other solutions were prepared as previously described.

c. Experimental procedures

In order to allow vesicles time to equilibrate with the counter-transport ion, one of the two above-mentioned buffers was used in place of Buffer #5 (see Section III.B.3.) for resuspension of the appropriate pellet. For each experiment, some vesicles were resuspended in Buffer #5 to serve as controls. These mixtures were allowed to stand overnight at $4^{o}C$. The following morning, the final spin was done, the supernatants removed, and the vesicles resuspended with no addition of buffer. Table III-4 shows the components and the volumes added for the types of samples used in these studies. The addition of radiolabelled compound, incubation, stopping of transport, and measurement of uptake was done in the manner previously described.

d. Calculations

There were no changes in the methods of calculating ^{3}H-PAH or ^{3}H-furosemide uptake from previous studies.

TABLE III-4. COMPONENTS OF SAMPLES FOR COUNTER-TRANSPORT STUDIES.

Sample Type	Solutions to be Combined (µl per sample)					
	Solution #1 (Mannitol 50mM Tris 6.9mM pH 7.0)	Mannitol 50mM Tris 150mM pH 7.0	Probenecid 50mM in Mannitol 50mM Tris 69mM pH 7.0	Vesicles 8-13mg/ml in Solution #1	Vesicles pre-incubated in counter-transport ion 0.1mM in Solution #1	^{3}H-transport ion 0.55mM + $MgCl_2$ 27.3mM in Solution #1
^{3}H-transport ion 0.1mM alone	20	20	—	9	—	11
^{3}H-transport ion 0.1mM + Probenecid 6.67mM	16	16	8	9	—	11
^{3}H-transport ion 0.1mM in vesicles containing countertransport ion	20	20	—	—	9	11

CHAPTER IV

EXPERIMENTAL METHODS FOR RENAL CLEARANCE STUDIES

A. Animal set-up

In order to measure renal clearance of an exogenous compound, the animal must be prepared to allow intravenous administration of the compound, collection of blood from a different vessel, and total collection of urine over a specified period of time. A number of techniques have been developed to do this. These include use of the carotid artery (203,204) or femoral artery (204-206) for collection of blood; catheterization of the jugular vein (203,204) or femoral vein (204-206) for administration of drug; and catheterization of the bladder (203), catheterization of the ureter (204), collection from the male rat penis (205) or cannulation of the bladder (206) for urine collection. The method used in these studies was described by Till (206) in her dissertation, and will be described here in similar detail.

1. Preparation for surgery

Male Sprague-Dawley rats weighing 205 gm to 506 gm were used in these experiments. Animals were kept in the Animal Care Facility at UCSF prior to surgery, and were not fasted. To anesthetize these animals for surgery, Pentobarbital Sodium Solution, 64.8 mg/ml (Fort Dodge Laboratories, Inc., Fort Dodge, Iowa) was administered intraperitoneally at a dose of 60 mg/kg. The use of pentobarbital as anesthetic in these experiments will be discussed in Section VII.A.

2. Surgical procedure for venous and arterial cannulation

a. Materials

Intramedic® non-radiopaque polyethylene tubing, PE-50, I.D. 0.023", O.D. 0.038" (Clay Adams, Parsippany, New Jersey); Monoject sterile disposable syringe, 6 cc; Monoject disposable hypodermic needles 23 gauge, 1 inch (Sherwood Medical Industries, Inc., Deland, Florida); 4-0 cotton suture (Ethicon Inc., Somerville, New Jersey); Sodium heparin injection (Liquaemin® Sodium 1,000 USP units/ml) (Organon, West Orange, New Jersey); Bacteriostatic sodium chloride injection, USP (normal saline solution) (Invenex, Chagrin Falls, Ohio).

b. Methods

Once anesthesia had been induced, rats were fastened to a temperature-controlled small animal operating table. Vascular cannulas were prepared in advance by the following procedure. Two 6 cc syringes, fitted with 23 gauge needles, were internally rinsed with 0.5 ml of sodium heparin solution, and the excess solution expelled. Each syringe was then filled with normal saline solution. Each needle was fitted with twelve to fifteen inches of PE-50 tubing and the end of the tubing was beveled to make insertion into the blood vessel easier. Finally the tubing was flushed with the solution in the syringes. This was done to prevent clotting in the tubing during the experiment.

Using scissors, a small (1.5-2 cm) incision was made in the skin of the right groin area. Forceps were used to expose the femoral artery

and vein. The vessels were cleaned of fascia using blunt curved forceps and were then separated.

In order to cannulate the vein, two ligatures were first placed around the vein---one at the proximal end and one at the distal end of the exposed vessel. The ligature at the distal end was tied tightly. This prevented excessive bleeding once the vessel had been cut. The ends of this ligature were taped to the table, in order to keep the vein taut and to facilitate cannulation. Iris scissors were used to make a small cut in the vein. The catheter entered the vein through this cut, and was moved into the vein until its end was past the proximal ligature. The ligatures were then tied tightly around the vein and the catheter, thus holding the catheter in place.

The artery was cannulated next. Again, ligatures were positioned at the proximal and distal ends of the exposed artery segment--however, neither of them was tied tightly at this point. The artery was clamped just before the proximal ligature, using a small artery forceps. A small cut was made in the artery, the catheter inserted and eased into the vessel up to the artery forceps. While holding the cannula in place with curved, blunt forceps, the artery forceps was removed, and the catheter was then moved a short distance further into the artery. Both ligatures were then tied tightly around the catheter and artery. A saline-soaked gauze pad was placed over the exposed vessels.

3. Surgical procedure for cannulation of the bladder

a. Materials

Intramedic® non-radiopaque polyethylene tubing, PE-90, I.D. 0.034", O.D. 0.050" (Clay Adams, Parsippany, New Jersey); Ferguson needle, 1/2 circle, taper point (The Torrington Company, Torrington, Connecticut); Monoject sterile disposable tuberculin syringe, 1 cc; Monoject hypodermic needle, 25 gauge, 5/8" (Sherwood Medical Industries, Inc., Deland, Florida). Other materials as previously described.

b. Methods

Using scissors, a slightly-to-the-right-of-midline incision was made in the same rat's abdomen. The bladder was exposed, and first drained of urine, using a 1 cc disposable syringe with a 25 gauge needle. Using a 1/2 circle taper point needle and 4-0 cotton suture, a purse-string suture was placed about 0.5 cm from the apex of the bladder. A small cut was made in the center of the sutured area, using iris scissors. A three inch piece of PE-90 tubing was placed in the bladder and tied tightly, using the purse-string suture. The end of the tubing placed in the bladder had been flanged earlier (by touching it to a heated hot plate), and this flange helped to keep the cannula from sliding out of the bladder incision. A saline-soaked gauze pad was then placed over the bladder.

4. Tracheotomy

Some animals showed signs of respiratory distress. In these animals, a tracheotomy was performed. An incision was made in the neck skin, using scissors, and the trachea exposed. A piece of 4-0 cotton suture was placed around the lower end of the exposed trachea, after which a small incision was made in the trachea, using iris scissors. A short (5 cm) piece of PE-205 tubing (Intramedic® non-radiopaque polyethylene tubing, PE-205, I.D. 0.062", O.D. 0.082"; Clay Adams, Parsippany, New Jersey) was inserted, and the previously-positioned suture used to tie it in place.

5. Maintenance

Figure IV-1 is a drawing of the rat surgical set-up. Figure IV-2 is a photograph of a representative experimental rat. The rat was kept on the operating table for the entire experiment. In order to maintain the body temperature of the rat at 37±0.5°C during an experiment, the following set-up was used. A rectal probe (YSI Model 402 small flexible vinyl rectal probe, Yellow Springs Instrument Company, Inc., Yellow Springs, Ohio) monitored the rat's body temperature. This probe was connected to a temperature control unit (YSI Model 73 ATD indicating controller, Yellow Springs Instrument Company, Inc., Yellow Springs, Ohio), which was connected to the heating element in the operating table, through a variable autotransformer (Staco, Inc., Dayton, Ohio). Anesthesia was maintained in the rat by giving 30 mg/kg sodium pentobarbital intraperitoneally as needed (approximately every hour).

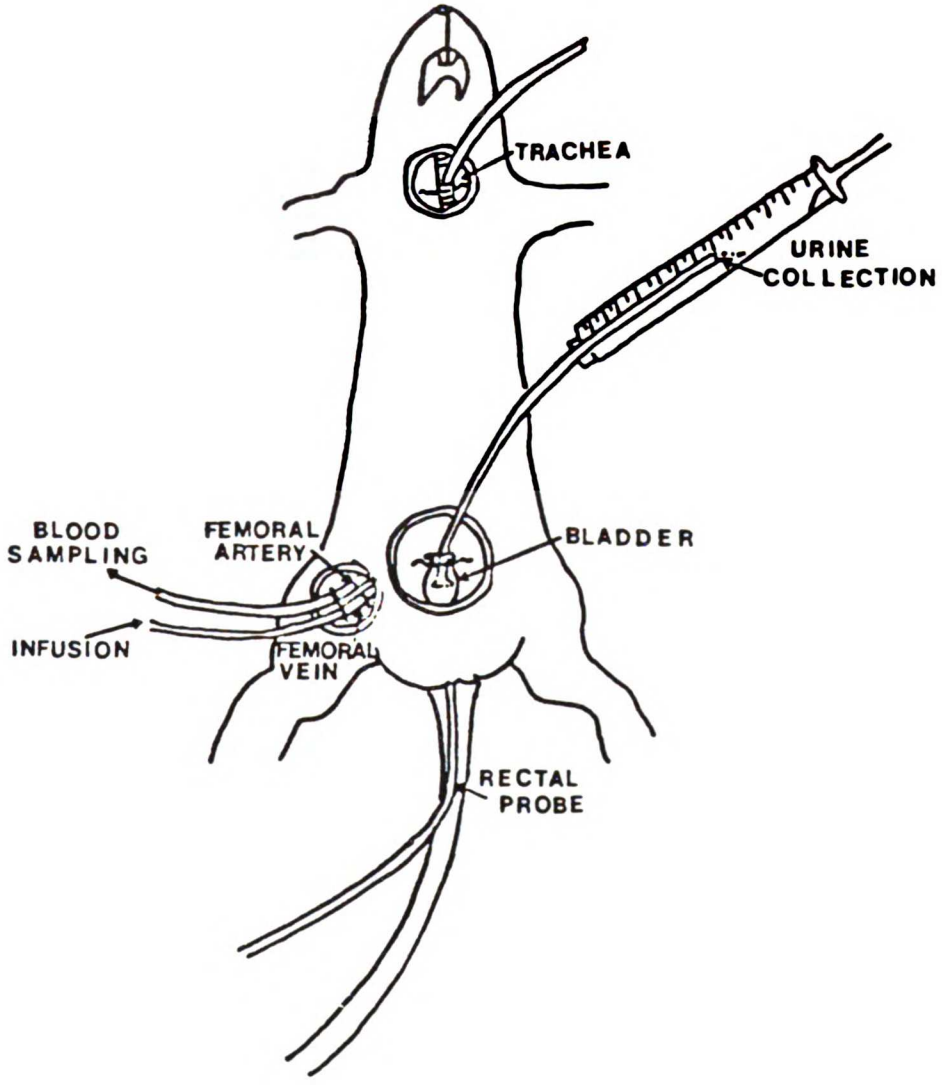

Figure IV-1. Schematic representation of rat surgical set-up (206).

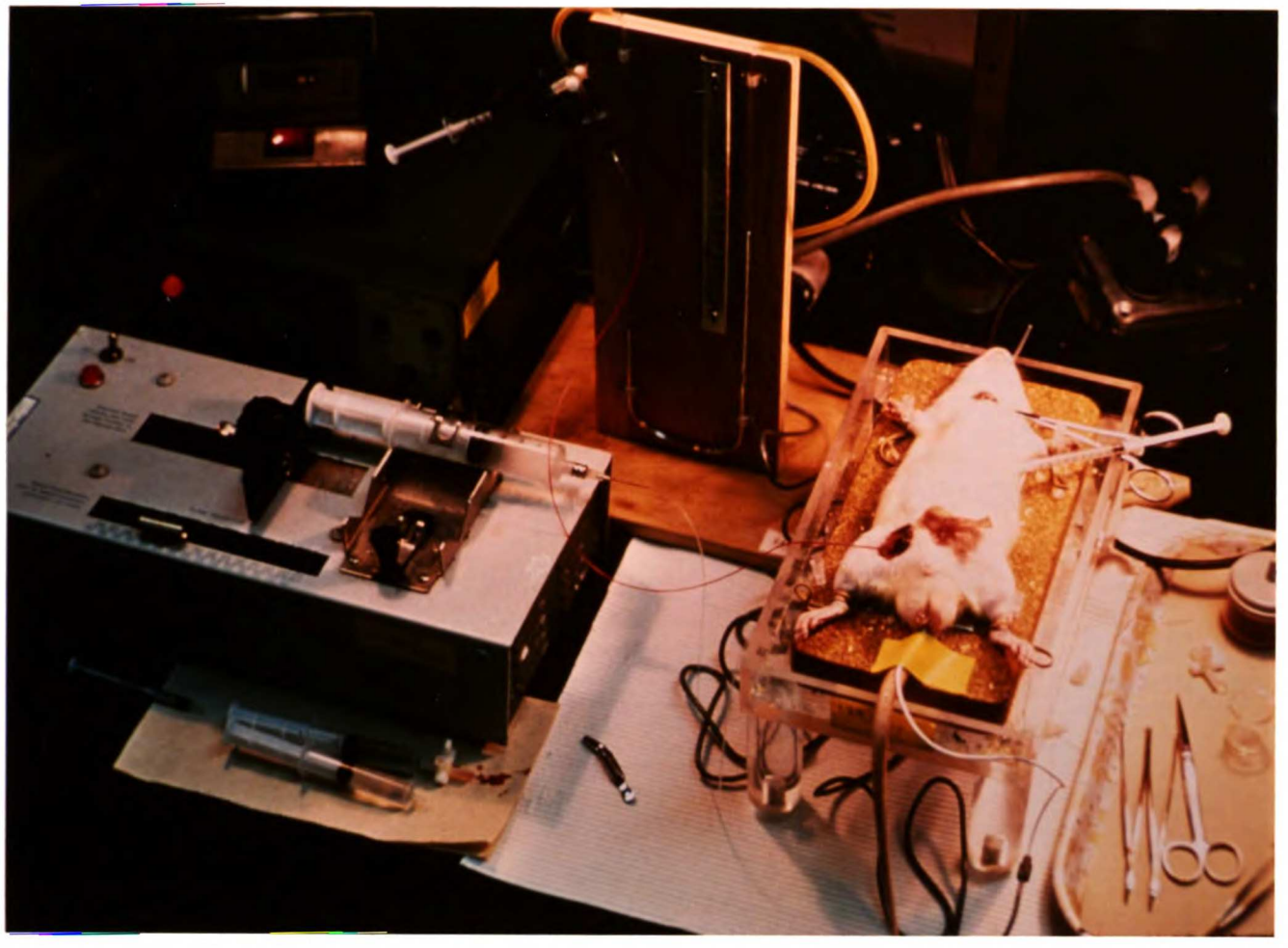

Figure IV-2. Photograph of rat surgical set-up (206).

The animal's blood pressure was monitored continuously during all experiments by use of a mercury manometer. This equipment was constructed to enable direct connection with the femoral artery cannula by use of a three-way stopcock. As soon as the experiment had been completed, the animal was sacrificed by intravenous injection of 0.4 ml euthanasia solution (Somlethol®, sodium pentobarbital 6 gr/ml in alcohol-propylene glycol base with water) (Med. Tech., Inc., Elwood, Kansas).

B. Methods of renal clearance studies

1. Bolus dose studies

a. Materials

Citric acid (Eastman Organic Chemicals, Rochester, New York); Mannitol, Sodium hydroxide, para-Aminohippuric acid (PAH) (Sigma Chemical Company, St. Louis, Missouri); Bacteriostatic sodium chloride injection, USP (Invenex, Chagrin Falls, Ohio); Eppendorf polypropylene micro test tubes, 1.5ml; Eppendorf centrifuge #5412 (Brinkmann Instruments, Inc., Westbury, New York); Harvard Apparatus compact infusion pump (Harvard Apparatus, Millis, Massachusetts); Digital Ionanalyzer pH meter, model 501 (Orion Research, Inc., Cambridge, Massachusetts); Miramark® combination electrode (Markson Science Inc., Del Mar, California); Furosemide injection, 20mg/2ml (IMS Limited, South El Monte, California); Monoject sterile disposable syringe, 35 cc (Sherwood Medical Industries, Inc., Deland, Florida).

b. Preparation of reagents

1) Citric acid, 26mM, was prepared by dissolving 49.92 mg citric acid in normal saline solution to make 10 ml. 2) PAH, 26mM, was prepared by dissolving 50 mg PAH in 10 ml of the above-mentioned citric acid solution. 3) Furosemide, 1 mg/ml, was prepared by diluting 1 ml of furosemide injection, 20 mg/ml with 9 ml normal saline solution. 4) Mannitol, 5 gm %, was prepared by dissolving 1.5 gm mannitol in 27 ml normal saline solution. The pH was adjusted to 7.4 using sodium hydroxide and the volume brought to 30 ml with normal saline solution.

c. Experimental procedures

After surgery had been completed, 0.4 ml of blood was removed via the femoral artery catheter, to serve as a blank plasma sample for that particular animal. Urine which had been withdrawn from the bladder prior to cannulation served as the blank urine sample.

The experiment was begun by administering either 3 or 4 mg furosemide per kg rat body weight, or 5 or 7 mg PAH per kg rat body weight, as a bolus dose via the femoral vein. Following this, an infusion of normal saline solution was begun in the furosemide studies. In the PAH studies, the infusion solution used was 5 gm% mannitol in normal saline solution. In both cases the infusion rate was 80 µl/min. The appropriate infusion was maintained for the entire time course of each experiment.

Table IV-1 shows the time intervals for urine collection and the (theoretical) times of plasma collection for the furosemide bolus dose

studies. Table IV-2 illustrates similar information for the PAH bolus dose studies.

Total urine was collected for each collection period. The volume was measured and, in the PAH bolus studies, pH was measured. Urine samples were placed in 1.5 ml micro test tubes, and stored at -20°C.

Plasma samples of 0.4 ml were withdrawn from the arterial cannula at the times indicated. Each sample was placed in a 1.5 ml micro test tube and spun for three minutes in an Eppendorf centrifuge. The plasma was removed and stored at -20°C. At the end of the experiment, the animal was sacrificed as described previously.

d. Calculations

PAH and furosemide concentrations were measured in plasma utilizing the assays described in Sections V.A. and V.B. Plots of PAH plasma concentration versus time and furosemide plasma concentration versus time were prepared, and half-lives for each drug's disappearance from plasma were determined. These results are presented and discussed in Sections VII.B.1. and VII.B.2.

2. Competition for transport studies

a. Materials

Inulin (Sigma Chemical Company, St. Louis, Missouri); other materials used were described in Section IV.B.1.a.

TABLE IV-1. THEORETICAL PLASMA SAMPLING TIMES AND URINE COLLECTION INTERVALS FOR FUROSEMIDE BOLUS DOSE STUDIES.

Sample #	Plasma Sampling Time (minutes)	Urine Collection Intervals (minutes)
Blank	Prior to dose	Upon cannulation of bladder
1	5	2.5-7.5
2	10.0	7.5-12.5
3	15.0	12.5-17.5
4	27.5	17.5-37.5
5	45.0	37.5-52.5
6	60.0	52.5-67.5
7	75.0	67.5-82.5
8	90.0	82.5-97.5

TABLE IV-2. THEORETICAL PLASMA SAMPLING TIMES AND URINE COLLECTION INTERVALS FOR PAH BOLUS DOSE STUDIES.

Sample #	Plasma Sampling Time (minutes)	Urine Collection Interval (minutes)
Blank	Prior to dose	Upon cannulation of bladder
1	1.25	0-2.5
2	5.0	2.5-7.5
3	10.0	7.5-12.5
4	15.0	12.5-17.5
5	25.0	17.5-32.5
6	40.0	32.5-47.5
7	55.0	47.5-62.5
8	70.0	62.5-77.5
9	85.0	77.5-92.5

b. Preparation of reagents

1) Citric Acid Solution 3.2mM was prepared by dissolving 61.44 mg citric acid in normal saline solution to make 100 ml total volume. This solution was prepared in advance and stored at room temperature. 2) A solution containing 1.134mM furosemide and 2 gm% inulin was prepared by dissolving 600 mg inulin in approximately 27 ml of Citric Acid Solution; 1.125 ml of furosemide (10mg/ml) solution was added, and the pH adjusted to 7.4 with sodium hydroxide. The volume was brought to thirty ml with normal saline solution, and the pH checked and re-adjusted to 7.4 if necessary. 3) A solution containing 3.193mM PAH, 5 gm% mannitol, and 2 gm% inulin was prepared by dissolving 18.6 mg PAH, 600 mg inulin, and 1.5 gm mannitol in approximately 28 ml of Citric Acid Solution. The pH was adjusted to 7.4 using sodium hydroxide and the volume brought to thirty ml with normal saline solution. The pH was then checked and re-adjusted to 7.4 if necessary. 4) A similar solution containing both 1.134mM furosemide and 3.193mM PAH was prepared by dissolving the PAH, inulin, and mannitol (same amounts as in solution #3 above) in 27 ml of Citric Acid Solution; 1.125 ml furosemide solution (10mg/ml) was added, and the pH adjusted to 7.4, using sodium hydroxide. The volume was brought to thirty ml with normal saline solution and the pH checked and re-adjusted to 7.4 if necessary. 5) A solution identical to #4, except that it lacked mannitol, was also prepared for some experiments. Masses, volumes, and pH used were the same as in other solutions detailed here. Solutions 2 through 5 were all prepared on the day of use.

c. Experimental procedures

After completion of surgery, blank plasma and urine were collected as described under in Section IV.B.1.c. Figure IV-3 illustrates the scheme followed for administration of infusion fluid and collection of plasma and urine samples. The experiment was begun by administering solution #2 or #3 to the animal, at a rate of 80 µl/min, for 80 minutes. If the solution administered contained furosemide (solution #2), it was immediately preceded by a loading dose of furosemide equal to 2 mg furosemide/kg rat body weight.

At the end of sixty minutes, total urine was collected for two 10 minute periods. The volume of urine was measured and the urine pH was immediately measured in some instances. In other animals, the pH of the urine was not measured. Fifty µl of urine was removed and diluted to five ml with distilled water. This solution was stored at $4^{o}C$ for assay of inulin content later. The rest of the urine was frozen at $-20^{o}C$ for later PAH or furosemide analysis.

A mid-point blood sample was taken during each urine collection period. These samples were collected and treated as detailed in Section IV.B.1.c.

At the end of the second collection period, the infusion solution was changed to solution #4 or #5. This solution was administered at 80 µl/min for 80 minutes. After sixty minutes of infusion, total urine was collected for two 10 minute clearance periods, and a mid-point blood sample was taken for each collection period. Urine and blood samples were treated as described previously in Sections IV.B.2.c. and IV.B.1.c., respectively. At the end of the last urine collection

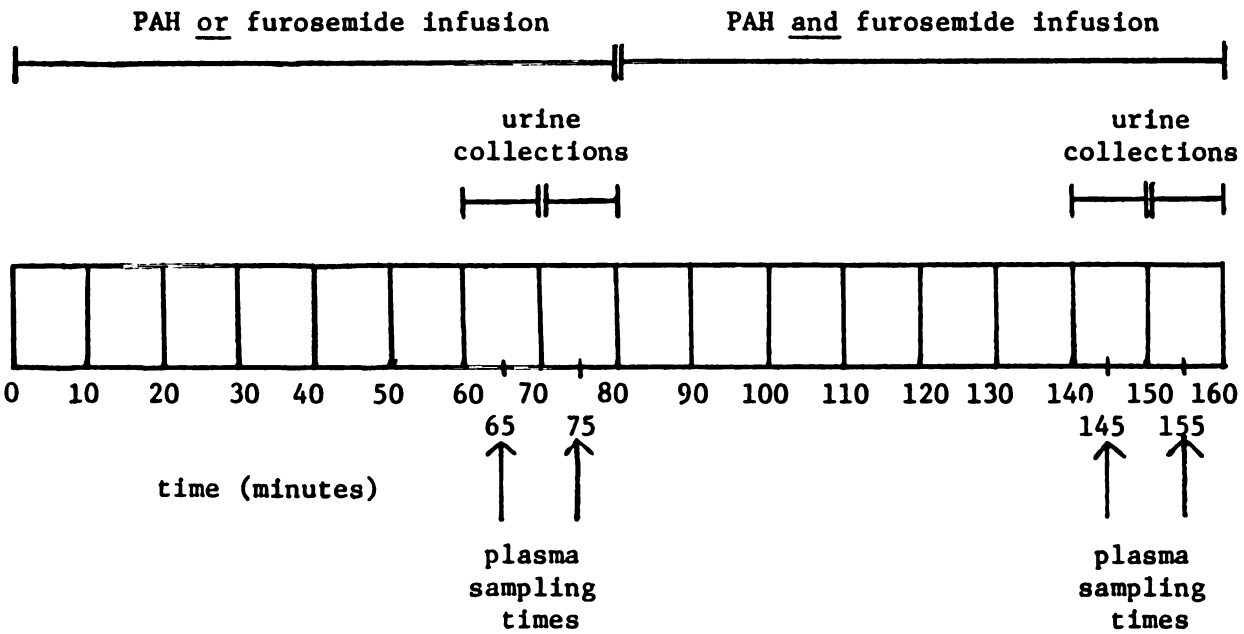

Figure IV-3. Graphical representation of experimental procedure--Competition-for-transport studies.

period, the animal was sacrificed as described earlier.

d. Calculations

PAH, furosemide, and inulin concentrations were measured in both plasma and urine samples. Renal clearance (CL_R), in ml/min/kg, for each compound was calculated by the following equation:

$$CL_R = \frac{C_u \times V_u}{C_p \times t_{uc} \times BW}$$

where C_u = concentration of compound in urine

V_u = volume of urine collected for that period

C_p = concentration of compound in plasma

t_{uc} = urine collection time interval (i.e., 10 minutes)

BW = rat body weight in kg

3. Renal failure studies

a. Induction of renal failure

i. Materials

Uranyl nitrate (uranium (VI) dinitrate oxide 99%) (Alfa Products, Danvers, Massachusetts); Monoject hypodermic needle, 27 gauge, ½ inch (Sherwood Medical Industries, Inc., Deland, Florida); other materials as described previously.

ii. Preparation of reagents

1) Solutions of uranyl nitrate 0.5 mg/ml, 1 mg/ml, and 3 mg/ml were prepared by dissolving 5, 10, or 30 mg of uranyl nitrate in 10 ml normal saline solution. These solutions were prepared on the day of use.

iii. Experimental procedures

Five days prior to clearance experiments, rats were anesthetized with 40 mg/kg sodium pentobarbital. After induction of anesthesia, a uranyl nitrate dose of 0.3, 1.0, or 3.0 mg/kg rat body weight was administered to each rat. Uranyl nitrate was administered via tail vein, in either a 0.5, 1.0, or 3.0 mg/ml solution, using a 1 cc disposable syringe and a 27 gauge needle. Rats were allowed to regain consciousness before they were returned to the Animal Care Facility.

b. PAH clearance studies in renally-damaged rats

i. Materials

Materials used were previously described under Section IV.B.1.a.

ii. Preparation of reagents

Solutions #1 and #3 from Section IV.B.2.b. were the solutions used in these experiments.

iii. Experimental procedures

After completion of surgery, blank blood and urine were collected as previously described (Section IV.B.1.c.). Figure IV-4 represents the time schedule for infusion of solution and collection of plasma and urine samples. An infusion of Solution #3, containing PAH, mannitol, inulin, citric acid, and sodium chloride was begun, and continued at 80 µl/min for 80 minutes. After sixty minutes, total urine was collected for two 10 minute periods, and blood was collected via the arterial catheter at the mid-point of each urine collection period. Blood and urine samples were treated as before. At the end of the second collection period, the animal was sacrificed as previously described.

iv. Calculations

Calculations of PAH and inulin renal clearances were done as described in Section IV.B.2.d.

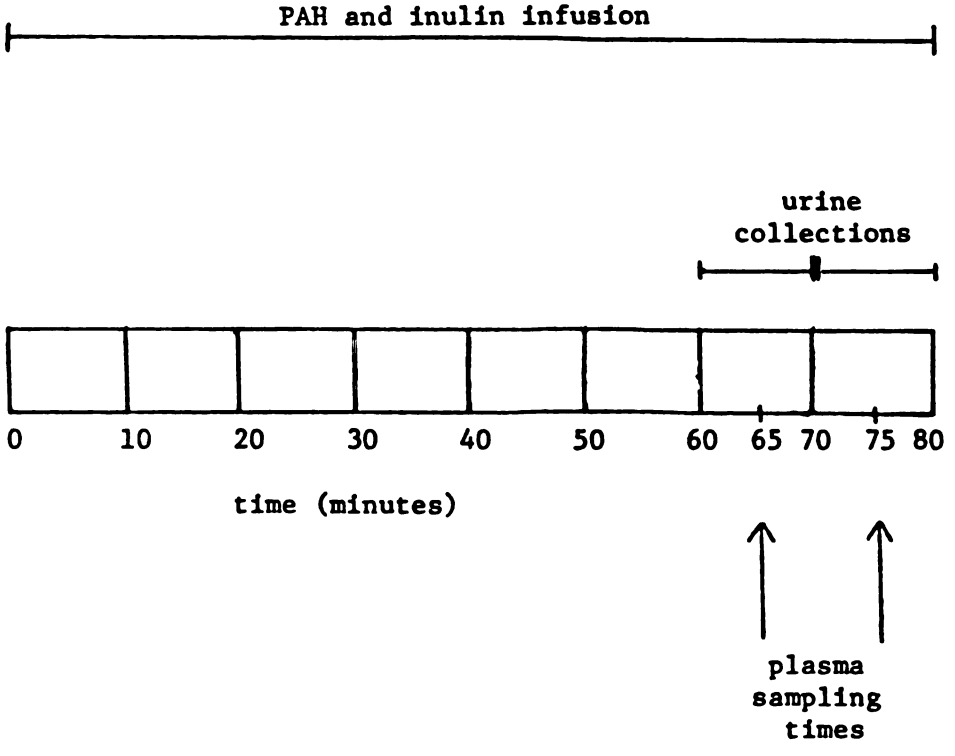

Figure IV-4. Graphical representation of experimental procedure--Renal failure studies.

CHAPTER V

ANALYTICAL METHODS

A. p-Aminohippuric acid assay

1. Previously reported techniques

The original assay for p-aminohippuric acid (PAH) was an application of the Bratton-Marshall reaction (207). This assay is a colorimetric reaction, in which the p-amino group of PAH is diazotized with HNO_2 and then coupled to N-(1-napthyl) ethylenediamine. The assay was originally developed for sulfonamide measurement, but was applied to PAH by Smith et al. (144).

There are two major disadvantages to the colorimetric assay for PAH. 1) The reagents involved will also react with other compounds, such as sulfonamides, thus preventing its use to measure PAH levels in patients taking these drugs. 2) The assay is not very sensitive, requiring at least 0.2 ml plasma or urine to measure 0.5 µg/ml concentration. The required sample volume may be decreased to 20 µl (208). However, the concentration required is then at least five times greater, and perhaps even higher. (The authors do not report assay sensitivity; however, they appear to never measure levels of sulfonamide lower than 20 µg/ml.) The studies described here required sensitivity of at least 1 µg/ml with a sample size of 20 µl. The Bratton-Marshall reaction does not provide this, and so was not appropriate for use in these studies.

A capillary gas chromatographic assay, using a nitrogen-phosphorus detector, was developed by Libeer et al. (209) in 1981. The sensitivity of the assay was not discussed in the publication. However, the assay requires both an extraction and a derivatization step, which we wished to avoid.

Brown et al. (210) and Shoup and Kissinger (211) have developed HPLC methods for analyzing PAH amounts in biological samples. The assay developed by Brown et al. (210) is quite sensitive (5 ng PAH on column); however, it suffers from an extremely unstable baseline, requiring solvent preparation at least 12-24 hours in advance and storage of the solvent in the pump. The assay of Shoup and Kissinger (211) is also quite sensitive (0.5 ng PAH on column). However, it requires an electrochemical detector which was not available in our laboratory.

A high performance liquid chromatographic (HPLC) technique for the measurement of p-aminobenzoic acid (PABA) was described by Ito et al. (212). Due to similarities in PABA and PAH structures, perhaps it could be adapted to measurement of PAH as well. This assay utilizes a reversed phase C_{18} column and an electrochemical detector. Aside from the electrochemical detector problem, it was only used to measure PABA levels of 50 µg/ml or greater, and this was not sensitive enough for our needs.

Based on the available assays, it was decided to develop a new assay for PAH. The following sections describe the cation exchange HPLC assay for PAH developed in this laboratory. (In March, 1984, Prueksaritanont et al. (213) published an HPLC assay for PAH, utilizing a C_{18} column, para-aminobenzoic acid as internal standard, and UV

detection at 254 nm.)

2. Experimental

a. Chemicals and instrumentation

p-Aminohippuric acid (PAH) (Sigma Chemical Company, St. Louis, Missouri); p-Aminobenzoic acid (PABA) (Eastman Organic Chemicals, Rochester, New York); Acetonitrile (J.T. Baker Chemical Company, Phillipsburg, New Jersey); Phosphoric acid (American Scientific Products, McGaw Park, Illinois); Partisil PXS 10/25 SCX column (Whatman Chemical Separation Inc., Clifton, New Jersey); Linear dual pen recorder, Model 300 (Linear Instruments Corporation, Irvine, California); Perkin-Elmer Series 2 liquid chromatograph, Perkin-Elmer LC-15 UV detector (Perkin-Elmer Corporation, Norwalk, Connecticut); WISP 710B automatic sampler (Waters Associates, Inc., Milford, Massachusetts); Thermolyne Maxi-mix vortex mixer (Thermolyne Corporation, Dubuque, Iowa); IEC centrifuge Model HN-SII (Damon/IEC Division, Needham Heights, Massachusetts); High speed analytical evaporator (Organomation Associates, Inc., Northborough, Massachusetts).

Water for all sample preparation and mobile phase preparation was distilled water de-ionized through a Nanopure de-ionizer (Sybron/Barnstead, Boston, Massachusetts). This water was then stored in covered glass containers until its use.

b. Preparation of reagents

1) A stock solution of PAH, 100 µg/ml, was prepared by dissolving 50 mg PAH in water to make 500 ml. This stock solution was diluted to 10 µg/ml, using 1 part PAH (100µg/ml) solution and 9 parts water. These solutions were prepared up to one month in advance and stored at 4°C. 2) PABA, 250 µg/ml, was prepared by dissolving 125 mg PABA in water to make 500 ml. This solution was also diluted to 100 µg PABA/ml, by combining 2 parts PABA (250 µg/ml) solution and 3 parts water. These solutions were also prepared up to 1 month in advance and stored at 4°C. 3) Mobile phase for HPLC assay contained 50% acetonitrile, 0.1% phosphoric acid in water. This solvent was prepared by mixing 500 ml acetonitrile, 1 ml phosphoric acid and adjusting the volume to 1000 ml with water. This solvent was filtered and de-gassed prior to its use.

c. Plasma sample preparation

Figure V-1 includes a flow diagram which illustrates the steps for preparation of plasma samples for PAH assay. Ten ml acetonitrile was combined with 50 µl PABA solution, 100 µg/ml. Two hundred µl of the acetonitrile/PABA solution was added to each 20 µl plasma sample.

Each sample was stirred on a vortex mixer and then centrifuged at 2400 rpm for ten minutes. The supernatant was transferred to a clean test tube and evaporated, under N_2, to dryness. Each sample was reconstituted by addition of 500 µl HPLC mobile phase (50% acetonitrile, 0.1% phosphoric acid), and mixing on a vortex mixer. Samples were then transferred to WISP® injection vials for assay.

d. Assay for PAH in plasma samples

The plasma assay for PAH was carried out using a WISP automatic injector, Perkin-Elmer Series 2 liquid chromatograph, Perkin-Elmer LC-15 UV detector, and Linear dual pen recorder. The mobile phase consisted of 50% acetonitrile, 0.1% phosphoric acid in water. The solvent flow rate was 2 ml/min, operating under isocratic and ambient temperature conditions. Ultraviolet absorbance detection was at 254 nm.

e. Urine sample preparation

Figure V-1 also contains a flow diagram for preparing urine samples for PAH assay. Five ml acetonitrile and 0.5 ml PABA solution, 250 µg/ml, were combined. One hundred µl of the acetonitrile/PABA mixture was added to each 20 µl urine sample.

Urine samples were treated in the same manner as plasma samples, including mixing, centrifugation, and evaporation steps. Each sample was finally reconstituted with 100 µl HPLC mobile phase, and transferred to a WISP® tube for injection into the HPLC system.

f. Assay for PAH in urine samples

The HPLC assay for PAH in urine samples was done under the same conditions as the plasma PAH assay.

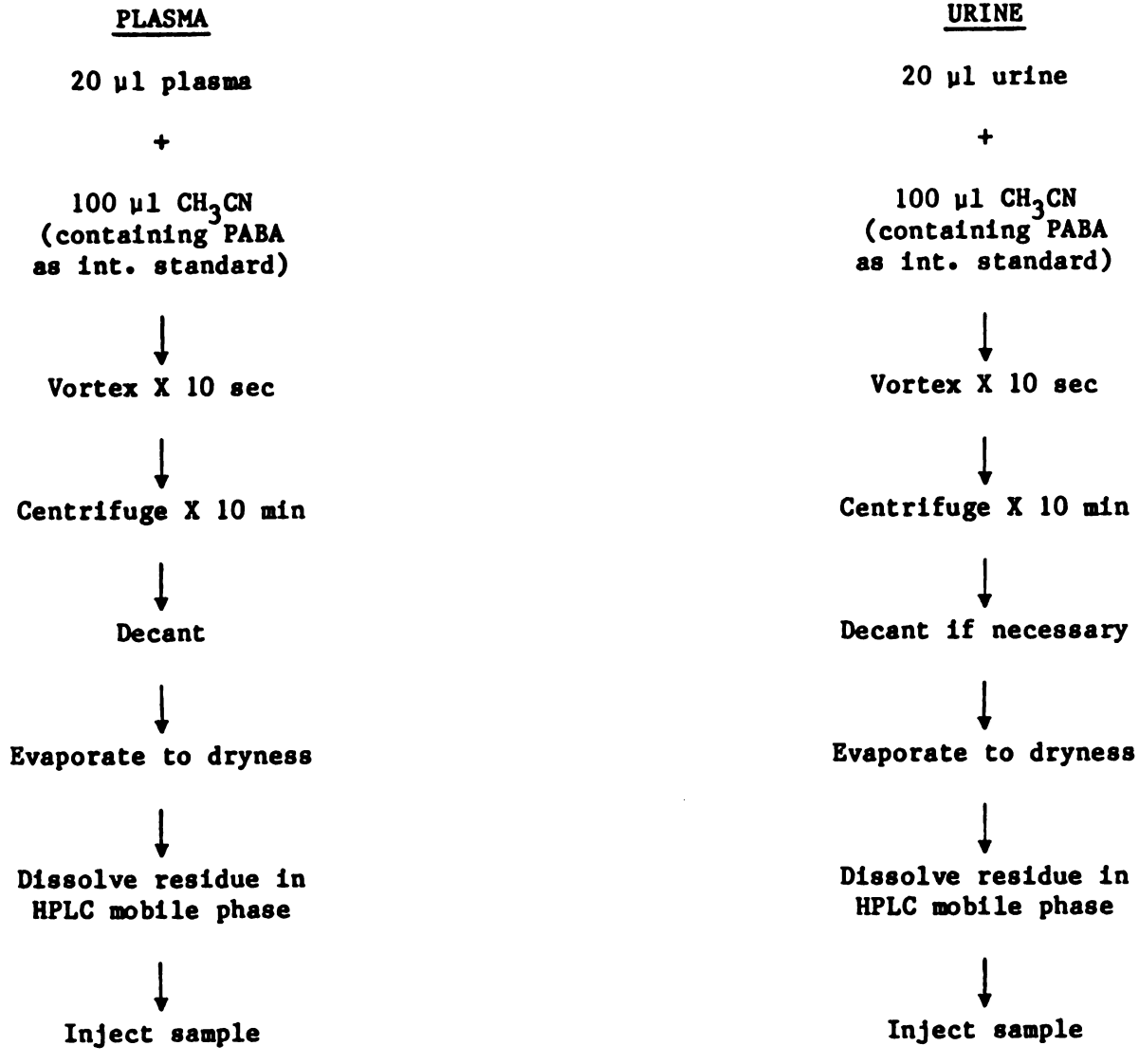

Figure V-1. Flow diagram for preparation of plasma and urine samples for PAH assay.

3. Results and discussion

Figure V-2 shows representative chromatographs from blank plasma and a sample of the same plasma spiked with PAH and PABA internal standard. The retention times are five minutes and eleven minutes for PABA and PAH respectively. This chromatograph shows no interference for either PAH or PABA peaks. Figure V-3 shows sample blank and PABA- and PAH-spiked urine chromatographs. No significant peaks are found to interfere with PAH or PABA in the urine samples.

Figure V-4 shows a representative plasma standard curve for PAH concentrations covering the range of 2 to 55 µg/ml plasma, using PABA as internal standard and a sample size of 20 µl. This set of data fits the straight line equation $y = (0.07274)x + 0.0573$, where x = PAH plasma concentration in µg/ml and y = PAH/PABA peak height ratio. For this set of data $r^2 = 0.9990$. PAH plasma concentrations as low as 0.7 µg/ml have been measured using the 20 µl sample size.

Figure V-5 is a representative standard curve for PAH urine samples. This standard curve covers the range of 20 to 1,050 µg/ml. Here the y-intercept = -0.01815 with a slope of 0.004245 and $r^2 = 0.9999$.

Standard curves of PAH in plasma were prepared and assayed on seven different days to determine the variability of the slopes and intercepts (Table V-1). The results show good linearity ($r^2 > 0.997$) over the concentration range studied, with little variability in slope and intercept. Standard curves for urine were similarly prepared and assayed. The results are shown in Table V-2. Good correlation ($r^2 > 0.996$) and limited variation in slope and y-intercept were seen with

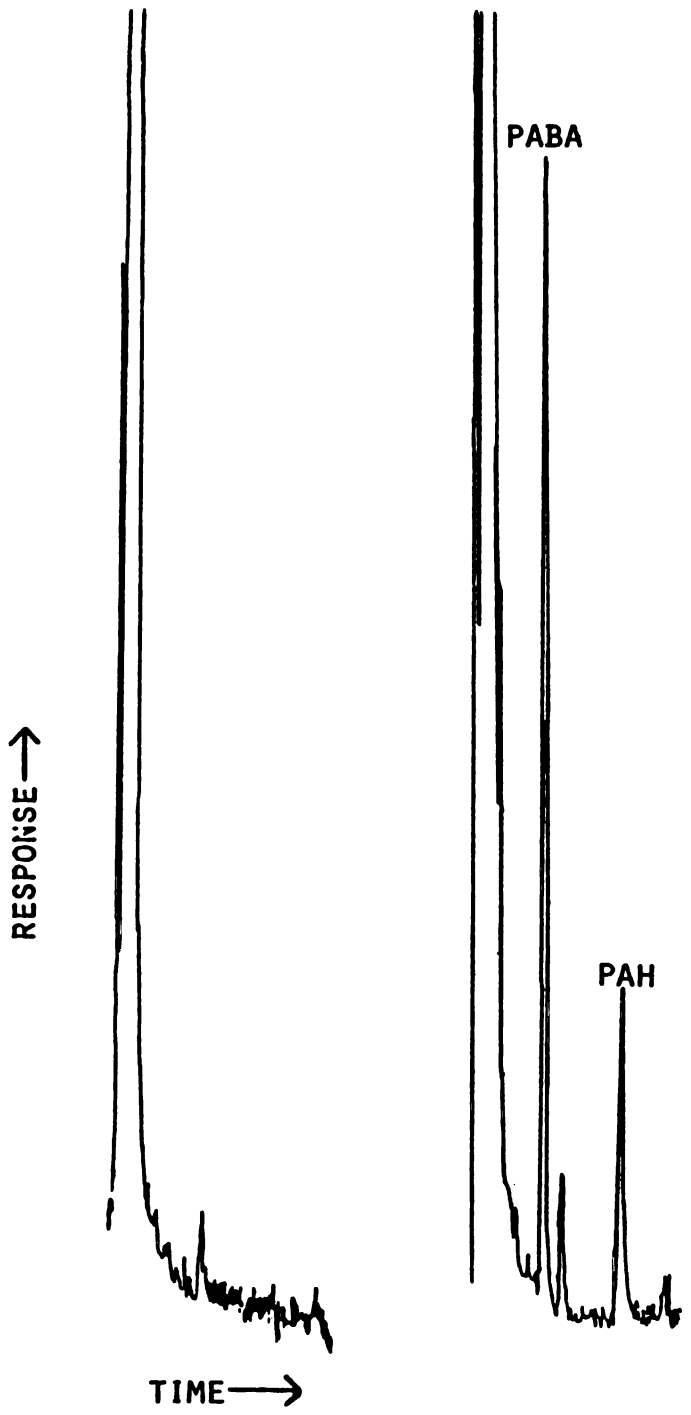

Figure V-2. Chromatographs of blank plasma and plasma spiked with PAH (2 µg/ml) and PABA.

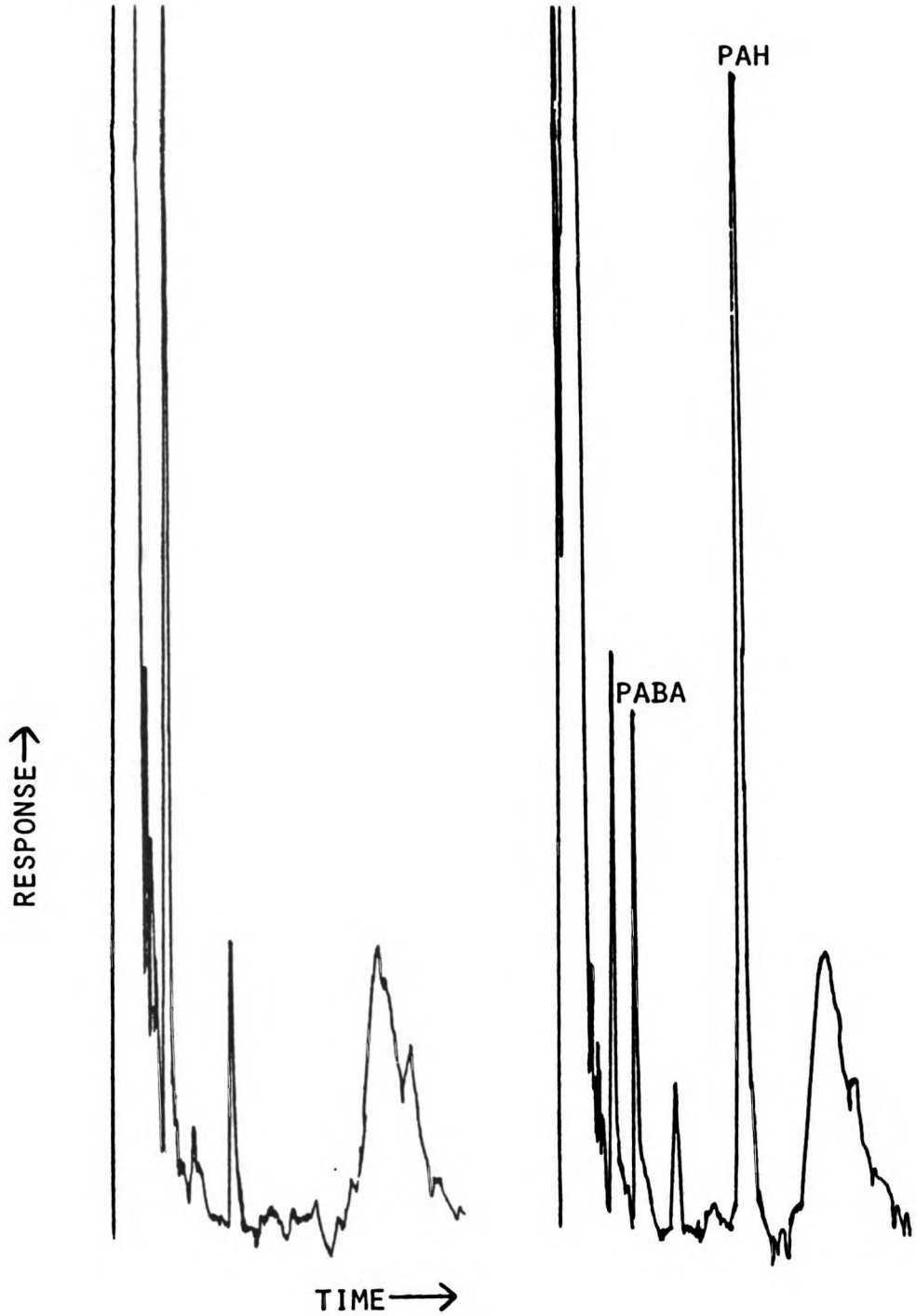

Figure V-3. Chromatographs of blank urine and urine spiked with PAH and PABA.

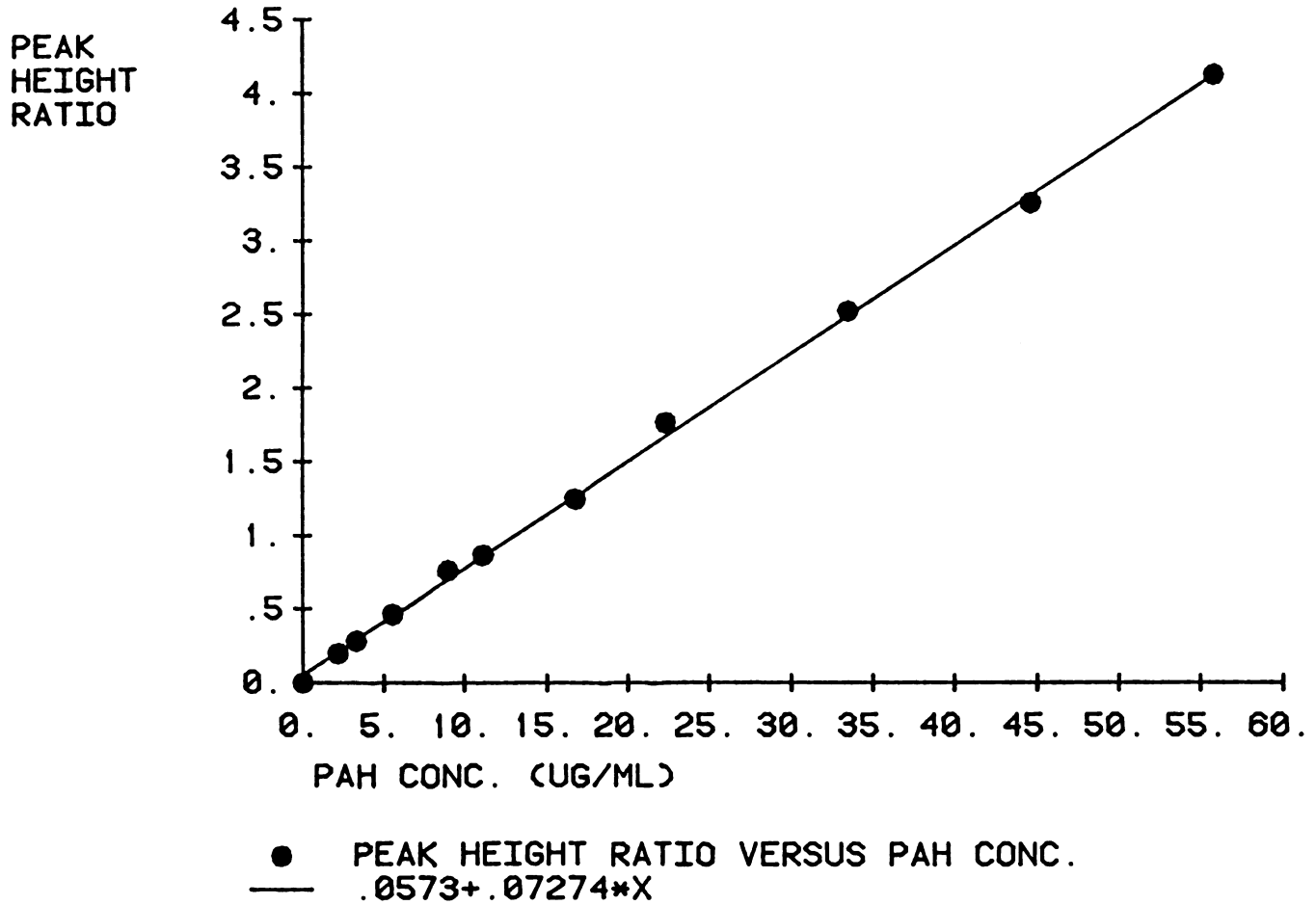

Figure V-4. Standard curve for PAH in plasma using PABA as internal standard. This curve fits the equation $y = (0.07274)x + 0.0573$, with $r^2 = 0.9990$.

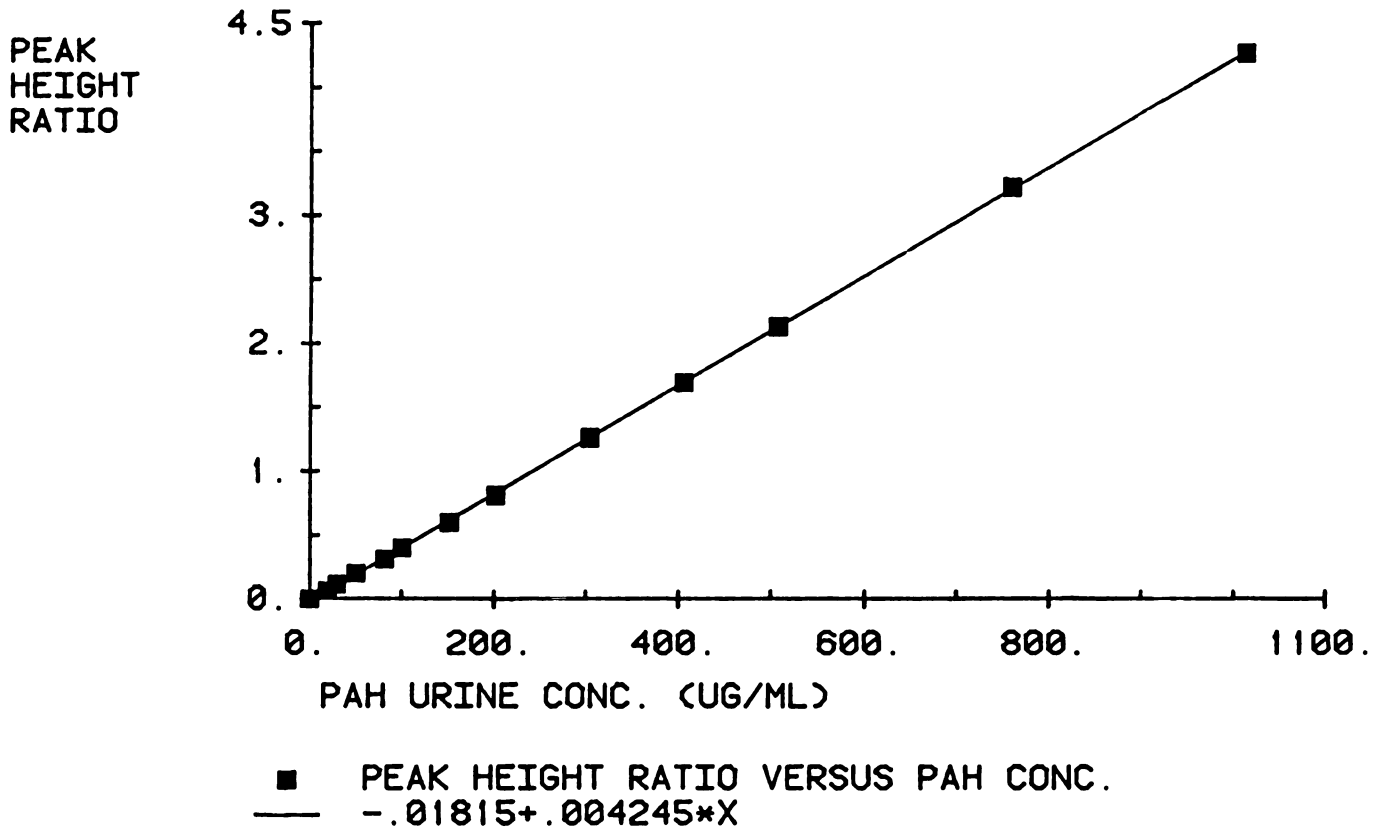

Figure V-5. Standard curve for PAH in urine using PABA as internal standard. This curve fits the equation $y = (0.004245)x - 0.01815$, with $r^2 = 0.9999$.

TABLE V-1. INTERDAY[a] VARIABILITY OF SLOPES, INTERCEPTS AND CORRELATION COEFFICIENTS DERIVED FROM THE STANDARD CURVES OF PAH IN PLASMA.

Curve #	Y-Intercept	Slope	r^2
1	-0.0537	0.0985	0.9987
2	-0.0138	0.0987	0.9934
3	0.0391	0.0843	0.9968
4	0.0150	0.0853	0.9981
5	-0.0206	0.0927	0.9977
6	-0.0074	0.0698	0.9976
7	0.0573	0.0727	0.9990
Mean	0.0023	0.0860	0.9973
S.D.	0.0371	0.0116	0.0019

[a]Standard curves were constructed on seven different days over an eleven month period.

TABLE V-2. INTERDAY[a] VARIABILITY OF SLOPES, INTERCEPTS AND CORRELATION COEFFICIENTS DERIVED FROM THE STANDARD CURVES OF PAH IN URINE.

Curve #	Y-Intercept	Slope	r^2
1	-0.0181	0.0042	0.9999
2	-0.0116	0.0022	0.9993
3	0.1135	0.0033	0.9917
4	0.1159	0.0030	0.9921
5	0.0358	0.0038	0.9977
6	-0.0203	0.0028	0.9987
Mean	0.0359	0.0032	0.9966
S.D.	0.0644	0.0007	0.0037

[a]Standard curves were constructed on six different days over an eleven month period.

the urine standard curves as well.

Tables V-3 and V-4 show intra-day variability for three PAH plasma concentrations and three PAH urine concentrations respectively. In general, the coefficient of variation (precision) and per cent difference from spiked concentration (accuracy) for these samples are within acceptable limits. Per cent deviation and coefficient of variation are somewhat high for the plasma concentration of 25 µg/ml. The cause of this is unknown.

Tables V-5 and V-6 contain interday variability for four PAH concentrations in plasma and urine respectively. Once again, all values for coefficient of variation and per cent error are reasonably low, with the exception of the coefficient of variation for the 2 µg/ml plasma concentration and the 100 µg/ml urine concentration. An explanation is not currently available for this variability.

The stability of PAH in plasma and urine was studied by assaying samples from a number of experiments and then re-assaying them six-and-one-half months later. Prior to and between assays, the samples were kept frozen at -20°C, except when they were thawed briefly in order to remove part of the sample for inulin assay. Results for plasma and urine are shown in Tables V-7 and V-8 respectively. These results indicate that there is quite a bit of variability in concentration upon re-assay of the samples.

Another group of samples was re-assayed approximately three-and-one-half months after the original assay. These samples were also kept at -20°C. However, they were not only thawed once to allow inulin assay, but were also inadvertently thawed and allowed to remain at room temperature for approximately 24 hours. These samples showed much

TABLE V-3. INTRADAY[a] VARIABILITY OF PAH CONCENTRATIONS IN SPIKED PLASMA SAMPLES.

Spiked Conc. (µg/ml)	Measured Conc. (µg/ml)	% Error[b]
10	Mean: 9.44 S.D.: 1.02 CV(%): 10.81	-5.6
25	Mean: 22.55 S.D.: 3.06 CV(%): 13.57	-9.8
50	Mean: 50.61 S.D.: 4.23 CV(%): 8.36	+1.22

[a]Mean values represent four different plasma samples.
[b]% Error = 100 X (Measured Conc. - Spiked Conc.)/Spiked Conc.

TABLE V-4. INTRADAY[a] VARIABILITY OF PAH CONCENTRATIONS IN SPIKED URINE SAMPLES.

Spiked Conc. (µg/ml)	Measured Conc. (µg/ml)	%Error[b]
50	Mean: 47.04 S.D. 2.21 CV(%): 4.70	-5.92
100	Mean: 104.38 S.D. 4.16 CV(%): 3.99	+4.38
200	Mean: 212.63 S.D. 13.20 CV(%): 6.21	+6.32

[a]Mean values represent four different urine samples.
[b]% Error = 100 X (Measured Conc. - Spiked Conc.)/Spiked Conc.

TABLE V-5. INTERDAY[a] VARIABILITY OF PAH CONCENTRATIONS IN SPIKED PLASMA SAMPLES.

Spiked Conc. (µg/ml)	Measured Conc. (µg/ml)	% Error[b]
2	Mean: 1.83 S.D.: 0.30 CV(%): 16.65	-8.52
5	Mean: 5.01 S.D.: 0.24 CV(%): 4.73	+0.25
10	Mean: 10.12 S.D.: 0.48 CV(%): 4.72	+1.18
50	Mean: 52.28 S.D.: 1.93 CV(%): 3.69	+4.56

[a]Mean values represent plasma samples analyzed on five different days over an eleven month period.
[b]% Error = 100 X (Measured conc. - Spiked Conc.)/Spiked Conc.

TABLE V-6. INTERDAY[a] VARIABILITY OF PAH CONCENTRATIONS IN SPIKED URINE SAMPLES.

Spiked Conc. (µg/ml)	Measured Conc. (µg/ml)	% Error[b]
50	Mean: 52.56 S.D.: 3.22 CV(%): 6.13	+5.12
100	Mean: 101.87 S.D.: 10.67 CV(%): 10.47	+1.87
200	Mean: 204.69 S.D.: 10.77 CV(%): 5.26	+2.34
500	Mean: 519.50 S.D.: 34.56 CV(%): 6.65	+3.90

[a]Mean values represent urine samples analyzed on five different days over an eleven month period.

[b]% Error = 100 X (Measured Conc. - Spiked Conc.)/Spiked Conc.

TABLE V-7. PAH STABILITY IN PLASMA SAMPLES[a].

Sample #	Original Measurement (µg/ml)	Second Measurement (µg/ml)	Ratio (Second/First)
1	5.07	4.46	0.88
2	7.11	8.69	1.22
3	7.29	3.49	0.48
4	4.82	3.74	0.78
5	6.79	4.96	0.73
6	4.01	3.96	0.99
7	7.33	7.26	0.99
8	5.10	4.26	0.84

[a]Samples were originally assayed on 1/22/83. Re-assay was performed on 8/3/83.

TABLE V-8. PAH STABILITY IN URINE SAMPLES[a].

Sample #	Original Measurement (mg/ml)	Second Measurement (mg/ml)	Ratio (Second/First)
1	0.58	0.57	0.98
2	0.57	0.52	0.91
3	0.48	0.45	0.94
4	0.83	0.63	0.76
5	0.65	0.92	1.42
6	0.82	0.77	0.94
7	0.74	0.50	0.68
8	0.84	0.87	1.04

[a]Samples were originally on 1/23/83. Re-assay was done on 8/3/83.

greater variability in the concentrations determined on the two different days. This appears to indicate that thawing and prolonged exposure to room temperatures may affect the stability of PAH in plasma and urine samples. Based on these results, it is recommended that samples be frozen at -20°C immediately after collection and that PAH concentrations be measured immediately after the samples are first thawed.

The use of PABA as internal standard posed a potential problem. PABA is a naturally-occurring substance in a number of species. If endogenous concentrations are high enough they might affect the PABA peak height in our assay and thus alter the accurate measurement of PAH concentrations. According to Altman and Dittmer (8) there is approximately 680 pg PABA/20 µl of plasma in humans. Mice (no data available for rats) have approximately 5.8 ng/20 µl plasma. One hundred ng PABA was added to each plasma sample. If rat plasma PABA concentrations are similar to those of man, the endogenous PABA creates no problem. If the levels are similar to those found in mice however, some increase in PABA peak height might occur due to endogenous PABA.

In order to investigate this further, plasma samples from sixteen rats given PAH were assayed without addition of internal standard. None of these samples showed a peak in the location of the PABA internal standard peak.

For urine, literature data (8) was available only for humans. This indicated that PABA is excreted in urine at a rate of 3 µg/kg body weight per day. Assuming a 70 kg person who makes two liters of urine per day, there would be 105 ng PABA/ml urine, or 2.1 ng/20 µl sample. Since 2.5 µg PABA is added to each sample as internal standard, it was

thought that endogenous PABA would not present a problem. However, urine samples from sixteen rats given PAH were also assayed without internal standard. Again, no peak was found in the PABA location, supporting the conclusion that endogenous PABA is not a deterrent to using PABA as internal standard in this assay.

In conclusion, an assay for PAH has been developed which is rapid, sensitive, reproducible and easy-to-do. It has been used extensively for samples from rat studies involving administration of PAH intravenously (see Chapters IV and VII).

B. Furosemide assay

1. Introduction

The assay for furosemide used in these studies was developed by Smith (214). It is a straightforward, easy-to-do assay with good sensitivity and reproducibility. Minor assay modifications were made for these experiments, but the assay remains unchanged overall.

2. Experimental

a. Chemicals and instrumentation

Furosemide (Sigma Chemical Company, St. Louis, Missouri); Sodium phenobarbital (Merck and Company, Inc., Rahway, New Jersey); Sodium hydroxide, 50% (w/w) (Mallinckrodt, Inc., Paris, Kentucky); Waters 440 UV detector (Waters Associates, Inc., Milford, Massachusetts); Perkin-

Elmer fluorescence spectrophotometer Model 204A, Perkin-Elmer 150 xenon power supply, Perkin-Elmer Series 3 liquid chromatograph (Perkin-Elmer Corporation, Norwalk, Connecticut); Pedersen dual pen recorder (Pedersen Intruments, Lafayette, California); C_{18} reversed phase analytical column, 10μ pore size, 25 cm length (Alltech Associates, Deerfield, Illinois); other materials as previously described.

b. Preparation of reagents

1) Furosemide, 41 μg/ml, was prepared by dissolving 4.1 mg furosemide in 50% acetonitrile/water to make 100 ml. This stock solution was also diluted 10-fold, with 50% acetonitrile/water, to make furosemide 4.1 μg/ml solution. These solutions were prepared up to 1 month in advance and stored at 4°C. 2) Sodium phenobarbital, 10 mg/ml, was prepared by dissolving 1.0 gm sodium phenobarbital in water to make 100 ml. This solution was prepared up to 1 month in advance and stored at 4°C. 3) Mobile phase, containing 22% acetonitrile, 0.1% phosphoric acid in water, was prepared by mixing 220 ml acetonitrile, 1 ml phosphoric acid, and bringing the volume to 1000 ml with water. The pH was adjusted to 4.3, using sodium hydroxide solution. This solution was filtered and de-gassed prior to use in the HPLC system.

c. Plasma sample preparation

Ten ml acetonitrile and 0.5 ml sodium phenobarbital solution (10 mg/ml) were combined. To each 25 μl furosemide plasma sample, 200 μl of the acetonitrile/sodium phenobarbital solution was added.

All samples were mixed on a vortex mixer and centrifuged at 2400 rpm for ten minutes. The supernatant was removed and evaporated to dryness under N_2. Samples were then reconstituted with 200 µl HPLC mobile phase (22% acetonitrile, 0.1% phosphoric acid, pH 4.3) and transferred to WISP® tubes for injection onto the HPLC system.

d. Assay for furosemide in plasma samples

The plasma assay for furosemide was carried out using a WISP 710B automatic injector, Perkin-Elmer Series 3 liquid chromatograph, Perkin-Elmer fluorescence spectrophotometer, Waters 440 UV detector, Alltech C_{18} reversed phase analytical column, and Pedersen dual pen recorder. Mobile phase consisted of 22% acetonitrile, 0.1% phosphoric acid in water, pH 4.3, with a solvent flow rate of 2 ml/min and operating under isocratic and ambient temperature conditions. Ultraviolet absorption was at 254 nm, and fluorescent detection was at 345 nm for excitation and 405 nm for emission. Retention times were 14.0 minutes for phenobarbital and 19.2 minutes for furosemide.

e. Urine sample preparation

Ten ml acetonitrile and 0.5 ml sodium phenobarbital (10 mg/ml) were combined. Two hundred µl of acetonitrile/sodium phenobarbital solution were added to each 25 µl furosemide urine sample.

Urine samples then followed the same mixing, centrifugation, evaporation and reconstitution steps as plasma samples. After reconstitution, urine samples were placed in WISP® tubes for HPLC assay.

f. Assay for furosemide in urine

The same equipment and conditions were used for assay of these samples as was used for assay of furosemide plasma samples.

3. Results and discussion

A representative standard curve for furosemide in plasma is shown in Figure V-6. For this set of plasma data the linear equation is $y = 0.044x - 0.0151$ ($r^2 = 0.9991$). This assay was utilized to measure furosemide plasma concentrations of 0.4 to 36 µg/ml. No interference from other compounds in plasma was noted.

Figure V-7 shows a standard curve for furosemide in urine. This data covers the range of 16 to 360 µg/ml, and fits the linear equation $y = 0.0076 - 0.0168$ ($r^2 = 0.9998$). Other components of urine did not interfere with this assay.

C. Purification of ^{3}H-furosemide

1. Introduction

^{3}H-Furosemide for vesicle studies (Chapters III and VI) was supplied by New England Nuclear in an ethanol solution. Unfortunately, furosemide decomposes in alcohol solution, so that after seven months, approximately 30% of the radioactivity was no longer associated with furosemide. This was determined by separation of an aliquot of ^{3}H-furosemide on HPLC, using furosemide plasma assay conditions. The

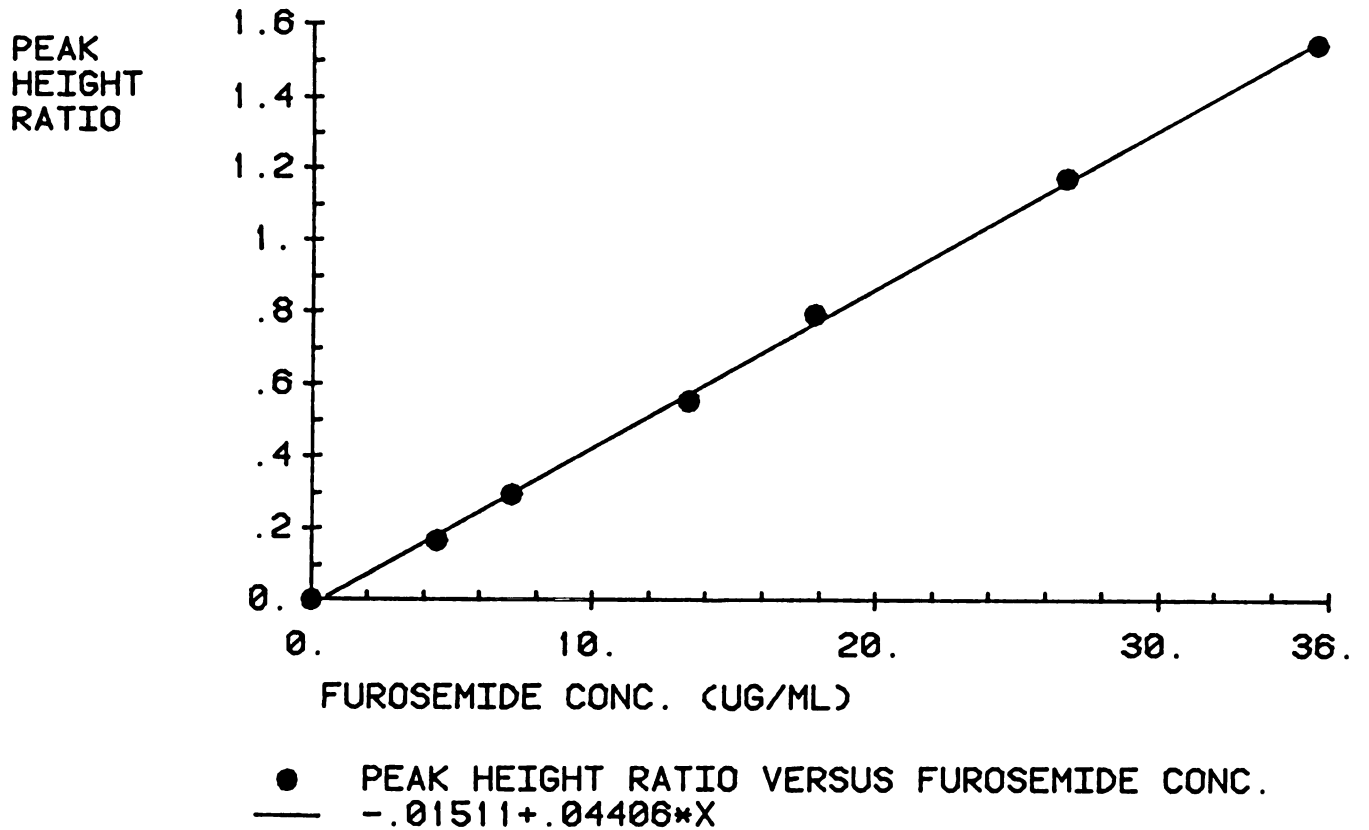

Figure V-6. Standard curve for furosemide in plasma using sodium phenobarbital as internal standard. This curve fits the equation $y = (0.04406)x - 0.01511$, with $r^2=0.9991$.

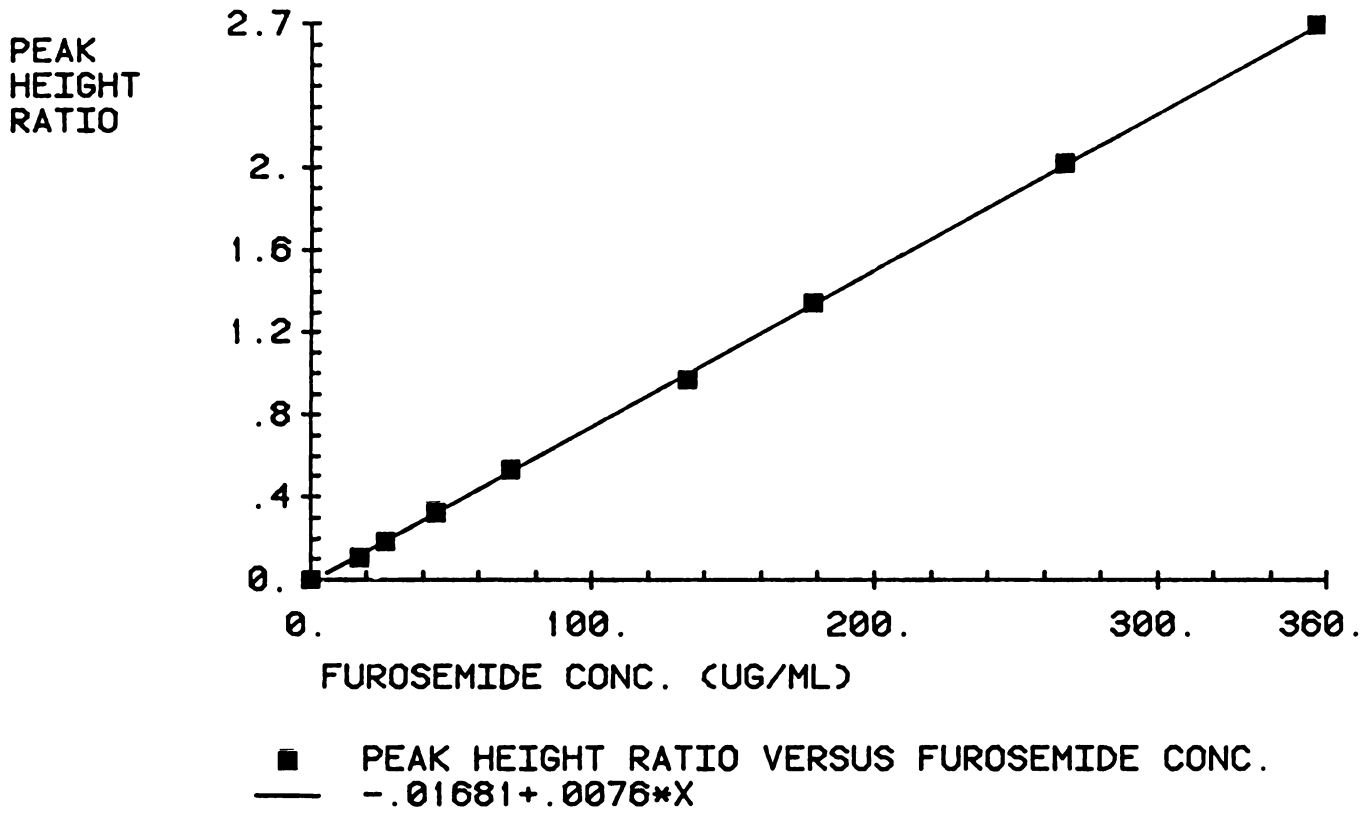

Figure V-7. Standard curve for furosemide in urine using sodium phenobarbital as internal standard. This curve fits the equation $y = (0.0076)x - 0.01681$, with $r^2=0.9998$.

following method was developed for purification of ^{3}H-furosemide.

2. Experimental

a. Chemicals and instrumentation

Trizma HCl (Sigma Chemical Company, St. Louis, Missouri); ^{3}H-Furosemide, Aquasol (New England Nuclear, Boston, Massachusetts); Rheodyne Model 7010 sample injector (Rheodyne Inc., Cotati, California); other materials as previously described.

b. Preparation of reagents

1) A solution of "cold" furosemide in acetonitrile was prepared by dissolving a small amount (several mg) of furosemide in acetonitrile in a disposable test tube. The concentration was unimportant and therefore was not determined. 2) HPLC mobile phase, 20% acetonitrile, 0.02 gm% Trizma HCl, pH 4.2 was prepared by dissolving 0.2 gm Trizma HCl in 200 ml acetonitrile and water to make 1000 ml. The pH was adjusted to approximately 4.2 using sodium hydroxide solution. This buffer was filtered and degassed prior to its use.

c. Purification procedures

The purification of ^{3}H-furosemide was carried out using a Rheodyne Model 7010 sample injector, Perkin-Elmer Series 3 liquid chromatograph, Alltech C_{18} reversed phase column, Waters 440 UV detector, Perkin-Elmer

fluorescent spectrophotometer Model 204A, and Pedersen dual pen recorder. Flow rate for the mobile phase was 2 ml/min, using isocratic and ambient temperature conditions. Ultraviolet detection was at 254 nm, with fluorescent excitation at 345 nm and emission at 405 nm.

Ten µl of "cold" furosemide in acetonitrile was injected onto the column and furosemide's retention time was noted. Injection of this same solution was repeated twice, to be certain that the retention time remained constant. Next, 15 µl of a solution (obtained from T. Blaschke, Stanford University) containing small amounts of ^{3}H-furosemide and much "cold" furosemide was injected. This was used as a standard, to determine that the breakdown product peaks were separated from the furosemide peak. Injection of this solution was repeated, followed by a 5-15 µl injection of ^{3}H-furosemide solution for purification. Collection of five minute fractions of HPLC eluent were begun as soon as the ^{3}H-furosemide for purification was injected. At two minutes before the expected appearance of the furosemide UV absorbance peak, we began collecting one minute fractions. This smaller fraction size was utilized throughout elution of the furosemide from the column. Just prior to the appearance of the furosemide peak, the fluorescence detection lamp was switched off, and the appearance of furosemide monitored by UV absorbance alone. After furosemide had been eluted from the column, we returned to collection of five minute fractions. These collections continued for at least 15 minutes of solvent wash and 20 minutes of column wash with 50% acetonitrile/water. All solvent eluted from the column after injection of radiolabelled compound was collected in scintillation vials and handled appropriately.

All fractions collected after injection of ^{3}H-furosemide for

purification were sampled for radioactivity. A 5 µl aliquot of each fraction was mixed with 10 ml Aquasol, and its radioactivity measured by scintillation counting. The remainder of each fraction was stored at 4°C while scintillation counting of the aliquots took place. Fractions containing furosemide which also contained the highest levels of radioactivity were combined (generally 2 or 3 one minute fractions) and evaporated to dryness under N_2. The purified, dried ^{3}H-furosemide was then stored at 4°C until its use in vesicle studies.

3. Results and discussion

Approximately 60-70% of total radioactivity in a sample was always found in the furosemide peak. Stability of this peak after purification was determined by allowing purified ^{3}H-furosemide to remain in HPLC solvent at 4°C for one week and then re-purifying a portion of the solution by HPLC. Virtually all (>99%) of the radioactivity was recovered in the newly-eluted furosemide peak. This indicates that the ^{3}H-furosemide was stable at 4°C for at least one week. Consequently, ^{3}H-furosemide was purified up to but not more than nine days in advance of its experimental use and stored at 4°C until used.

D. Inulin assay

1. Introduction

Inulin is an exogenously-administered compound used to measure glomerular filtration rate. It was included in infusion solutions

administered to rats in both competition for transport studies and renal failure studies (see Chapters IV and VII). The assay used for this compound is a colorimetric assay described by Till (206).

2. Experimental

a. Chemicals and instrumentation

Trichloroacetic acid (Matheson Coleman and Bell, Norwood, Ohio); Anthrone (J.T. Baker Chemical Company, Phillipsburg, New Jersey); Sulfuric acid (Allied Chemical, Morristown, New Jersey); Dubnoff metabolic shaking incubator (water bath) (GCA/Precision Scientific, Chicago, Illinois); Inulin (Sigma Chemical Company, St. Louis, Missouri); Perkin-Elmer LC-55 spectrophotometer (Perkin-Elmer Corporation, Norwalk, Connecticut).

b. Preparation of reagents

1) Trichloroacetic acid (TCA) solution, 9.3%, was prepared by dissolving 9.3 gm TCA in water to make 100 ml. This solution was prepared in advance and stored at room temperature. 2) Sulfuric acid, 70%, was prepared by mixing 225 ml sulfuric acid, 93.2%, and water to make 300 ml. Due to heat of mixing, the addition of water was done a small amount (i.e. 20 ml) at a time with the solution allowed to cool between additions. This solution was prepared in advance and stored at room temperature. 3) Anthrone Solution, 0.2% in 70% sulfuric acid, was prepared by dissolving 0.2 gm anthrone in 100 ml 70% sulfuric acid.

This solution was prepared on its day of use. 4) Inulin standard solutions were prepared by dissolving 16 mg of inulin in 100 ml of water. Aliquots were then diluted to 12, 8, 4, 2, 1, and 0.5 mg inulin per 100 ml water. These solutions were prepared on the day of use.

c. Plasma sample preparation

Seventy-five µl plasma samples were mixed with 1.5 ml water and 0.75 ml 9.3% TCA solution. This mixture was stirred on a vortex mixer and spun at 2400 rpm for 10 minutes. After centrifugation, the supernatant from each sample was placed in a clean test tube.

d. Urine sample preparation

Urine samples had been diluted 100-fold at the time of collection, as noted in Section IV.B.2.c. These diluted samples were diluted 5-fold again with water prior to assay.

e. Assay for inulin in plasma and urine samples

A 0.2 ml aliquot of plasma supernatant, urine dilution, or inulin standard solution was combined with 2.0 ml Anthrone Solution. Samples were stirred on a vortex mixer and incubated at 37^{o}C for one hour in a Dubnoff shaker/waterbath (speed = 35 oscillations/ minute). After incubation, samples were cooled to room temperature and absorbance was read at 620 nm.

3. Results and discussion

A representative graph of ΔA_{620} versus inulin concentration in mg per cent is shown in Figure V-8. For this particular set of data, the linear equation which describes it is $y = (0.0477)x - 0.0012$ ($r^2 = 0.9995$). This standard curve demonstrates linearity over a concentration range of 0.5 to 12 mg per cent inulin. Low blank readings indicate negligible interference by endogenous compounds.

It is possible that the addition of mannitol as a diuretic in some samples could interfere with this reaction. However, Till (206) has reported this interference to be non-existent. Other exogenous compounds (furosemide, PAH) would not be expected to cause any interference.

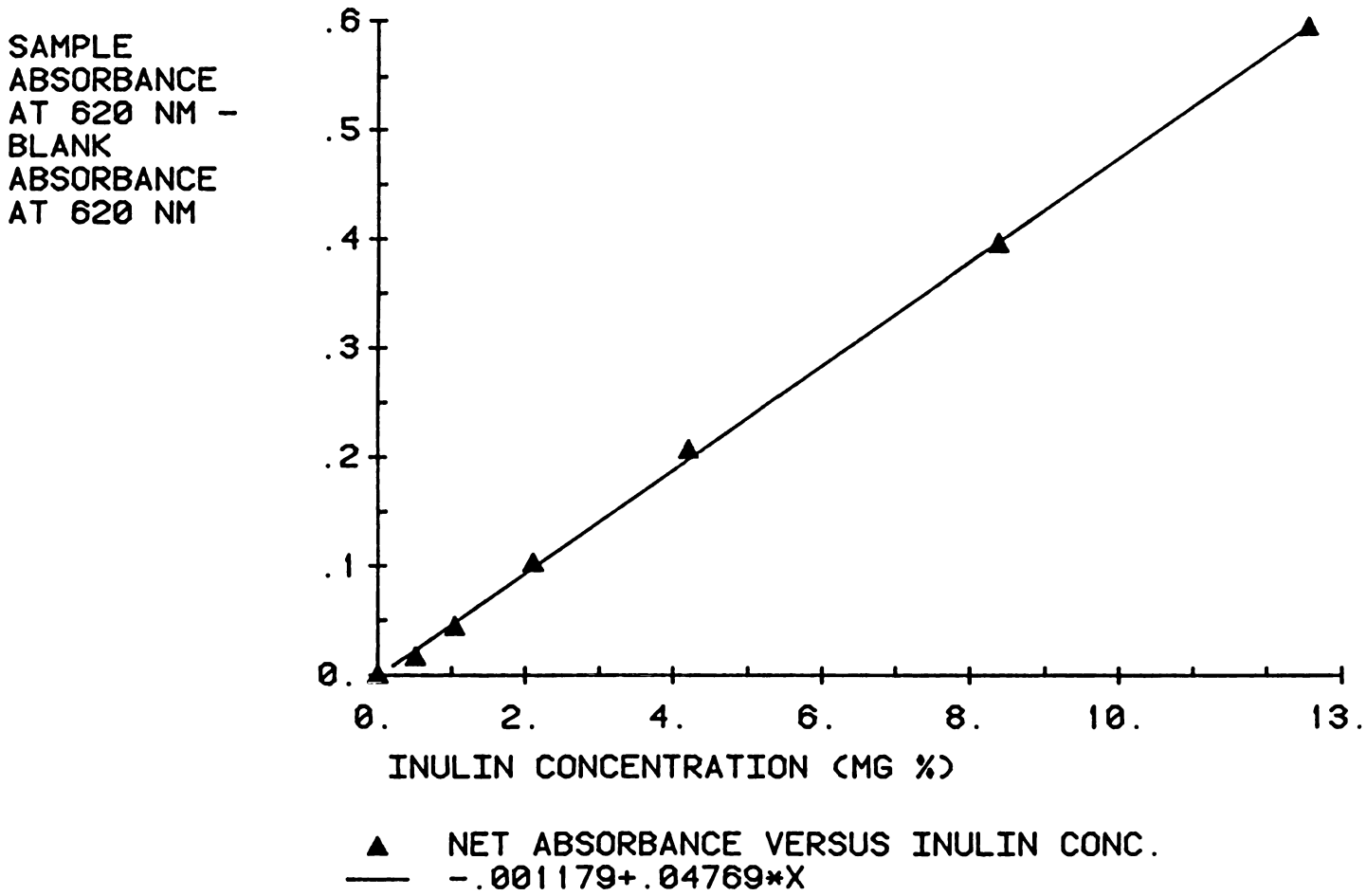

Figure V-8. Standard curve for inulin in water. This curve fits the equation $y = (0.04769)x - 0.001179$, with $r^2=0.9995$.

CHAPTER VI

VESICLE RESULTS

A. Introduction

Several types of experiments were done using vesicles prepared by the sucrose density gradient method of Mamelok et al. (94). Results from the various types of studies will be reported and discussed separately, with comparison of two or more types of studies following presentation of all appropriate data.

B. Effect of furosemide on PAH transport

1. Vesicles pre-incubated with furosemide for thirty minutes

a. Results

A sample graph of pmole PAH uptake/mg protein versus time is shown in Figure VI-1. This graph illustrates significant inhibition of PAH uptake by probenecid. It also shows furosemide inhibition of PAH uptake. It appears that, although a 0.1mM concentration of furosemide did not effectively inhibit uptake of 0.1mM PAH, 0.5mM and 1.0mM furosemide concentrations did decrease PAH uptake considerably.

Average results from studies investigating furosemide's effect on PAH uptake are shown in Table VI-1. The number of experiments for each value is indicated on the table, with four determinations of each value from each experiment. These average results indicate that probenecid

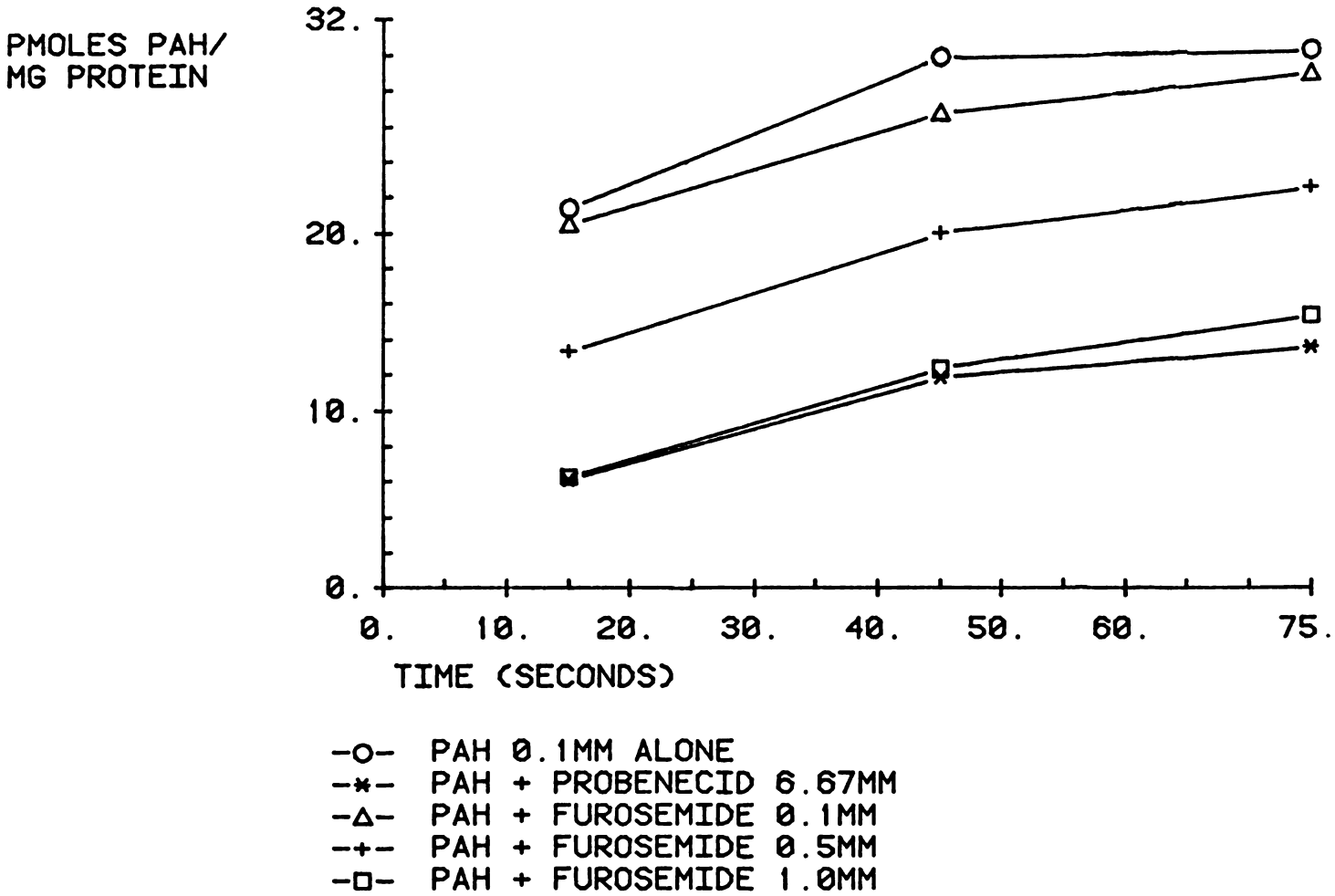

Figure VI-1. PAH uptake versus time. Furosemide and probenecid added at least thirty minutes prior to PAH addition.

TABLE VI-1. PAH UPTAKE IN BASAL-LATERAL MEMBRANE VESICLES.
EFFECT OF PROBENECID AND FUROSEMIDE ON PAH UPTAKE.
ADDITION OF FUROSEMIDE THIRTY MINUTES PRIOR TO ADDITION OF PAH.

Incubation Time (seconds) (n= number of experiments[a])	Uptake of PAH (pmoles PAH/ mg protein)	Organic Anion Components of Samples			
		Percent Inhibition of PAH Transport			
	PAH 0.1mM alone	PAH 0.1mM + Probenecid 6.67mM	PAH 0.1mM + Furosemide 0.1mM	PAH 0.1mM + Furosemide 0.5mM	PAH 0.1mM + Furosemide 1.0mM
5 (n=3)	15.6±8.2	45.2±24.0%[b]	6.0±13.6%[b]	26.3±6.3%	16.1±7.5%
10 (n=3)	23.3±9.9	51.2±9.5%	-4.8±20.2%	40.5±5.2%	37.0±8.1%
15 (n=6)	28.1±15.8	63.2±8.3%	18.3±16.1%	42.6±11.7%	52.9±14.1%
45 (n=4)	29.9±10.5	49.6±10.8%	17.4±44.8%	46.4±24.3%	55.8±6.7%
75 (n=4)	29.2±6.6	35.8±21.2%	7.9±20.2%	18.1±6.5%	38.7±9.1%
3600 (n=6)	59.6±19.7	15.9±16.4%	-1.4±14.7%	7.1±27.2%	9.4±22.1%

[a]Each experiment included 4 identical samples for each time point and set of sample components.

[b]Only two experiments are included in these values. Values are therefore Mean ± Range.

inhibited the uptake of 0.1mM PAH extensively. This inhibition reached a maximum at 15 seconds, and then decreased with increasing incubation time.

At 0.1mM furosemide concentration, slight inhibition of PAH uptake was seen at 15 seconds. However, other time points did not show an inhibition of PAH uptake by this furosemide concentration. For 0.5 and 1.0mM furosemide concentrations, PAH uptake was inhibited extensively. In fact, at 45 and 75 seconds, 1.0mM furosemide appeared to inhibit PAH uptake to approximately the same degree as did 6.67mM probenecid.

b. Discussion

Probenecid, 6.67mM, was used to ensure maximum inhibition of PAH uptake and thus give an indication of the viability of the vesicular membranes. In all experiments, significant inhibition of PAH uptake was seen using probenecid. Thus, the vesicles were believed to be viable and transporting PAH by means of a carrier-mediated transport system which could undergo competitive inhibition.

Other researchers have used inhibition of PAH uptake by probenecid as an indication of vesicle viability. Berner and Kinne (81), Sheikh and Moller (215), Kinsella et al. (82), Eveloff et al. (95), Miller (96), Mamelok et al. (94), Kasher et al. (91) and Hori et al. (97) have all used probenecid as an inhibitor of PAH carrier-mediated transport in basal-lateral membrane vesicles. Results from these researchers' work are presented in Table VI-2. Although different species, as well as different PAH and probenecid concentrations were used in these studies, similar levels of inhibition of PAH uptake were seen. Results obtained

TABLE VI-2. EFFECT OF PROBENECID ON PAH UPTAKE BY BASAL-LATERAL MEMBRANE VESICLES. DATA AVAILABLE IN THE LITERATURE.

Reference	Species	PAH Concentration (M)	Probenecid Concentration (M)	Incubation Time (seconds)	% Inhibition
Mamelok et al. (94)	rabbit	1×10^{-4}	6.7×10^{-3}	15 60	60% 65%
Berner & Kinne (81)	rat	1×10^{-5}	5×10^{-4}	60	53%
Sheikh & Moller (215)	rabbit	(not given)	1×10^{-3}	60	87%
Kinsella et al. (82)	dog	5×10^{-5}	1×10^{-2}	15	67%
Eveloff et al. (95)	flounder	5.8×10^{-5}	5×10^{-3}	20	75%
Miller et al. (96)	flounder	1×10^{-5}	5×10^{-3}	15	26%
Kasher et al. (91)	dog	5.0×10^{-5}	5×10^{-3}	15	50%
Hori et al. (97)	rat	1.25×10^{-4}	1×10^{-4} 1×10^{-3}	60 60	20% 35%

here agree with published data. In general, the inhibition of PAH uptake by probenecid is taken as evidence of a carrier-mediated transport system.

In the work presented here, the degree of PAH uptake inhibition observed with 1.0mM furosemide was similar to that seen with probenecid. These results may indicate that furosemide is a potent inhibitor of PAH carrier-mediated transport. No other studies of the interaction between furosemide and PAH in basal-lateral membranes have been reported in the literature. However, an interaction between PAH and furosemide, and its effect on the transport of PAH, has been examined using other experimental models. In possum cortical slices, Miller and Morris (216) found 81% inhibition of 0.015mM PAH uptake in the presence of 0.75mM furosemide. In isolated perfused rabbit kidneys, Bito and Baroody (87) found that 29μM furosemide caused 50% inhibition of 0.1μM PAH secretion. Two groups of researchers have looked at furosemide inhibition of PAH transport in brush border membranes. Blomstedt and Aronson (85) obtained approximately 83% inhibition of 1.0μM PAH uptake in the presence of 1.2mM furosemide. Kahn et al. (84) saw 70% inhibition of 2.0μM PAH uptake with 0.2mM furosemide, and 90% inhibition with 2.0mM furosemide concentration. The results presented here fit well with these literature values.

A study involving inhibition of basal-lateral membrane PAH uptake by other organic anion drugs has been reported by Kasher et al. (91). Using dog basal-lateral membranes, they report that cephaloridine and cefazolin inhibited 50μM PAH uptake by 46 and 49%, respectively, with inhibitor concentrations of 5mM. These results, when compared to the results involving furosemide presented here, indicate that furosemide's

ability to inhibit PAH uptake is at least comparable to that of cephaloridine and cefazolin. Given that the PAH concentration used here was two times that used by Kasher et al. (91), and that the maximum furosemide concentration was only one-fifth the cephalosporin concentration used by Kasher et al., there is a possibility that the ability of furosemide to inhibit PAH transport is even greater than that of the cephalosporins.

Due to the limited solubility of furosemide in water, higher concentrations were not used. Both cephalosporins used by Kasher et al. (91) are soluble in water and do not present this problem. If higher levels of furosemide as inhibitor were used, perhaps even greater inhibition of PAH uptake would be demonstrated.

Other similar work, involving inhibition of PAH uptake in basal-lateral membranes by other organic anion drugs, has not been reported to date. More extensive work, involving other drugs, will provide a better basis for comparison of these results.

2. No pre-incubation with furosemide

a. Results

Two experiments were done, in which samples were prepared and incubated for thirty minutes, at 37°C, without furosemide as inhibitor. Just prior to addition of ^{3}H-PAH, furosemide was added to the appropriate samples.

A representative graph of pmole PAH uptake/mg protein versus time is shown in Figure VI-2. Average results of these experiments are shown

in Table VI-3. Probenecid again extensively inhibited the uptake of PAH. The lowest furosemide concentration appeared to inhibit PAH uptake at five and ten seconds; however, later time points did not exhibit this inhibition.

For higher (0.5 and 1.0mM) concentrations of furosemide, inhibition of PAH uptake was seen for all sampling times. Again, inhibition of PAH uptake at the highest (1.0mM) furosemide concentration was similar to that seen with probenecid.

b. Discussion

These studies indicate that furosemide is able to inhibit the uptake of PAH, even when it is added immediately (< 5 seconds) before the PAH solution is added. Probenecid was added at least thirty minutes prior to addition of ^{3}H-PAH. This was done because of lack of information about the "on time" of probenecid—the time it takes for probenecid to bind effectively to the carrier. It is important that probenecid be able to attach to the carrier; otherwise it would not be known if the vesicles were functional, or if there were only a methodological problem. In the case of furosemide, however, it was of interest to see if the drug could inhibit the uptake of PAH when both compounds were presented to the vesicles at approximately the same time. These results indicate that furosemide is able to inhibit PAH uptake under both sets of conditions—when added at least thirty minutes prior to addition of ^{3}H-PAH, and when added immediately prior to ^{3}H-PAH addition.

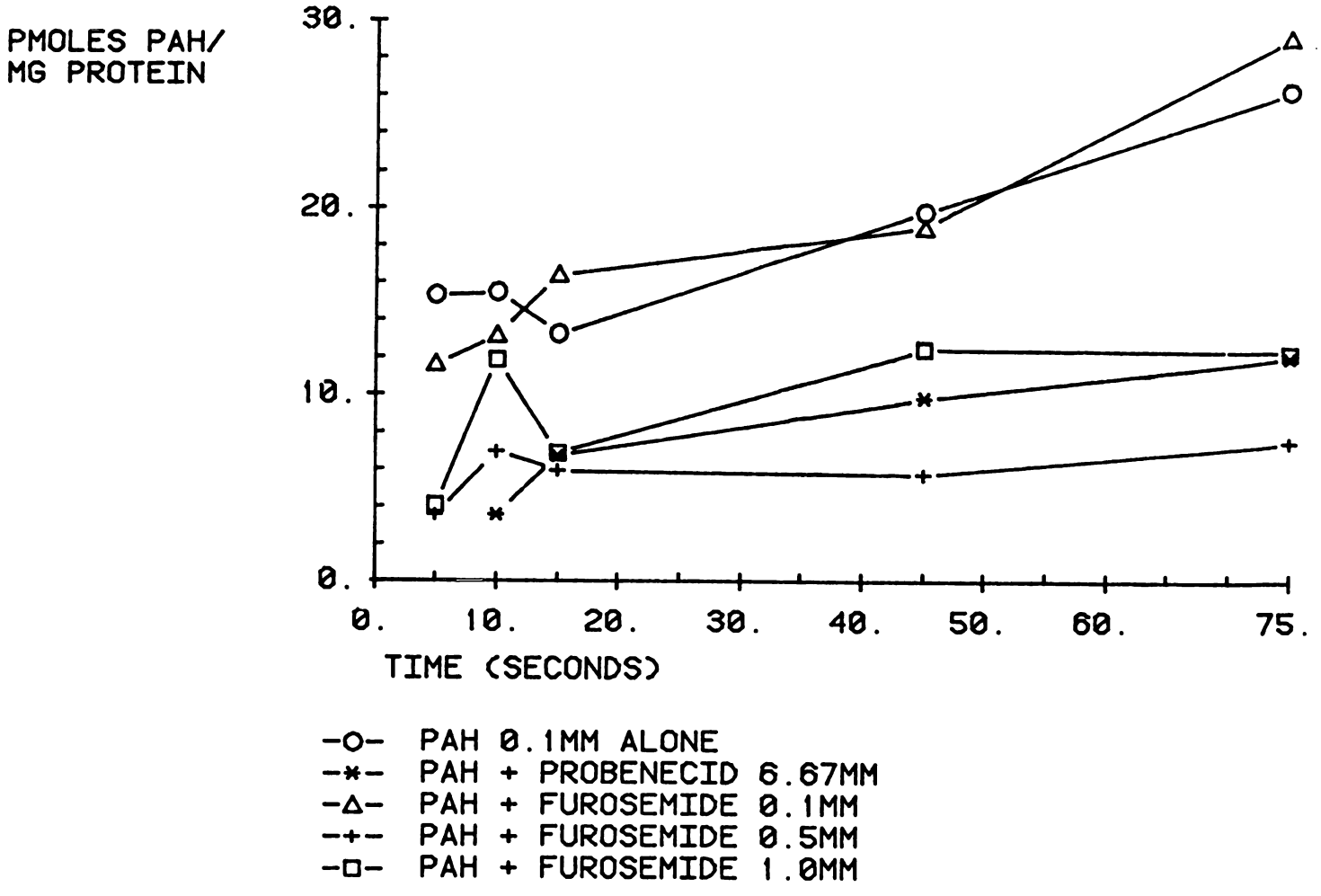

Figure VI-2. PAH uptake versus time. Furosemide added less than five seconds prior to PAH addition.

TABLE VI-3. PAH UPTAKE BY BASAL-LATERAL MEMBRANE VESICLES.
EFFECT OF PROBENECID AND FUROSEMIDE ON PAH UPTAKE.
ADDITION OF FUROSEMIDE IMMEDIATELY PRIOR TO ADDITION OF PAH.

Incubation Time (seconds) (n = number of experiments[a])	Uptake of PAH (pmoles PAH/ mg protein)	Organic Anion Components of Samples — Percent Inhibition of PAH Uptake			
	PAH 0.1mM alone	PAH 0.1mM + Probenecid 6.67mM	PAH 0.1mM + Furosemide 0.1mM	PAH 0.1mM + Furosemide 0.5mM	PAH 0.1mM + Furosemide 1.0mM
5 (n=2)	14.8±0.5	73.8±26.2%	33.0±8.7%	54.2±22.8%	62.8±10.8%
10 (n=2)	17.3±1.9	70.5±6.8%	27.0±6.8%	54.5±0.9%	36.6±13.4%
15 (n=2)	19.3±6.1	55.6±6.3%	7.7±31.4%	56.9±1.2%	54.6±6.4%
45 (n=2)	27.5±7.8	55.6±4.8%	14.0±9.9%	68.2±3.5%	47.5±10.1%
75 (n=2)	29.4±3.2	48.7±5.6%	-5.1±5.9%	46.1±25.7%	46.4±7.0%
3600 (n=2)	66.6±16.1%	16.6±4.9%	4.8±13.9%	4.2±9.5%	11.8±12.9%

[a]Each experiment included 4 identical samples for each time point and set of sample components. Values shown here represent Mean ± Range.

Comparison of early time points for all furosemide concentrations, as well as later time points for 0.5mM furosemide under the two conditions, may indicate increased inhibition of PAH uptake when furosemide is added immediately prior to PAH addition. In general, these differences are not statistically significant. Such a real difference could be caused by increasing non-specific binding of furosemide to the vesicles over time. By adding furosemide thirty minutes prior to adding PAH, some of the furosemide may bind to the membrane, thus decreasing the free furosemide concentration available to competitively inhibit the uptake of PAH. If furosemide is added just prior to PAH addition, this binding and subsequent decrease in concentration will be lessened. Binding of furosemide to the membrane will be discussed in Section IV.D.1.

Here again, inhibition of PAH uptake by 0.5 and 1.0mM furosemide was close to that seen with 6.67mM probenecid. It appears that furosemide is able to cause extensive inhibition of PAH transport, even when presented to the carrier just prior to PAH addition. It may well be that furosemide has an "on time" similar to that of PAH, and/or has a higher affinity for the carrier.

C. Effect of PAH on furosemide transport

1. Non-purified ^{3}H-furosemide

No pre-incubation with PAH

a. Results

Results of a representative study observing the effect of PAH on furosemide uptake are shown in Figure VI-3. These samples had PAH added immediately (< 5 seconds) before addition of furosemide. This study indicated that, although inhibition of furosemide uptake by probenecid occurred, inhibition by PAH was less apparent. There appeared to be much scatter in the data, which made it more difficult to determine a true inhibitory effect.

Average results from five experiments studying the effect of PAH on furosemide's uptake by basal-lateral membrane vesicles are shown in Table VI-4. These results differed significantly from those obtained when inhibiting PAH uptake by furosemide. Based on these average data, PAH did not appear to have a significant effect on furosemide's uptake by basal-lateral membrane vesicles. Furosemide uptake was inhibited by probenecid. However, its percent of uptake inhibition (35.4% at 15 seconds) was less than that seen with PAH uptake inhibition due to probenecid (55.6%). This decreased inhibition was seen at all time points. It should also be noted that the apparent furosemide uptake, in pmoles/mg protein, was significantly greater than apparent PAH uptake under similar conditions.

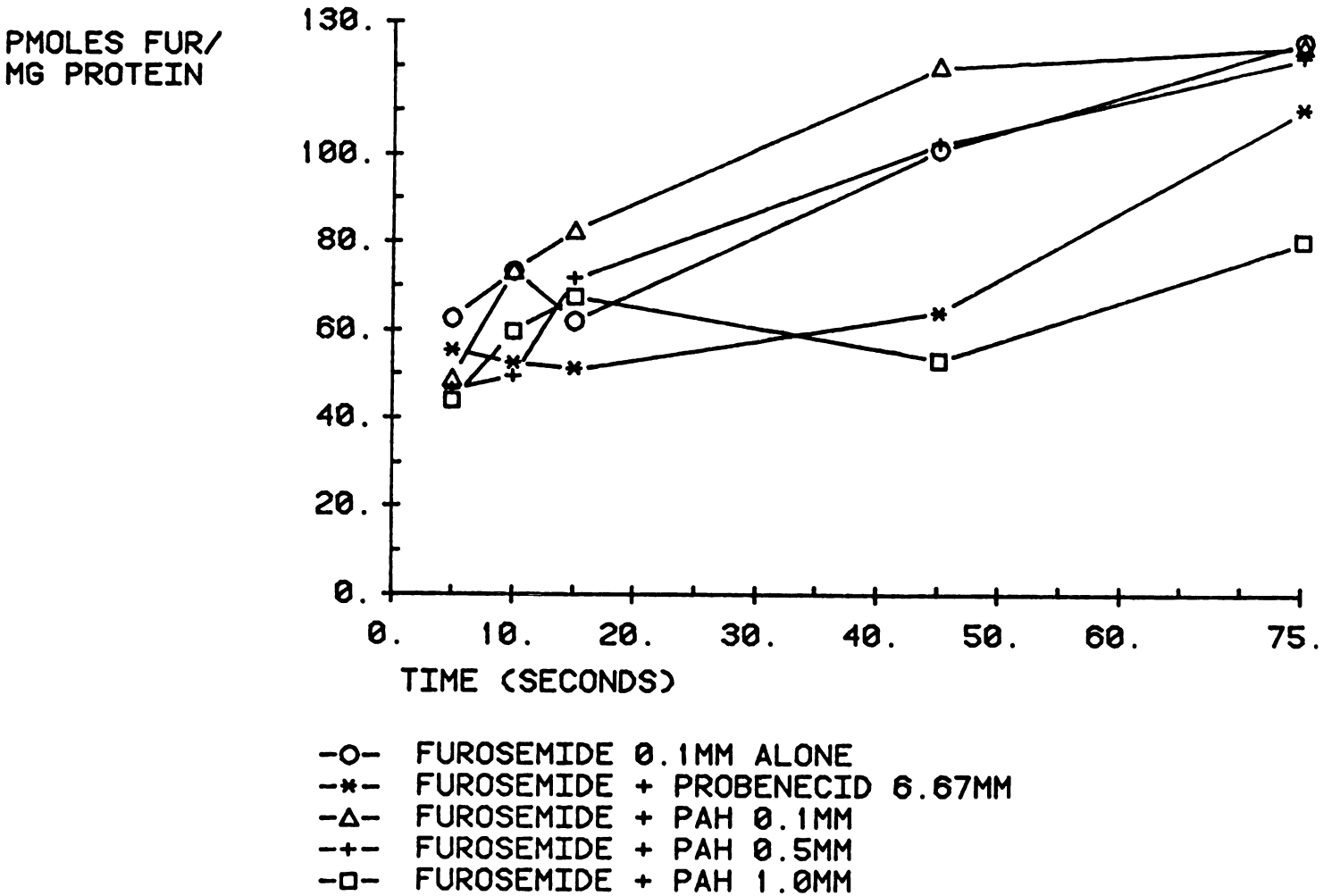

Figure VI-3. Furosemide (FUR) uptake versus time, using non-purified furosemide. This experiment used ^{3}H-furosemide as supplied by New England Nuclear. PAH was added less than five seconds prior to furosemide addition.

TABLE VI-4. FUROSEMIDE UPTAKE BY BASAL-LATERAL MEMBRANE VESICLES.
EFFECT OF PROBENECID AND PAH ON FUROSEMIDE UPTAKE.
NON-PURIFIED FUROSEMIDE, ADDITION OF PAH IMMEDIATELY BEFORE ADDITION OF FUROSEMIDE.

Incubation Time (seconds)	Organic Anion Components of Sample				
	Furosemide Uptake (pmoles furosemide/ mg protein)	Inhibition of Furosemide Uptake (Percent Inhibition)			
(n = number of experiments[a])	Furosemide 0.1mM alone	Furosemide 0.1mm + Probenecid 6.67mM	Furosemide 0.1mM + PAH 0.1mM	Furosemide 0.1mM + PAH 0.5mM	Furosemide 0.1mM + PAH 1.0mM
5 (n=4)	80.6±65.0	23.8±13.6%	1.7±24.4%	-7.2±40.9%	-2.1±34.6%
10 (n=4)	107.0±74.3	36.0±13.2%	6.6±26.7%	18.0±32.0%	7.7±16.1%
15 (n=4)	107.8±77.1	16.9±21.6%	-3.6±21.6%	-9.9±16.2%	-13.9±18.7%
45 (n=4)	166.8±124.6	35.4±9.4%	2.4±43.9	-4.2±31.4%	7.1±48.3%
75 (n=4)	191.0±125.3	28.1±13.0%	16.6±18.7%	12.1±10.4%	2.4±33.1%
3600 (n=4)	457.8±96.6	10.2±30.0%	6.8±41.6%	4.6±32.1%	-5.9±15.6%

[a]Each experiment included 4 identical samples for each time point and set of sample components.

b. Discussion

There are obvious differences between the effect of furosemide on PAH uptake, and the effect of PAH on furosemide uptake. Furosemide definitely decreases PAH uptake by basal-lateral membranes, whereas PAH does not appear to significantly decrease furosemide uptake. Furosemide also appears to be taken up by vesicles to a higher concentration than is PAH. These differences may be attributed to any or all of the following possible reasons. 1) Furosemide may, in fact, be transported more rapidly and/or more extensively than PAH, due to a higher affinity for the carrier, i.e., more rapid "on" and "off" carrier times, etc. This increase in rate of transport might then cause furosemide uptake to be greater than PAH uptake at the times studied. Braunlich (217) found that furosemide accumulates more extensively than does PAH in rat renal cortical slices. The results shown here may further support those presented by Braunlich. 2) The ^{3}H-furosemide used was perhaps not pure, and so radiolabelled breakdown products were either also being taken up into the vesicle, and/or were binding to the vesicular membrane. 3) Furosemide may non-specifically bind extensively to the vesicle membrane, so that actual uptake is significantly less than apparent uptake. Furosemide uptake was significantly inhibited by probenecid. This is evidence that furosemide is being transported by an anion carrier system. However, it is possible that probenecid only inhibits some non-specific binding of furosemide, and that transport does not actually take place. The following studies were designed to determine which of these possibilities was responsible for the differences seen in the data.

2. Purified ^{3}H-furosemide

Vesicles pre-incubated with PAH for thirty minutes

a. Introduction

One concern was whether or not purity of ^{3}H-furosemide could be affecting uptake results. ^{3}H-Furosemide was greater than 99% radiochemically pure when provided by New England Nuclear in an ethanol solution. Unfortunately, furosemide is not stable in alcohol solution over long periods of time. Seven months after receipt of the ^{3}H-furosemide, its purity was re-checked. A five µl aliquot was injected onto a C_{18} column, using the conditions of the furosemide assay for plasma or urine developed in this laboratory (see Section V.B.). One minute fractions were collected, and UV detection at 254 nm was used to determine the exact location of the furosemide peak. The decay of tritium was determined, using a Beckman scintillation counter.

Approximately 30% of the radioactivity in the ^{3}H-furosemide solution was found to be associated with fractions other than those containing furosemide. It was decided to purify the ^{3}H-furosemide, and this was done as described in Section V.C. Purified ^{3}H-furosemide was then used in subsequent uptake experiments. The following results were obtained from studies using purified ^{3}H-furosemide, in which vesicles were incubated with appropriate inhibitors (none, probenecid, or PAH) for at least thirty minutes prior to furosemide addition.

b. Results

Two sample graphs of furosemide uptake versus time is shown in Figures VI-4 and VI-5. A significant inhibition of furosemide uptake by probenecid was seen once again in both experiments. However, there appeared to be definite inhibition of furosemide uptake in the presence of PAH in Figure VI-4 whereas Figure VI-5 shows more scatter in the data, and therefore less obvious inhibition of furosemide uptake.

Table VI-5 shows average results from four experiments involving furosemide uptake, in which purified ^{3}H-furosemide was used. At fifteen seconds, uptake of furosemide was 103.6 pmole/ mg protein. This is similar to values obtained using non-purified ^{3}H-furosemide. Based on standard deviations, the data from purified preparations was generally more consistent between experiments than was the data using non-purified ^{3}H-furosemide. The average data shows inhibition of furosemide uptake by PAH. However, due to scatter in the data, there are large standard deviations in the values seen, and consequently the inhibition is not statistically significant. Probenecid inhibited furosemide uptake by 51.1% at fifteen seconds. This is greater inhibition by probenecid than was seen with non-purified ^{3}H-furosemide transport studies. This increased inhibition holds true for other incubation times as well.

c. Discussion

The results of furosemide uptake using purified ^{3}H-furosemide were similar to those seen with non-purified ^{3}H-furosemide. Furosemide uptake under control conditions reached similar levels at various time

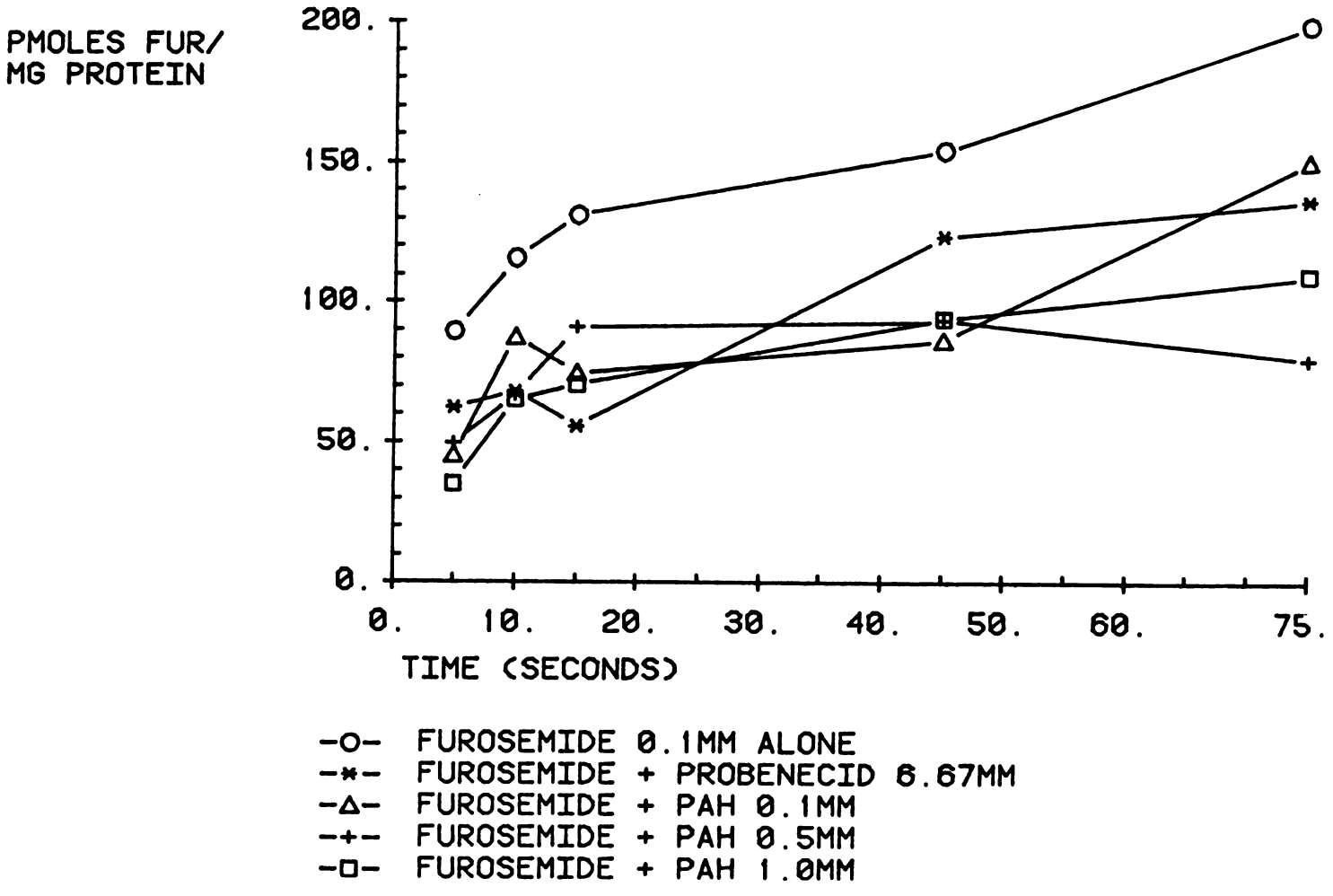

Figure VI-4. Furosemide (FUR) uptake versus time, using purified furosemide. Radiolabelled furosemide was purified as described in Section V.C. PAH was added at least thirty minutes prior to furosemide addition.

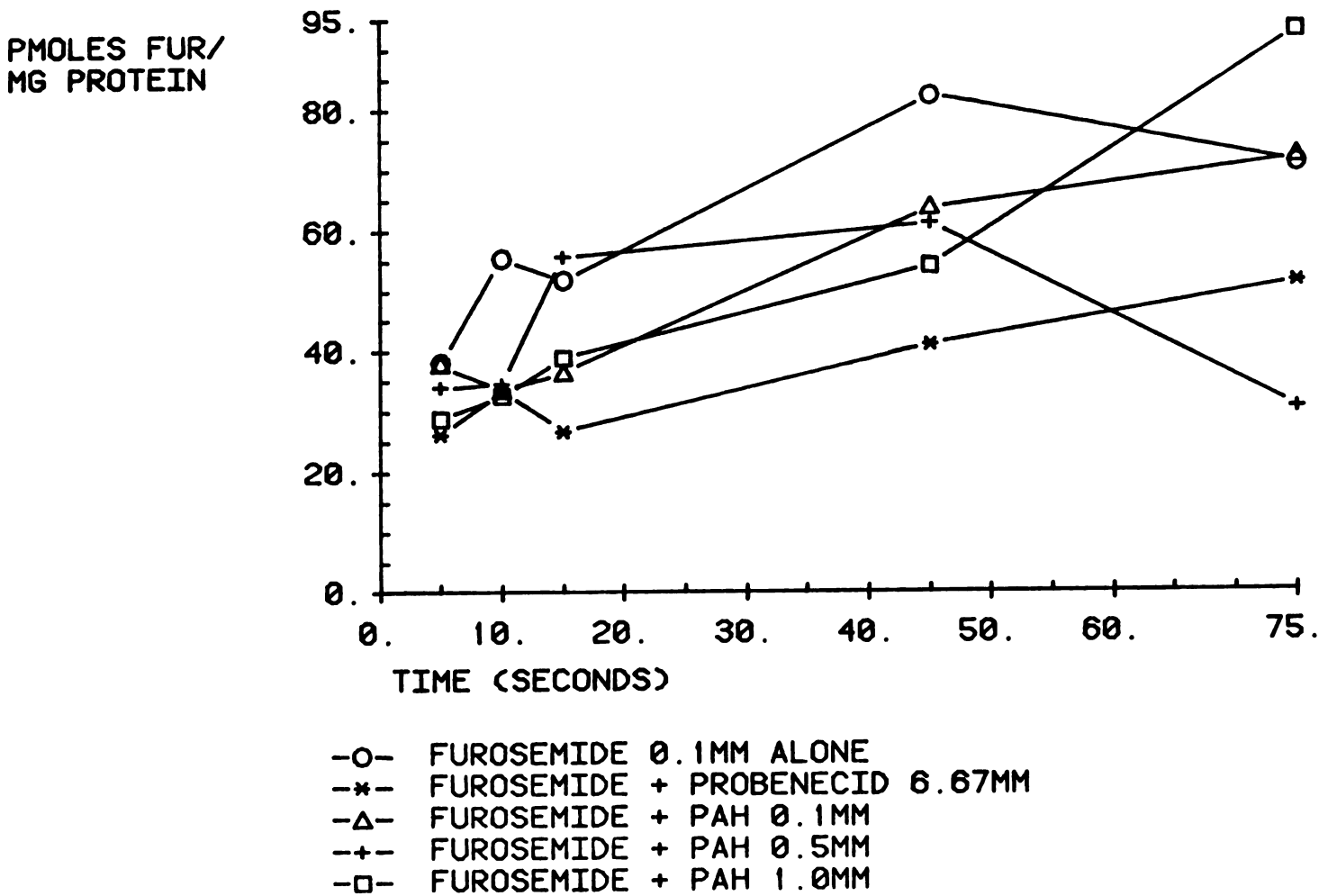

Figure VI-5. Furosemide (FUR) uptake versus time, using purified furosemide. Same conditions as Figure VI-4.

TABLE VI-5. FUROSEMIDE UPTAKE BY BASAL-LATERAL MEMBRANE VESICLES.
EFFECT OF PROBENECID AND PAH ON FUROSEMIDE UPTAKE.
PURIFIED FUROSEMIDE, ADDITION OF PAH THIRTY MINUTES PRIOR TO ADDITION OF FUROSEMIDE.

Incubation Time (seconds)	Organic Anion Components of Sample				
	Furosemide Uptake (pmoles furosemide/ mg protein)	Inhibition of Furosemide Uptake (Percent Inhibition)			
(n = number of experiments[a])	Furosemide 0.1mM alone	Furosemide 0.1mM + Probenecid 6.67mM	Furosemide 0.1mM + PAH 0.1mM	Furosemide 0.1mM + PAH 0.5mM	Furosemide 0.1mM + PAH 1.0mM
5 (n=4)	65.8±21.7	39.0±10.9%	1.4±34.2%	18.0±18.2%	28.8±23.6%
10 (n=4)	96.0±39.6	40.7±7.2%	14.5±22.8%	21.2±23.6%	22.9±28.1%
15 (n=4)	103.6±38.1	51.5±5.8%	28.7±16.8%	15.7±16.8%	31.5±10.5%
45 (n=4)	130.6±37.8	42.4±15.8%	11.7±27.3%	26.3±9.6%	36.3±9.3%
75 (n=4)	148.1±56.1	36.3±9.2%	25.2±21.2%	41.0±20.3%	17.0±33.9%
3600 (n=4)	298.7±111.0	31.6±5.1%	13.1±10.4%	15.7±14.9%	21.4±8.0%

[a]Each experiment included 4 identical samples for each time point and set of sample components.

points whether purified or non-purified radiolabelled furosemide was used. This appears to indicate that the impurities in the ^{3}H-furosemide were not affecting its apparent uptake. However, these results may also be due to a combination of non-specific binding of radiolabelled breakdown products and a decreased ^{3}H-furosemide uptake. These two factors combined could result in apparent uptake values the same as those seen with purified ^{3}H-furosemide. As a result, this does not indicate that purification of the ^{3}H-furosemide is of no value.

Upon examining standard deviations as a measure of variability in the data, there seems to be somewhat less variability in the experiments utilizing purified ^{3}H-furosemide. This decreased variability may be due to the use of purified ^{3}H-furosemide. The radiolabelled breakdown products may have been binding non-specifically to the vesicle membranes. More variability would be expected from non-specific binding, as was seen here. Consequently, the purification of ^{3}H-furosemide appeared useful for decreasing variability in the data.

Inhibition of furosemide uptake by probenecid is also enhanced in vesicles transporting purified material. This change may also be attributed to the removal of radiolabelled breakdown products of furosemide. With less apparent uptake due to non-specific binding of radiolabelled breakdown products, a higher percentage of apparent uptake will be due to actual uptake, with a correspondingly higher percentage of apparent uptake inhibitable by probenecid. Due to the changes in variability of data and increased probenecid-inhibitable uptake, it was deemed worthwhile to purify the ^{3}H-furosemide to be used in further transport experiments.

As stated under Results for this section (Section VI.C.2.b.), PAH may have a significant effect on the uptake of radiolabelled furosemide in these experiments. One experiment definitely indicated this (Figure VI-4), while the others tend to demonstrate this effect also. Unfortunately, due to scatter in the data, a statistically significant inhibition of furosemide uptake by PAH is not seen. One reason may be the addition of PAH at least thirty minutes prior to furosemide addition. The PAH may not be able to compete for carrier binding under these conditions--it may bind to the membrane in other locations, for example, and not be available for competitive inhibition of transport. The following experiments were done to answer this question.

3. Purified ^{3}H-furosemide with PAH

   No pre-incubation

   a. Results

Two experiments were done, using purified ^{3}H-furosemide, in which PAH, as an inhibitor, was added immediately prior to (< five seconds before) ^{3}H-furosemide addition. Average results are shown in Table VI-6. Furosemide uptake in control vesicles was again similar to other experiments reported here, as was probenecid inhibition of furosemide uptake. Also, once again inhibition of furosemide uptake by 0.1mM, 0.5mM and 1.0mM PAH was seen. However, due to variability in the data, this inhibition was again not statistically significant.

TABLE VI-6. FUROSEMIDE UPTAKE BY BASAL-LATERAL MEMBRANE VESICLES.
EFFECT OF PROBENECID AND PAH ON FUROSEMIDE UPTAKE.
PURIFIED FUROSEMIDE, ADDITION OF PAH IMMEDIATELY PRIOR TO ADDITION OF FUROSEMIDE.

Incubation Time (seconds)	Organic Anion Components of Sample				
	Furosemide Uptake (pmoles furosemide/ mg protein)	Inhibition of Furosemide Uptake (Percent Inhibition)			
(n = number of experiments[a])	Furosemide 0.1mM alone	Furosemide 0.1mM + Probenecid 6.67mM	Furosemide 0.1mM + PAH 0.1mM	Furosemide 0.1mM + PAH 0.5mM	Furosemide 0.1mM + PAH 1.0mM
5 (n=2)	55.7±7.5	72.8±16.8%	41.7±10.4%	55.1%[b]	32.8±21.6%
10 (n=2)	84.6±10.8	54.8±2.5%	24.0±18.7%	47.2±24.3%	48.9±13.5%
15 (n=2)	87.4±3.1	56.4±10.7%	33.0±19.2%	41.6±11.4%	49.4±7.8%
45 (n=2)	101.0±29.1	30.2±5.7%	8.7±4.9%	26.2±42.8%	44.6±8.6%
75 (n=2)	108.8±29.1	64.0±23.1%	7.1±17.3%	-8.2±37.3%	49.4±12.7%
3600 (n=2)	359.3±9.40	29.0±4.7%	23.4±4.5%	27.6±4.9%	18.5±15.8%

[a]Each experiment included 4 identical samples for each time point and set of sample components. Values shown here indicate Mean ± Range.

[b]One experiment only.

4. Discussion

These results are similar to those described in previous sections. This may suggest that PAH is able to inhibit furosemide transport by basal-lateral membranes. Finally, this inhibition of furosemide transport by PAH may be further evidence that the two compounds share a common transport system.

D. Furosemide binding studies

1. Binding of furosemide to vesicles

a. Introduction

In order to partially quantify the extent to which binding of furosemide to the membrane affects apparent furosemide uptake, experiments were done with vesicles under various osmotic conditions. The osmolarity of the medium inside the vesicles was not changed from that used in other uptake studies. However, the osmolarity of the medium surrounding the vesicles was changed. As the osmolarity of the solution outside the vesicle increases, the water of the solution inside the vesicle will move out of the vesicle, in an attempt to equalize the osmotic pressure on both sides of the membrane. Movement of water from inside to outside will cause the vesicles to shrink. Eventually, at infinite external osmolarity, there will be no water left inside the vesicles, and thus no intravesicular volume. As a result, no transport of compounds will take place, and apparent transport will, in actuality,

be binding to the membrane.

In order for this method to be effective, a compound which will not cross the membrane must be used to increase the osmolarity of the extravesicular medium. The compound chosen for these studies was sucrose because it is not transported across basal-lateral membranes.

b. Results

Results of representative osmolarity binding studies are shown in Figures VI-6, VI-7 and VI-8. These three experiments were all done on the same day, using vesicles from the same preparation. This was done to insure that interday variability in uptake by vesicle preparations would not be a factor in these results. This will be discussed further in Section VI.D.2.b. These figures are plots of pmole furosemide uptake/mg protein versus 1/total osmolarity of the surrounding medium. A line was fitted to each graph, with slope, y-intercept, r and r^2 determined. The y-intercept represents "uptake" when the internal vesicular volume has been shrunk to zero. This "uptake" is then in fact binding to the membrane. In each plot, the point corresponding to 17.24 on the x-axis represents uptake in vesicles under normal uptake conditions--i.e., no sucrose added to the medium.

As Figure VI-6 indicates, the average furosemide uptake after fifteen seconds of incubation in vesicles to which sucrose had not been added was 87.4 pmoles furosemide/ mg protein. The y-intercept of the line fitted to this data was 15.2 pmoles furosemide/ mg protein. This represented 17.4% of the uptake in unaffected vesicles.

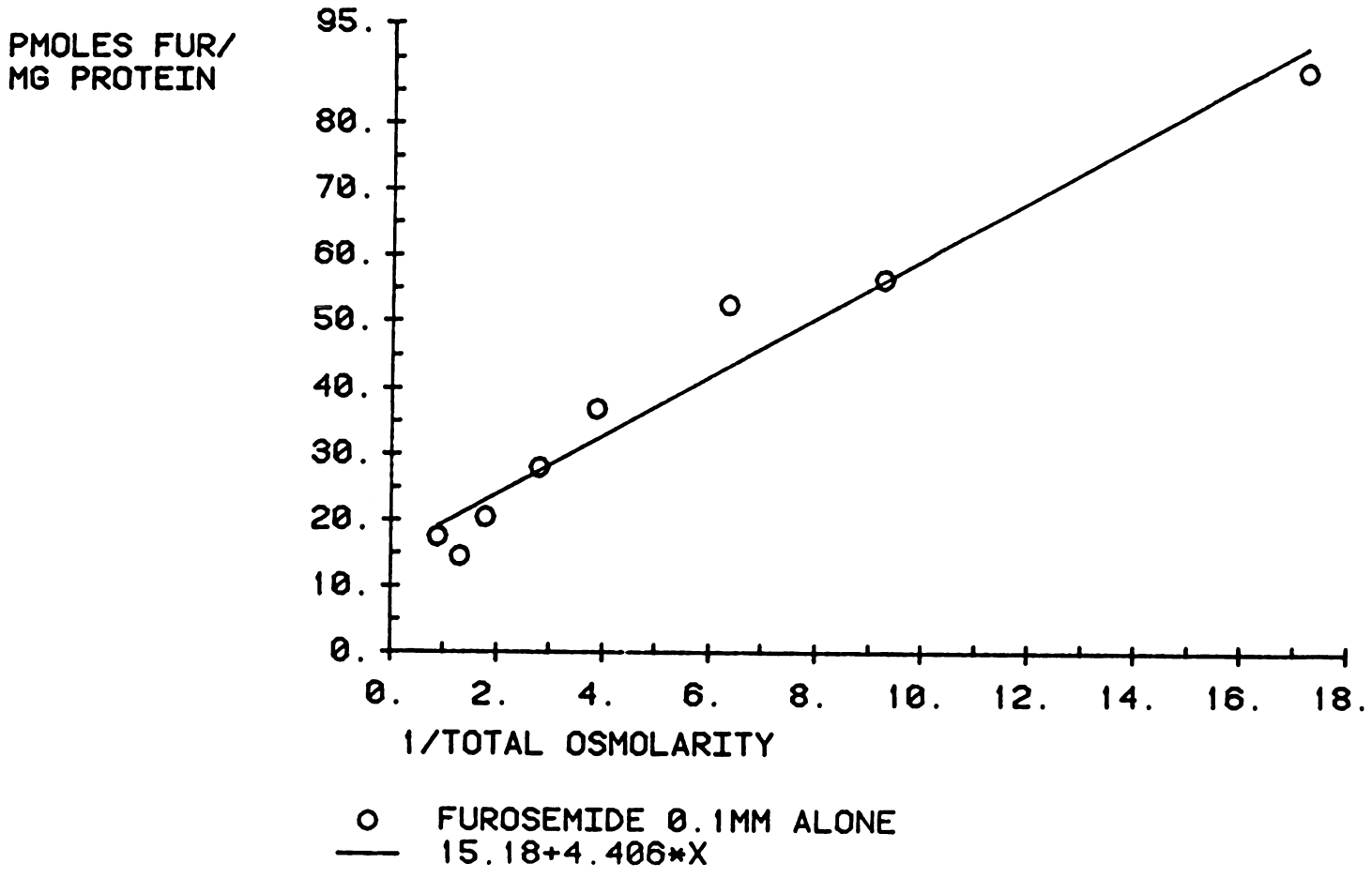

Figure VI-6. Furosemide (FUR) uptake after fifteen seconds incubation time versus 1/total osmolarity of the external medium. The amount of furosemide binding to the membranes is represented by the y-intercept, here equal to 15.18 pmoles/mg protein. For the fit line, r^2=0.9600.

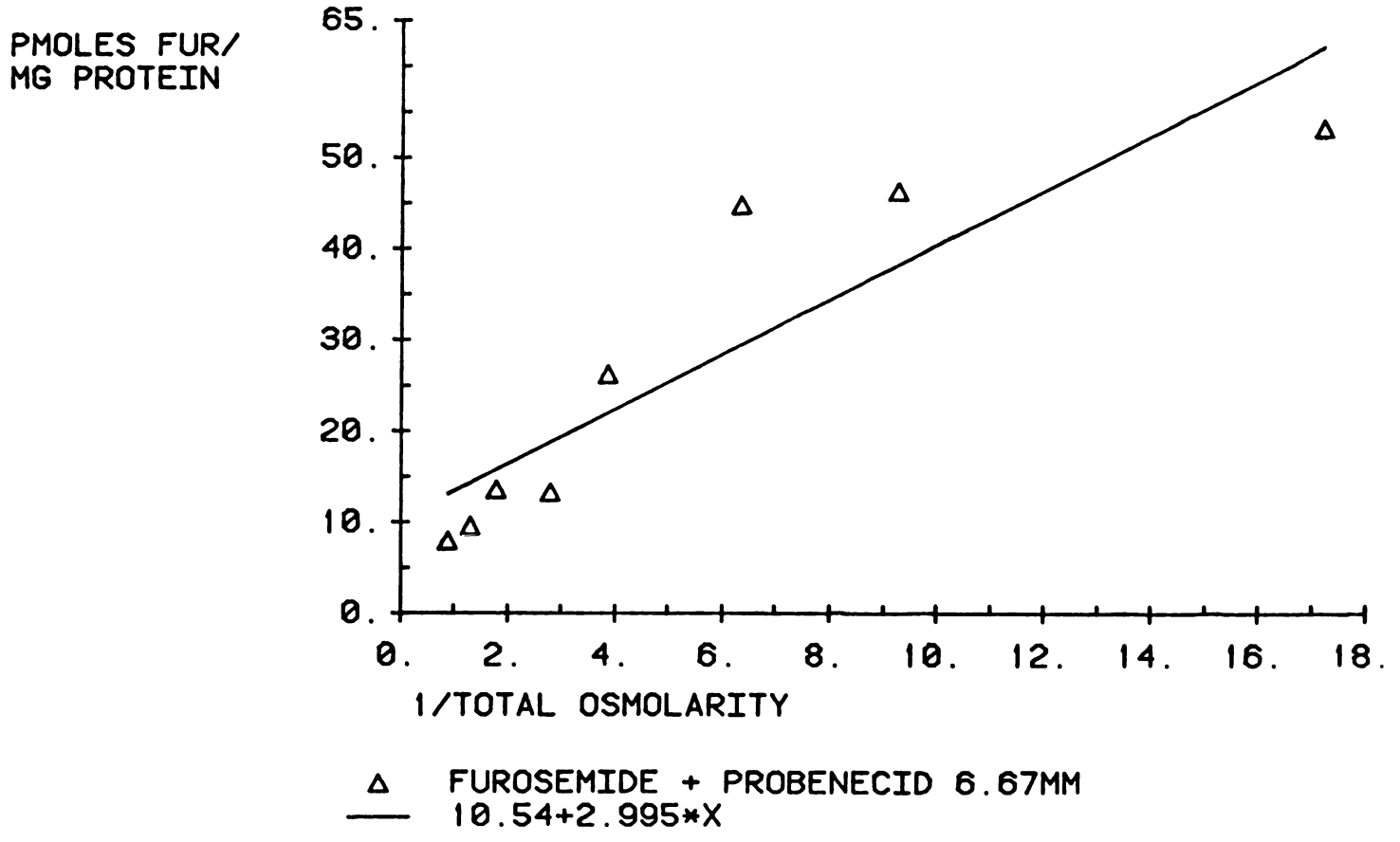

Figure VI-7. Furosemide (FUR) uptake in the presence of probenecid after fifteen seconds incubation time versus 1/total osmolarity of the external medium. For this experiment, binding of furosemide equals 10.54 pmoles/mg protein and r^2=0.8003.

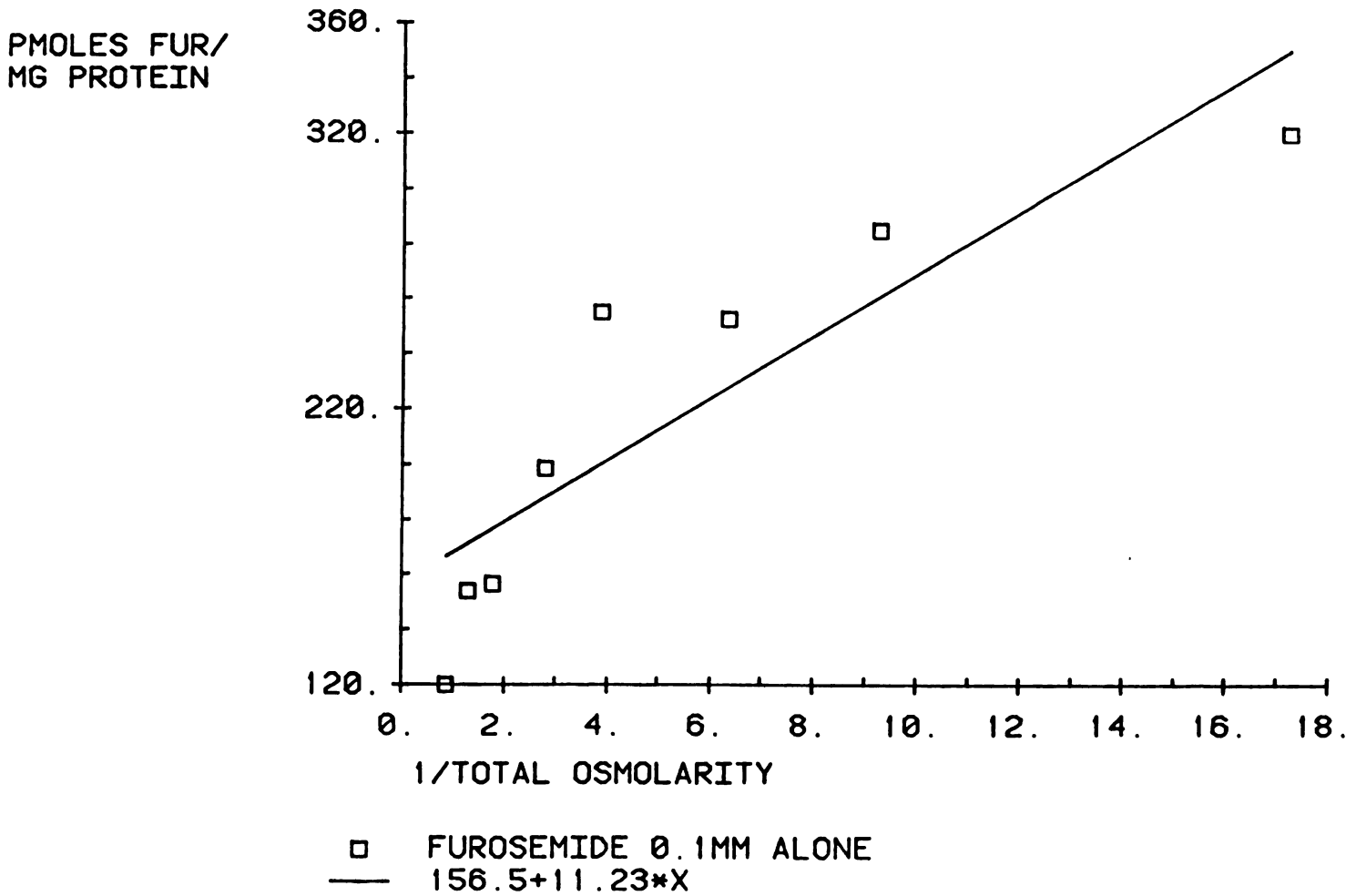

Figure VI-8. Furosemide (FUR) uptake after one hour incubation time versus 1/total osmolarity of the external medium. Furosemide binding to membranes is 156.5 pmoles/mg protein, and r^2=0.7706.

Figure VI-7 shows the results obtained in samples containing 6.67mM probenecid. All other conditions remained the same. Here the furosemide uptake was 53.2 pmoles/mg protein in vesicles not treated with sucrose. The amount of furosemide binding was 10.6 pmoles/mg protein, or 19.9% of apparent uptake in untreated vesicles.

For samples incubated one hour (Figure VI-8), the uptake in samples containing no sucrose was 320.0 pmole furosemide/mg protein. The y-intercept for this graph is 156.5 pmoles furosemide/mg protein. This value is 48.8% of uptake in untreated vesicles.

c. Discussion

The method of increased extravesicular osmolarity to measure binding to vesicles has been widely used (81,82,85,92-94). Other methods have also been used to determine binding. These methods include high-speed, lengthy centrifugation (218), standard filtration techniques (219) and disruption of vesicles by addition of distilled water, as described by Warnock and Yee (195) and Berner et al. (220). Since these studies required comparison of available PAH data with the furosemide data generated here, the method chosen was that commonly used in PAH binding studies--i.e., osmolarity changes.

These results indicate that furosemide does bind to basal-lateral membrane vesicles. Results of ^{3}H-PAH binding studies, done by Mamelok et al. (94) show that PAH is approximately 21% bound to basal-lateral membrane vesicles after two hours of incubation. Berner and Kinne (81) found 10% of PAH uptake to be binding to basal-lateral membranes, and Kinsella et al. (82) found less than 10% of PAH uptake due to binding.

However, their samples were only incubated for twenty and ten minutes, respectively. The longer incubation time of Mamelok et al. (94) may give rise to increased binding. Also, Berner and Kinne (81) and Kinsella et al. (82) used different species (rat and dog) than the rabbit, which was used by Mamelok et al. (94). Species differences may give rise to these differing results.

The studies presented here indicate that the binding of furosemide to vesicles is greater than that seen with PAH. The binding of furosemide appears to be significant even at early time points, and increases substantially with time until nearly 50% of apparent uptake at one hour is due to binding. Such extensive binding complicates the measurement of furosemide's actual uptake. It was of interest to attempt to decrease this binding by some method. Competition for non-specific binding sites seemed to be a reasonable way to decrease furosemide's binding. The following study was designed to determine if such competition could be demonstrated, and if the results would be useful for future studies.

2. Inhibition of furosemide binding

a. Results

Experiments were done in which vesicles were pre-incubated in buffer containing 0.1mM sulfisoxazole. Other vesicles from the same preparation were left in buffer without sulfisoxazole. All vesicles were stored at $4^{o}C$ overnight and then removed from the buffer by centrifugation the following morning (see Section III.D.2.c.). Both

sets of vesicles were then used for osmolarity binding experiments.

Results are shown in Figures VI-9 and VI-10. Figure VI-9 is an identical experiment to the one presented in Figure VI-8. The only difference is that the two experiments were done on two different days. It is presented here because it served as the control experiment on the day when the sulfisoxazole binding inhibition experiment was done. As can be seen, sulfisoxazole did decrease the binding of furosemide to vesicles by 62.3% after one hour's incubation. The data for samples containing sulfisoxazole (Figure VI-10) also fit a straight line equation better, with $r^2 = 0.943$, versus $r^2 = 0.767$ for untreated vesicles.

b. Discussion

The addition of sulfisoxazole to vesicles appears to decrease binding of furosemide to the vesicles. To date, extensive binding to basal-lateral membrane vesicles of a transported compound has not been reported in the literature. As a result, a method has not been developed for overcoming this problem. This study attempted to rectify this.

Sulfisoxazole was chosen as a possible inhibitor of furosemide binding. Smith and Benet (221) have reported that sulfisoxazole decreases furosemide binding to plasma proteins. Since this effect could perhaps be extrapolated to vesicle membranes, sulfisoxazole's action was studied.

The results obtained, though somewhat successful, were disappointing. Sulfisoxazole did inhibit furosemide binding and removed

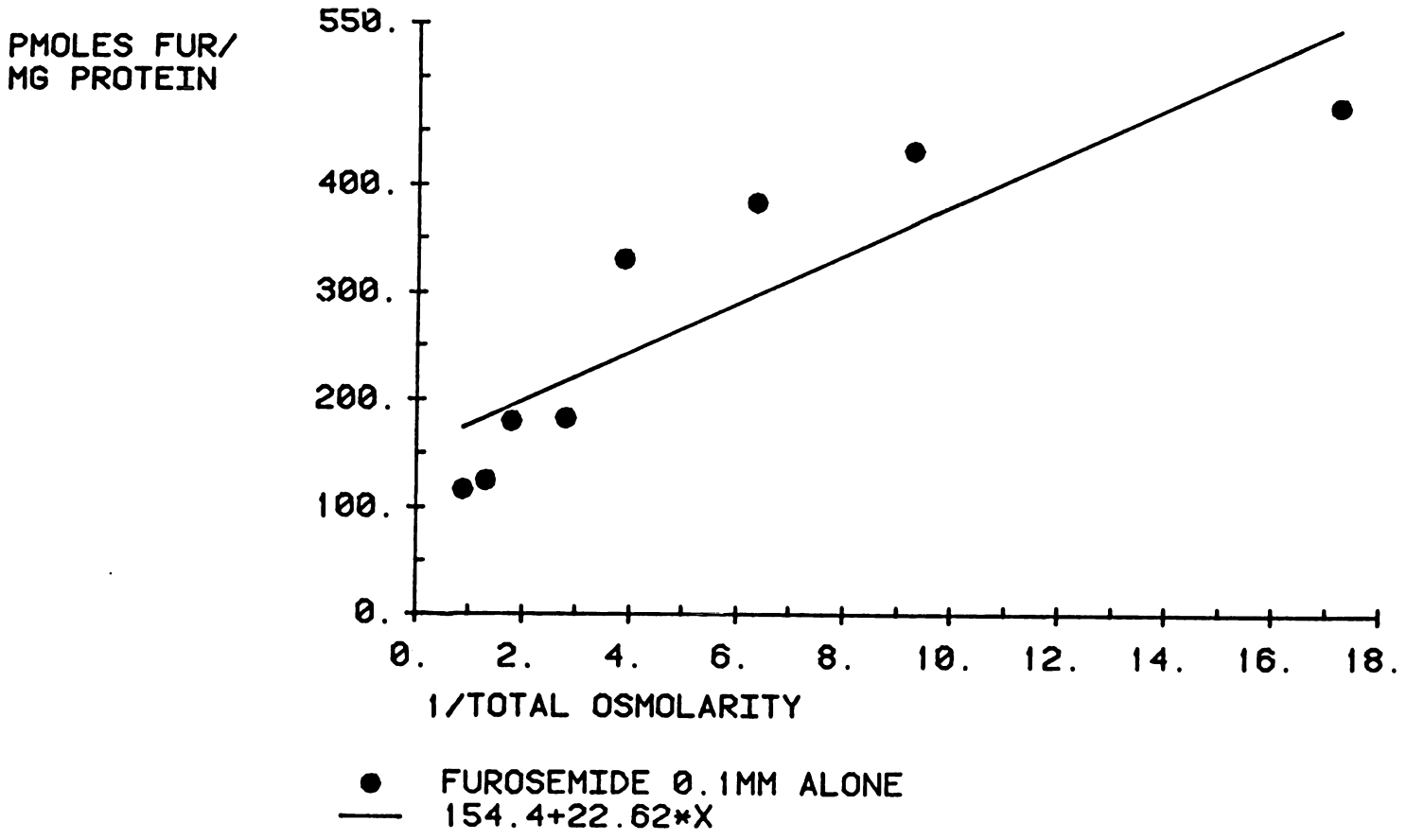

Figure VI-9. Furosemide (FUR) uptake after one hour incubation time versus 1/total osmolarity of the external medium--control for (without) sulfisoxazole (Figure VI-10). Here, 154.5 pmoles furosemide per mg protein is bound to the membrane, and r^2=0.767.

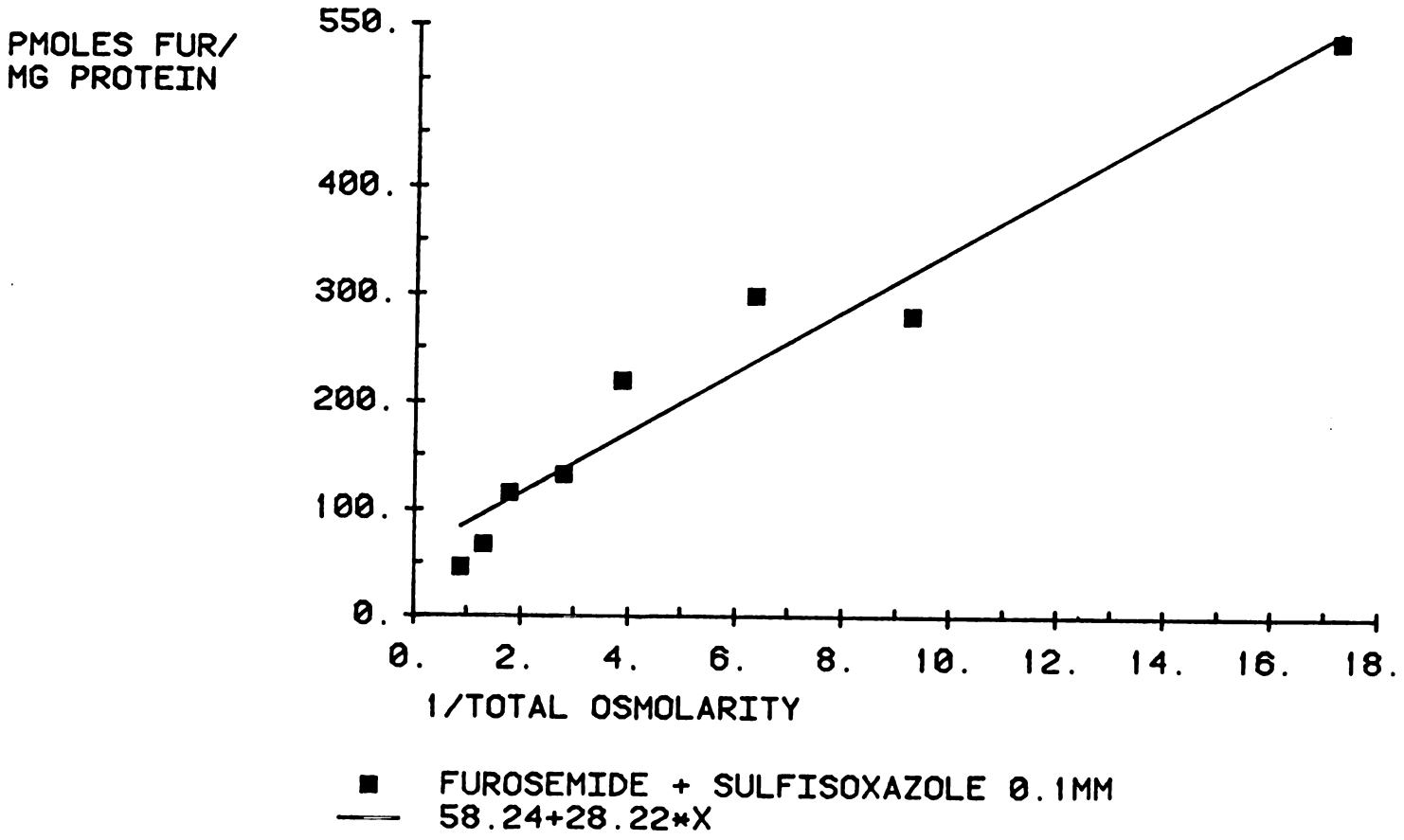

Figure VI-10. Furosemide (FUR) uptake after one hour incubation time versus 1/total osmolarity of the external medium--effect of sulfisoxazole 0.1mM. Furosemide is bound to the membranes at 58.24 pmoles/mg protein and r^2=0.943.

some of the scatter in the data. However, a significant portion of furosemide binding remained. Also, sulfisoxazole is a sulfonamide which, like PAH and furosemide, is secreted by the proximal tubule (222). The location of sulfonamide secretion is believed to be identical to that of PAH. Addition of sulfisoxazole to samples in which PAH and furosemide competition for transport was to be studied would only complicate the experiment, by supplying yet another potential competitor. It was decided that these factors made it impractical to use sulfisoxazole as a binding inhibitor on a regular basis.

E. Furosemide counter-transport studies

Effect of pre-loading with PAH

Use of purified radiolabelled furosemide

1. Results

Three experiments were performed in which vesicles were incubated in PAH 0.1mM in Solution #1 at 4°C overnight. Vesicles not pre-incubated in PAH solution were also available to serve as controls. The uptake of furosemide in control vesicles, with and without probenecid, and its uptake in the vesicles pre-incubated with PAH were examined. Table VI-7 shows the average results for these three experiments. It appears that probenecid causes inhibition of furosemide uptake. These results are similar to those seen in Tables VI-4, VI-5 and VI-6.

These results also indicate that pre-incubation with 0.1mM PAH in buffer generally causes a decrease or no significant change in furosemide uptake. No evidence for countertransport stimulation of ^{3}H-

TABLE VI-7. FUROSEMIDE UPTAKE BY BASAL-LATERAL MEMBRANE VESICLES.
EFFECT OF PRE-LOADING VESICLES WITH PAH PRIOR TO FUROSEMIDE UPTAKE STUDIES.

Incubation Time (seconds)	Organic Anion Components of Sample		
	Furosemide Uptake (pmoles furosemide/ mg protein)	Effect on Furosemide Uptake (Percent of Control)	
(n = number of experiments[a])	Furosemide 0.1mM alone (Controls)	Furosemide 0.1mM + Probenecid 6.67mM	Furosemide 0.1mM in Vesicles Pre-loaded with PAH 0.1mM
5 (n=3)	91.33±49.00	58.99±6.08%	95.93±41.68%
10 (n=3)	129.99±69.67	52.15±20.05%	64.69±12.86%
15 (n=3)	137.24±14.03	58.86±13.65%	59.52±19.17%
45 (n=3)	150.86±37.71	81.03±27.77%	86.69±12.06%
75 (n=3)	160.61±42.43	81.69±17.67%	72.95±31.86%
3600 (n=3)	262.27±11.77	81.78±13.63%	95.61±7.80%

[a]Each experiment included 4 identical samples for each time point and set of sample components.

furosemide uptake is seen here.

2. Discussion

The presence of probenecid inhibition of ^{3}H-furosemide uptake indicates that carrier-mediated transport of furosemide is taking place. The presence of countertransport stimulation by PAH would provide further evidence for same-carrier-mediated transport of PAH and furosemide. Unfortunately, this stimulation is not seen. It is possible that the two compounds are not transported by the same carrier and inhibition of PAH uptake by furosemide, as discussed earlier, is due to something other than competition for the carrier.

However, it is also possible that PAH decreases the binding of ^{3}H-furosemide to the vesicle membranes, so that the "apparent uptake" of furosemide is decreased. Due to the relatively high binding of furosemide to membranes, an effect of decreased binding by PAH could easily negate the effect of any countertransport taking place.

F. PAH counter-transport studies

Effect of pre-loading with furosemide

1. Results

Table VI-8 provides average data for three experiments in which a portion of the vesicles was pre-incubated with furosemide 0.1mM. The average values for PAH uptake at all time points are shown in this table. These values are similar to those obtained in previous

TABLE VI-8. PAH UPTAKE BY BASAL-LATERAL MEMBRANE VESICLES.
EFFECT OF PRE-LOADING VESICLES WITH FUROSEMIDE PRIOR TO PAH UPTAKE STUDIES.

Incubation Time (seconds)	Organic Anion Components of Sample		
	PAH Uptake (pmole PAH/ mg protein)	Effect on PAH Uptake (Percent of Control)	
(n = number of experiments[a])	PAH 0.1mM alone (Controls)	PAH 0.1mM + Probenecid 6.67mM	PAH 0.1mM in Vesicles Pre-loaded with Furosemide 0.1mM
5 (n=3)	22.87±7.86	28.32±19.71%	59.57±13.43%
10 (n=3)	18.74±2.26	43.21±47.59%	113.37±11.47%
15 (n=3)	16.84±4.96	30.34±11.94%	176.38±83.71%
45 (n=3)	23.26±12.51	41.30±26.14%	97.89±46.39%
75 (n=3)	23.06±10.09	41.72±12.70%	122.05±30.84%
3600 (n=3)	49.16±13.64	72.79±7.68%	110.35±43.22%

[a]Each experiment included 4 identical samples for each time point and set of sample components.

experiments (Tables VI-1 and VI-2). Probenecid caused significant inhibition of PAH uptake. These average data also show that PAH uptake was increased over control values at four of six incubation times when vesicles were equilibrated with 0.1mM furosemide in advance. Only the five second incubation time demonstrated a significant decrease in PAH uptake when compared to controls.

2. Discussion

The control values for PAH uptake with and without probenecid obtained in these experiments were found to be similar to values obtained in other studies presented previously in this chapter. These results indicate that carrier-mediated transport of PAH is taking place.

Pre-loading of vesicles with 0.1mM furosemide appears to cause some increased uptake of PAH. Although these average values are not significantly different from control values (100%), they do demonstrate a serious trend toward increased uptake of PAH. More experiments would perhaps decrease some of the variability seen in these results.

A number of researchers have examined the effect of excess intravesicular concentrations of PAH on uptake of radiolabelled PAH from outside to inside vesicles. Hori et al. (97) demonstrated up to a 100% increase in PAH uptake in basal-lateral membrane vesicles containing a ten-fold higher PAH concentration inside the membrane. Eveloff et al. (95) found both increased influx and efflux of radiolabelled PAH when brush border membranes were presented with excess PAH on the alternate surface. Kasher et al. (92) also demonstrated an increased uptake of radiolabelled PAH in the presence of a large PAH gradient out of the

vesicles. Berner and Kinne (81) and Kinsella et al. (82) both found stimulation of ^{3}H-PAH transport by a reverse gradient of unlabelled PAH. This stimulation was seen only in basal-lateral membranes. Neither group saw this effect in brush border membranes.

No work demonstrating trans-stimulation of PAH uptake by basal-lateral membranes, using a reverse gradient of a different compound, has been reported. The results presented here indicate that the uptake of PAH may be trans-stimulated by furosemide. As stated before, the lack of trans-stimulation of furosemide uptake by PAH may be due to decreases in vesicle binding, leading to a decrease in "apparent" transport.

G. Conclusions

There are obviously questions left unanswered by this work. How may the binding of furosemide to the membrane be eliminated, so that the actual uptake of furosemide may be studied? Why was counter-transport stimulation by PAH of furosemide uptake not observed? What effect will other organic anion drugs have on the transport of PAH and furosemide? Further experiments are needed to answer these and other questions. However, the work presented here provides answers to some basic questions involving transport of these two compounds, as well as raises other points that must be considered when utilizing this type of methodology. This work demonstrates that: 1. Furosemide and PAH uptake by basal-lateral membrane vesicles are both inhibitable by probenecid. This provides evidence for a carrier-mediated process(es) for the transport of furosemide and PAH. 2. Furosemide inhibits the uptake of PAH by basal-lateral membrane vesicles. This is evidence for a shared

transport system for the two molecules. 3. PAH showed only limited inhibition of furosemide uptake under certain conditions (high PAH concentrations, addition of PAH immediately prior to furosemide addition). This may indicate that PAH has less affinity for the carrier than does furosemide, but does utilize the same carrier. 4. Furosemide binding to vesicles is extensive, and increases with time. This complicates measurement of actual furosemide uptake, and introduces more variability into the data. Furosemide binding can be decreased by addition of sulfisoxazole; however, this drug then becomes a further complicating factor in transport studies. 5. Countertransport stimulation of furosemide uptake by PAH was not seen. Countertransport of PAH uptake by furosemide was demonstrated. The problem of furosemide binding to vesicles may be causing the lack of apparent countertransport stimulation of furosemide uptake.

CHAPTER VII

RENAL CLEARANCE STUDIES

RESULTS AND DISCUSSION

A. Introduction

These experiments were performed as described in Chapter IV. In all experiments, animals were anesthetized with sodium pentobarbital, 60 mg/kg rat body weight. Pentobarbital was chosen as the anesthetic based on the satisfactory results obtained by Till and Benet (119), Smith and Benet (57), Harvey and Malvin (204) and Brennan et al. (223). Kau et al. (205) have used ketamine as anesthetic for this type of procedure and have obtained comparable results. Although Kau et al. (205) state that Guignard and Peters (224) found a depression of renal function when pentobarbital was used for anesthesia, no evidence of this is apparent in the publication. Also, Till and Benet (119), Smith and Benet (57), Harvey and Malvin (204) and Brennan et al. (223), as well as Dev et al. (225) found no change from normal values for renal function parameters when using this barbiturate. Due to these overwhelmingly positive results, pentobarbital was used for anesthesia in these experiments.

B. Bolus dose studies

1. Furosemide

a. Results

Bolus doses of either three or four mg furosemide/kg rat body weight were administered to four rats, as described in Section IV.B.1. Graphs of furosemide plasma concentration versus time for these rats are shown in Figures VII-1 and VII-2. Data from these experiments is presented in Table VII-1. Data from rats #1, #2 and #4 were fit to a one-compartment model. A two-compartment model was used for Rat #3.

As these results indicate, furosemide followed one-compartment-body-model behavior reasonably well for three of the four rats. It appears that rats #1 and #2 show some two-compartment characteristics in their handling of furosemide. However, due to limited data, a one-compartment model was used. Half-lives ranged from 17.3 to 27.2 minutes with a mean of 23.5±5.4 (S.D.) minutes for these animals. Rat #3 showed obvious two compartment characteristics (Figure VII-2). For this animal, $t_{1/2_\alpha}$ was 11.3 minutes and $t_{1/2_\beta}$ equaled 98.6 minutes.

Animal #3 exhibited a furosemide peak concentration at t = 11.0 minutes, with a lower concentration at the earlier (4.8 minute) time point. In animal #4 the plasma concentration of furosemide did not significantly change over the first fifteen minutes of the experiment. These first time points for rats #3 and #4 look as if an absorption phase is taking place. However, since these doses were given by IV bolus, there should not be an absorption phase. These results will be

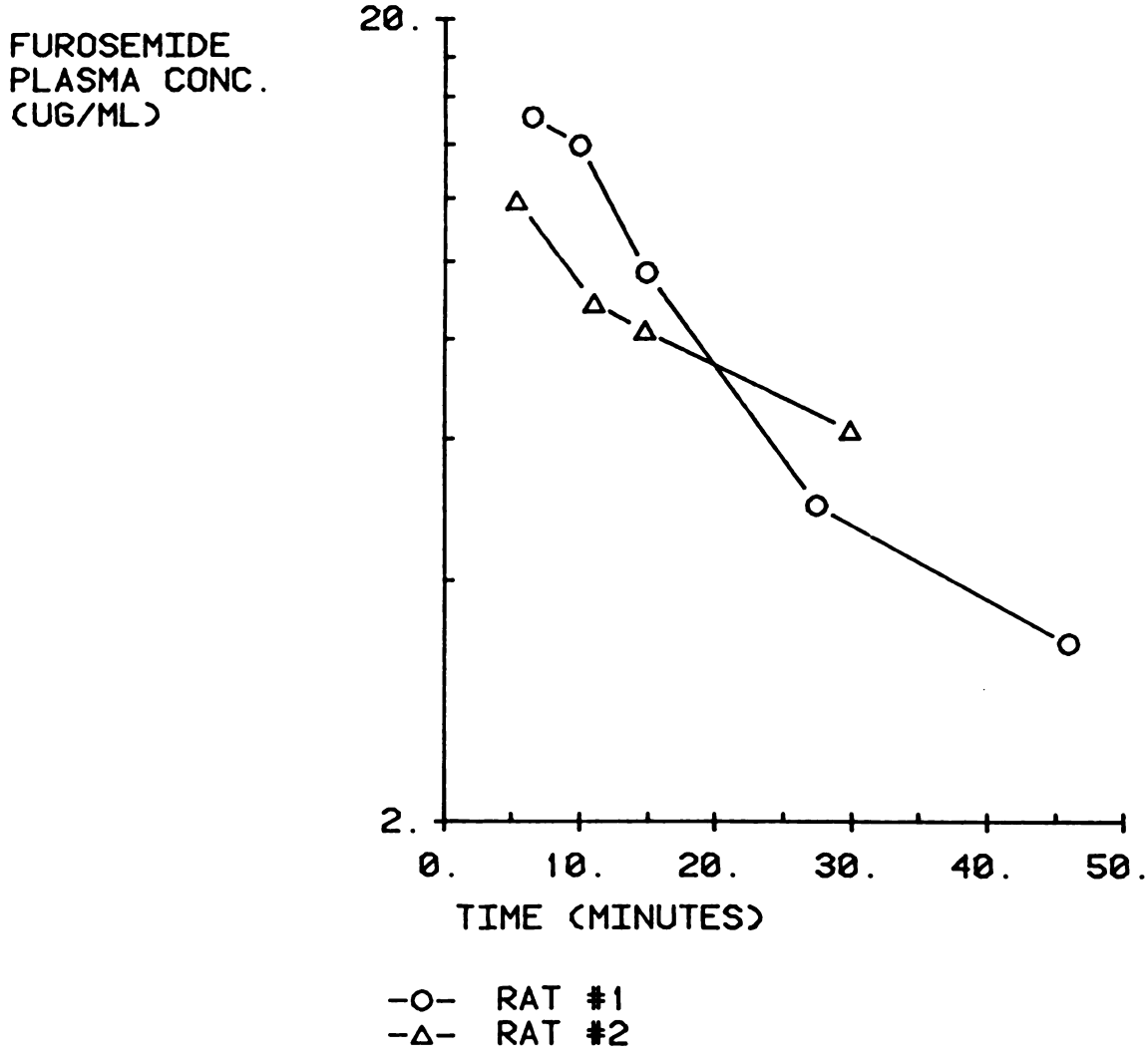

Figure VII-1. Furosemide plasma concentration versus time for 4 mg/kg bolus doses.

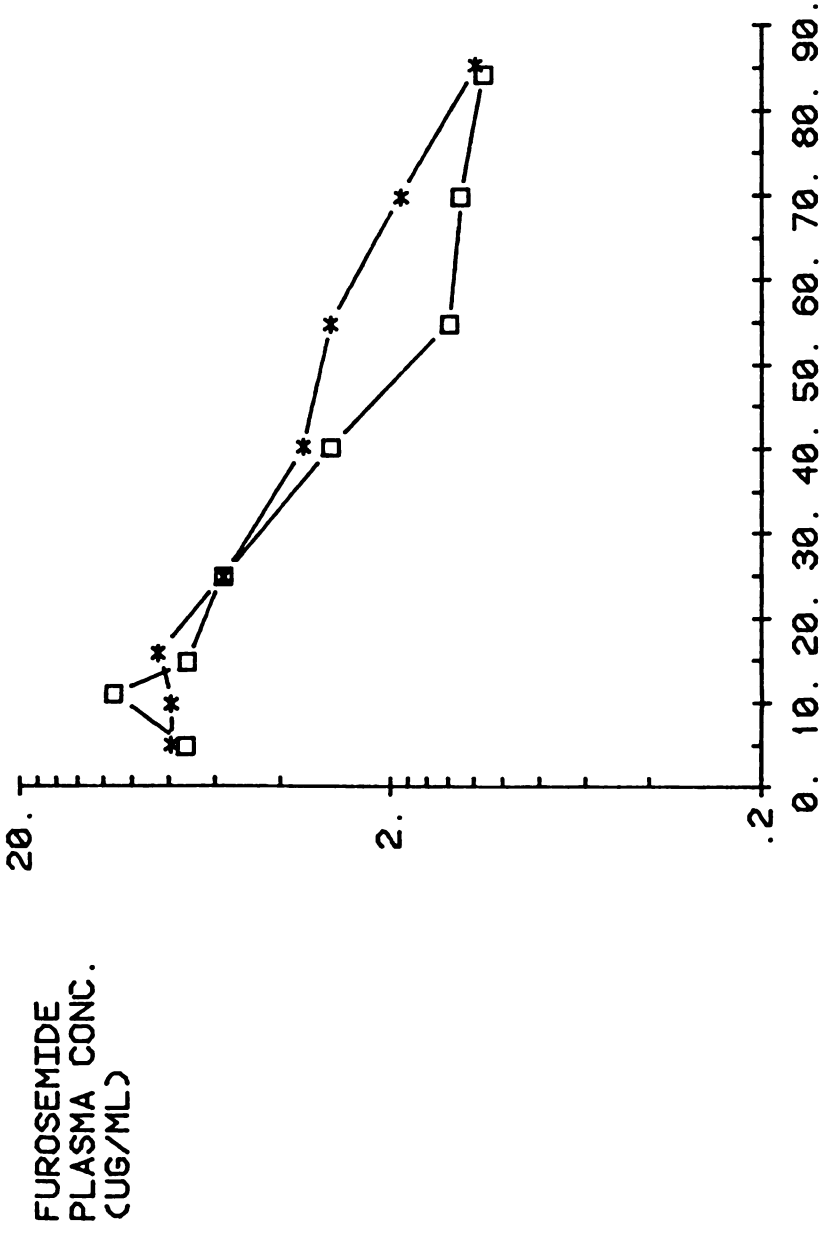

Figure VII-2. Furosemide plasma concentration versus time for 3 mg/kg bolus doses.

TABLE VII-1. RESULTS FROM FUROSEMIDE BOLUS DOSE STUDIES

Rat #	Dose (mg/kg)	Time of Sample (min)	C_p (μg/ml)	$t_{1/2\alpha}$ (min)	$t_{1/2\beta}$ (min)	AUC_α (μg/ml-min)	AUC_β (μg/ml-min)
1	4	6.5	15.1	—	17.3	—	465.6
		10.0	13.9				
		15.0	9.7				
		27.5	5.0				
		46.0	3.3				
2	4	5.4	11.9	—	27.2	—	492.2
		11.1	8.8				
		14.8	8.2				
		30.0	6.1				
3	3	4.7	7.2	11.3	98.6	260.6	293.4
		11.0	11.1				
		14.7	7.1				
		24.8	5.6				
		40.0	2.9				
		54.7	1.4				
		69.7	1.3				
		84.1	1.1				
4	3	4.8	7.8	—	25.9	—	433.8
		9.8	7.8				
		15.8	8.4				
		24.8	5.6				
		40.1	3.4				
		54.2	2.9				
		69.6	1.9				
		85.1	1.2				

examined further in the following discussion.

b. Discussion

The purpose of these experiments was to determine if a priming dose of furosemide should be used in steady-state competition for transport studies. Smith and Benet (57) have published work correlating the diuretic response to the urinary excretion rate of furosemide. They also demonstrated no correlation between diuretic response and furosemide steady-state plasma levels. Leenen (226) looked at the dose-response relationship between furosemide dose and diuresis or cardiovascular effects. He did not measure plasma or urine furosemide levels. Chakrabarti and Brodeur (227) have examined the effect of fasting on total and free concentrations of furosemide in plasma and in kidney tissue slices. Prandota and Wilimowski (228) gave a 1 mg/kg intravenous dose of furosemide, and found two compartment characteristics, with $t_{1/2_\alpha}$ = 8.8 minutes and $t_{1/2_\beta}$ = 72.0 minutes. Finally, Hammarlund and Paalzow (173) gave doses of 10 and 40 mg furosemide/kg rat body weight and found that the data obtained was best fit by a three compartment model. For the low dose, the terminal $t_{1/2}$ = 28.9 minutes, while the 40 mg/kg dose gave a terminal $t_{1/2}$ of 49.2 minutes.

The doses of furosemide used here (3 and 4 mg/kg) are between the 1 mg/kg used by Prandota and Wilimowski and the 10 and 40 mg/kg doses of Hammarlund and Paalzow. The half-lives calculated from this data are not inconsistent with those found by the other researchers. Although for three of the four rats the data has been fit to a one compartment

model, additional plasma sampling times in these studies might have increased the suitability of this data for the multi-compartment models observed by others (173,228).

The presence of an "absorption phase" in animals 3 and 4 was curious. Hammarlund and Paalzow (173) do not report anything of this nature, and they sampled plasma early and frequently. Prandota and Wilimowski (228) do appear to have a slightly lower initial level of furosemide. Also, Lee et al. (229) have noted a "dip" in furosemide plasma concentrations three to five minutes after administering an IV dose to rabbits. Although this "dip" is not at the initial sampling time in their studies, it did occur at approximately the same time as did the low plasma levels of furosemide observed in the current studies. It may be that if earlier plasma samples had been taken in our studies the results would also indicate a decrease in furosemide concentration at this time, followed by an increased level and then the expected decline.

As stated before, the intent of this work was to determine if a bolus loading dose of furosemide would be needed in competition for transport studies, in order to achieve steady state by the start of the first clearance period (sixty minutes into the infusion). Since approximate (90% of) steady-state levels will be reached in 3.3 $t_{1/2}$'s it is essential to know the $t_{1/2}$ of the compound. With a mean $t_{1/2}$ of 23.5 minutes (for rats #1, #2 and #4), it should take approximately 78 minutes to reach 90% of steady state plasma levels of furosemide. This is near the end of the second clearance period, and might cause problems with analysis of the data. Also, the obvious furosemide two compartment characteristics of rat #3 as well as the possible two-compartment

characteristics of rats #1 and #2 were worrisome. When calculating the contribution to total AUC from each phase (α and β) for Rat #3, it was found that the β phase contributed 53% of the total AUC. If other animals also exhibited a β phase with a similarly long $t_{1/2}$, steady state plasma levels might not be reached for well over four hours. This was unacceptable and it was decided to use a bolus loading dose of furosemide in order to approach steady-state levels more rapidly.

2. PAH bolus dose studies

a. Results

Four rats were administered a dose of either five or seven mg PAH/kg rat body weight. Plasma concentrations of PAH were determined and graphs of PAH plasma concentration versus time are shown in Figures VII-3 and VII-4. Data from these studies are shown in Table VII-2. PAH appeared to follow two compartment kinetics in all four rats at these doses. Terminal $t_{1/2}$'s range from 12.1 to 26.6 minutes, averaging 19.3±5.9 minutes. Alpha-phase half-lives were significantly shorter, in the range of 3.1 to 7.4 minutes, with a mean of 4.9±1.9 minutes. In these studies, at least 55% of the total AUC was contributed by the β phase.

b. Discussion

The purpose of these experiments was the same as that of the furosemide bolus dose studies--to determine if a PAH bolus dose was

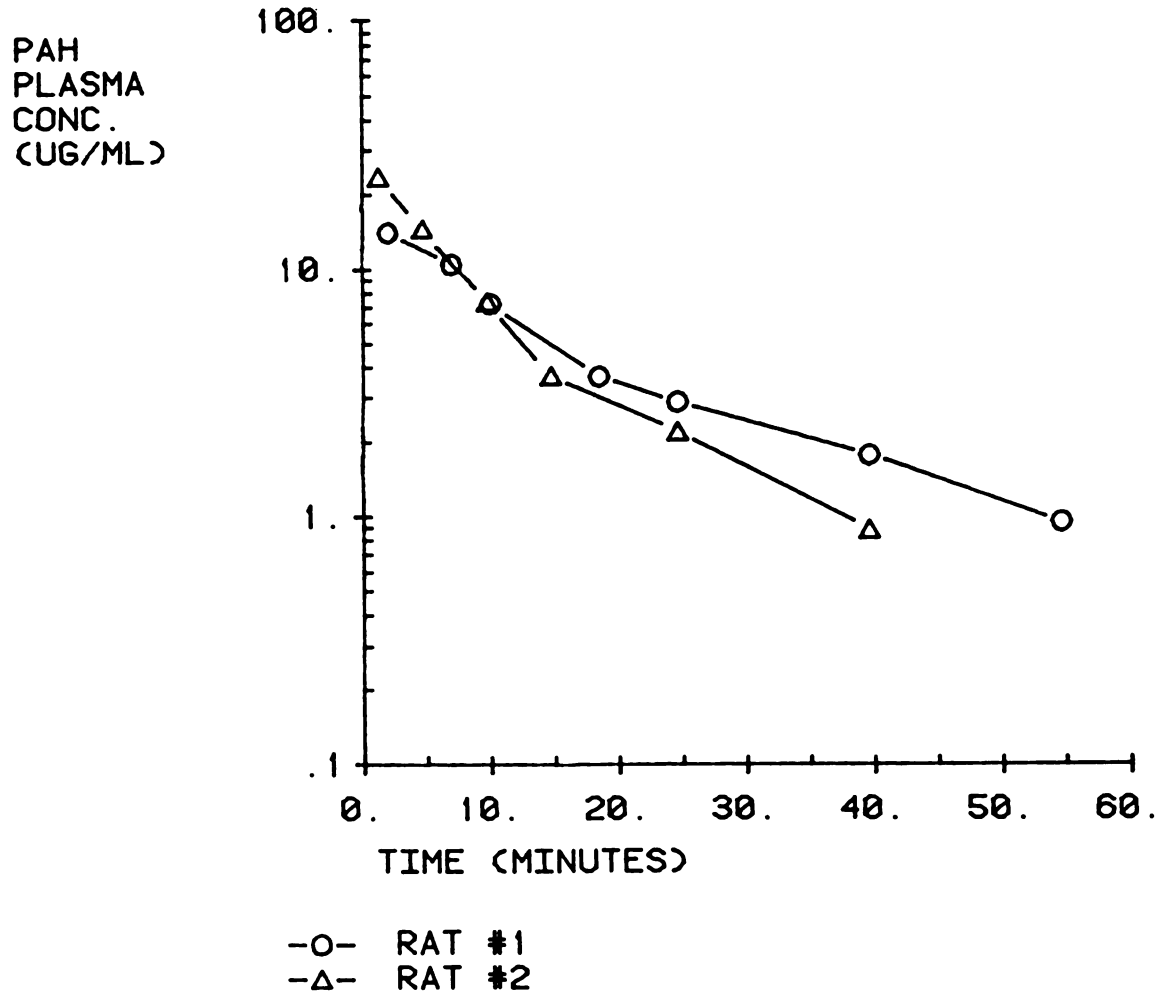

Figure VII-3. PAH plasma concentration versus time for 7 mg/kg bolus doses.

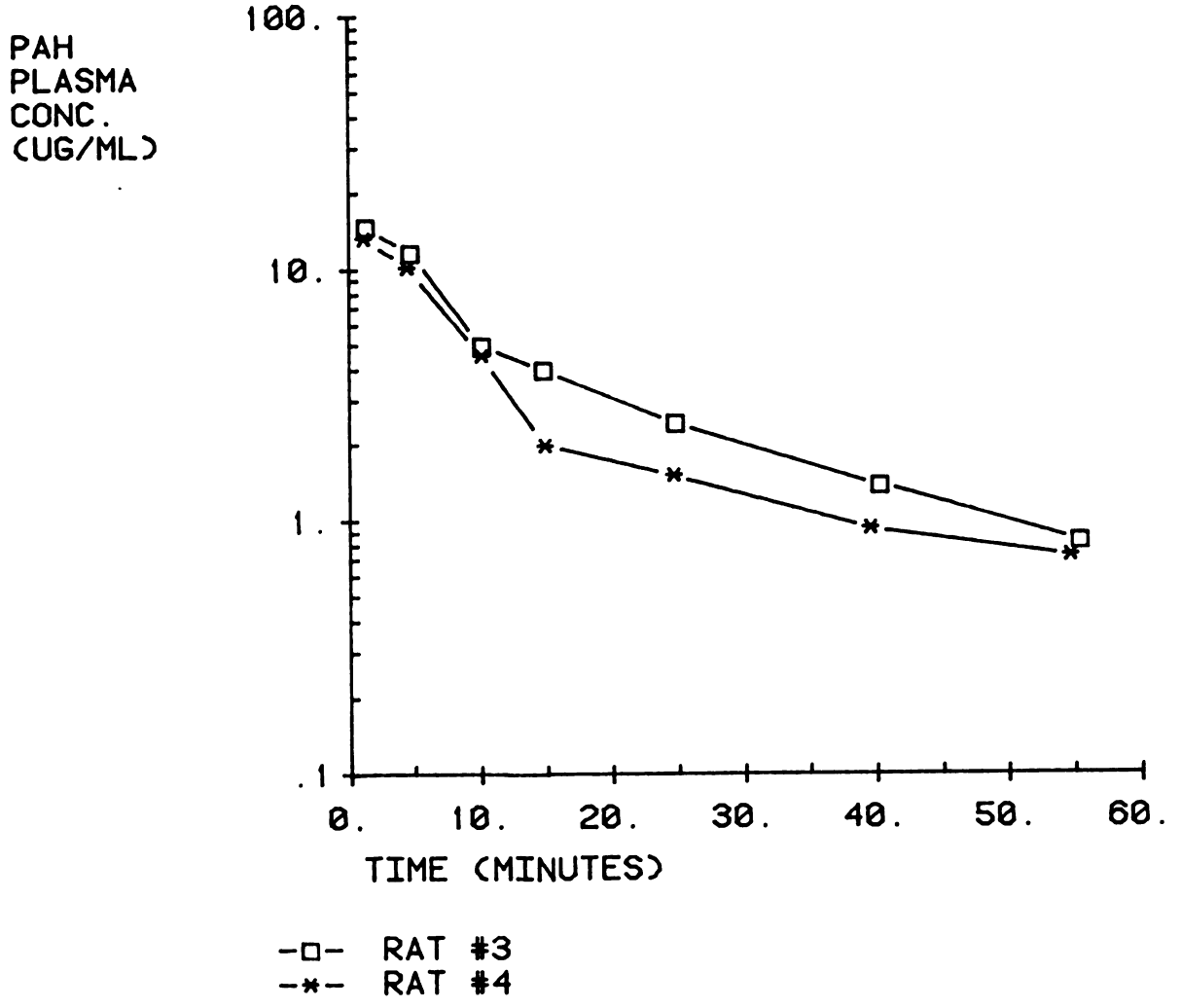

Figure VII-4. PAH plasma concentration versus time for 5 mg/kg bolus doses.

TABLE VII-2. RESULTS FROM PAH BOLUS DOSE STUDIES.

Rat #	Dose (mg/kg)	Time of Sample (min)	C_p (μg/ml)	$t_{1/2\alpha}$ (min)	$t_{1/2\beta}$ (min)	AUC_α (μg/ml-min)	AUC_β (μg/ml-min)
1	7	2.0	13.9	5.0	18.6	73.0	197.0
		7.0	10.4				
		10.1	7.2				
		18.5	3.6				
		24.7	2.9				
		39.7	1.8				
		54.7	0.9				
2	7	1.2	23.6	3.1	12.1	95.0	151.8
		4.8	14.4				
		9.8	7.3				
		14.8	3.7				
		24.7	2.2				
		39.7	0.9				
3	5	1.4	14.7	7.4	19.7	109.4	163.3
		4.8	11.5				
		10.1	4.9				
		14.8	3.9				
		24.8	2.4				
		40.2	1.4				
		55.4	0.8				
4	5	1.2	13.3	4.0	26.6	82.4	109.1
		4.5	10.1				
		10.1	4.5				
		14.9	2.0				
		24.6	1.5				
		39.5	0.9				
		54.7	0.7				

required in order to reach steady-state levels reasonably quickly in the competition-for-transport studies. Since PAH's clearance and extraction ratio are related to renal plasma flow, virtually all work to date describes only these two parameters. No one has reported a $t_{1/2}$ for PAH in rats. With PAH's high renal clearance, one might expect PAH to have a short $t_{1/2}$. As these data show, the initial $t_{1/2}$ ($t_{1/2_\alpha}$) for PAH in rats is indeed quite short, with a mean of 4.9±1.9 minutes. However, after 15-25 minutes, the decline in PAH plasma concentration slows down, with a mean $t_{1/2_\beta}$ of 19.3±5.9 minutes. There was not a significant difference in the half-lives when comparing five and seven mg/kg PAH doses.

Once again, these experiments were done to determine if a bolus dose of PAH should be administered prior to starting the infusion. As with furosemide, using the $t_{1/2}$ to determine when 90% of steady-state levels would be reached was the criteria selected. However, with PAH it also became important to know which (if either) of the two $t_{1/2}$'s was the more important in determining when steady state would be reached. This could be determined by calculating the AUC's under the α and β portions of the plasma concentration-time curves. If one phase contributed significantly more than the other to the total AUC, its $t_{1/2}$ would be more important to consider in determining when steady-state levels would be reached.

The percent AUC found under the β phase in these rats was always greater than 55% of the total AUC. This indicates that $t_{1/2_\beta}$ is more important in determining when steady state will be reached than is $t_{1/2_\alpha}$. It was determined that 90% of steady-state levels would be reached approximately 64 minutes into the infusion if the α component

were totally ignored. This is the longest possible time to steady state and the true time is likely to be much shorter due to the α contribution. Since the animal would be close to steady state at the start of the first clearance period (sixty minutes into the infusion), it was decided not to give a PAH bolus dose.

C. Competition for transport studies

1. Effect of PAH on furosemide clearance

a. Results

Table VII-3 shows the results obtained from these interaction studies. As described in Chapter IV, these studies were done by first infusing furosemide solution for sixty minutes, followed by two 10 minute clearance periods, during which the infusion continued. At the end of this time, the infusion solution was changed to one containing both furosemide and PAH. Again, the infusion was administered for sixty minutes, followed by two 10 minute clearance periods during which the infusion was continued as well.

Plots of CL_F/CL_{IN} versus furosemide $C_{p_{ss}}$, GFR (CL_{IN}) versus $C_{p_{ss}}$ and urine flow rate versus furosemide urinary excretion rate are shown in Figures VII-5 through VII-7. The plot of CL_F/CL_{IN} versus $C_{p_{ss}}$ appears to show a decrease in clearance ratio with increasing furosemide plasma concentration for samples containing furosemide alone. However, the correlation is not statistically significant ($r = -0.5687$, $p>0.1$). This correlation is similar to that seen by Smith and Benet (57). When

TABLE VII-3. RESULTS FROM FUROSEMIDE-PAH INTERACTION[a] STUDY.
EFFECT OF PAH ON FUROSEMIDE RENAL CLEARANCE.

Rat #	+ or - PAH[b]	Weight (kg)	Urine Flow (ml/min)	ΔAe/Δt (μg/min)	$C_{p_{ss}}$ (μg/ml)	CL_F (ml/min-kg)	Urinary pH	CL_{IN} (ml/min-kg)	CL_F/CL_{IN}
1	-	0.317	0.122	7.48	10.44	2.27	—[c]	6.35	0.36
	+		0.085	3.63	10.92	1.04	—[c]	9.41	0.11
2	-	0.306	0.093	2.98	2.63	3.74	—[c]	8.82	0.42
	+		0.081	3.18	3.00	3.76	—[c]	9.65	0.39
3	-	0.330	0.080	2.73	4.10	2.01	—[c]	2.89	0.70
	+		0.064	2.10	4.59	1.38	—[c]	2.37	0.58
4	-	0.346	0.072	4.91	9.17	1.62	4.82	5.75	0.28
	+		0.030	1.72	13.49	0.37	5.11	2.46	0.15
5	-	0.429	0.111	8.21	6.58	3.00	5.32	8.10	0.37
	+		0.040	3.22	7.37	1.02	5.25	3.29	0.31
6	-	0.440	0.112	5.37	7.42	1.66	5.56	6.99	0.24
	+		0.082	4.82	8.63	1.27	5.54	7.27	0.17
7	-	0.255	0.092	6.56	8.20	3.38	5.24	8.55	0.40
	+		0.064	2.76	11.24	1.03	5.28	5.16	0.20
8	-	0.260	0.112	6.25	7.64	3.26	5.06	8.10	0.40
	+		0.076	2.68	10.30	1.03	5.22	6.18	0.17

[a]Study was performed by infusion of furosemide, 30.0 μg/min, for eighty minutes followed by infusion of furosemide, 30.0 μg/min plus PAH, 49.6 μg/min, for eighty minutes.

[b]Values are the means for 2 ten-minute clearance periods. Furosemide-alone clearance periods were between 60 and 80 minutes during the first infusion. Furosemide-plus-PAH clearance periods were between 60 and 80 minutes during the second infusion, or 140 to 160 minutes total infusion time.

[c]Urinary pH values not available.

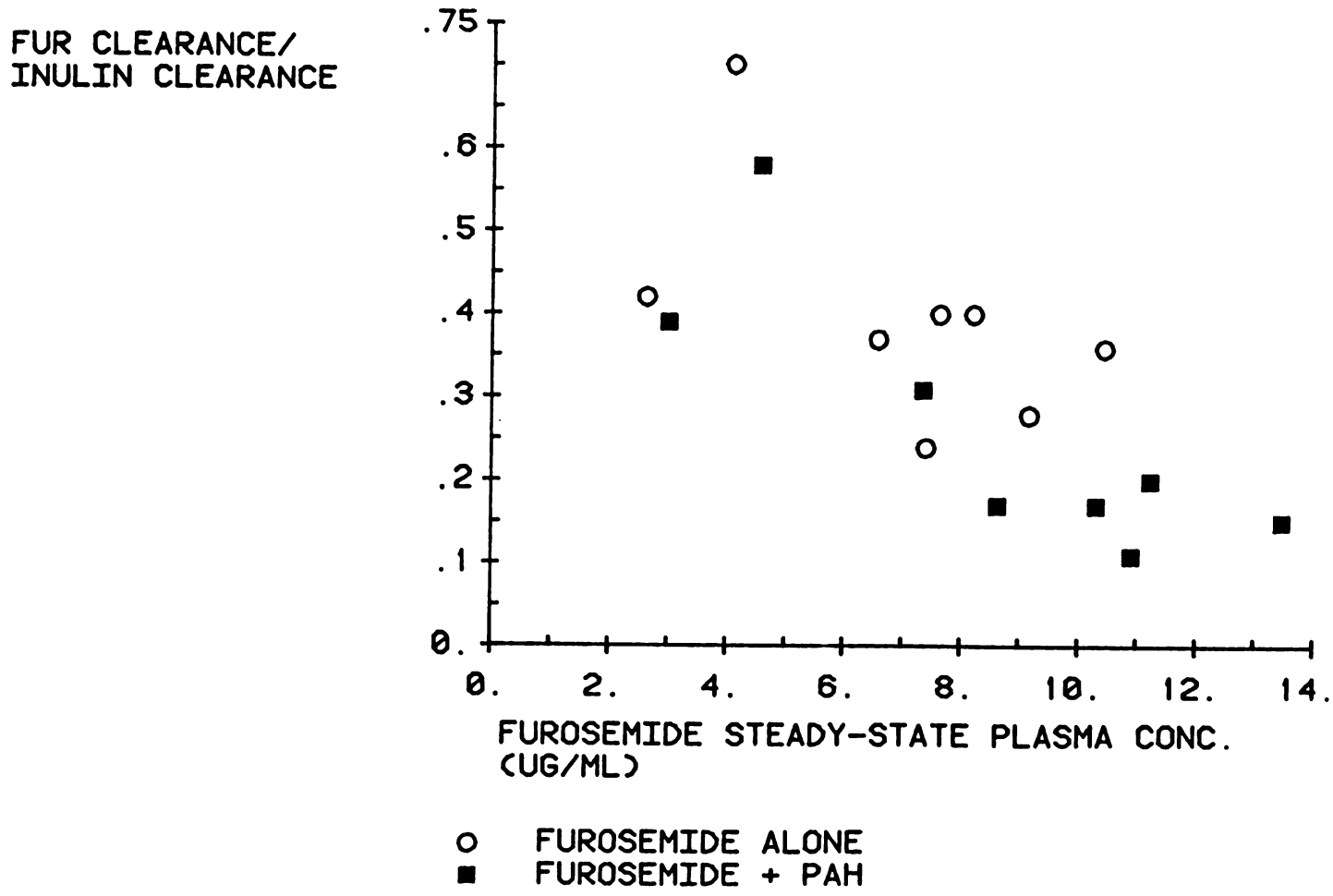

Figure VII-5. Relationship between CL_F/CL_{IN} and furosemide steady-state plasma concentration.

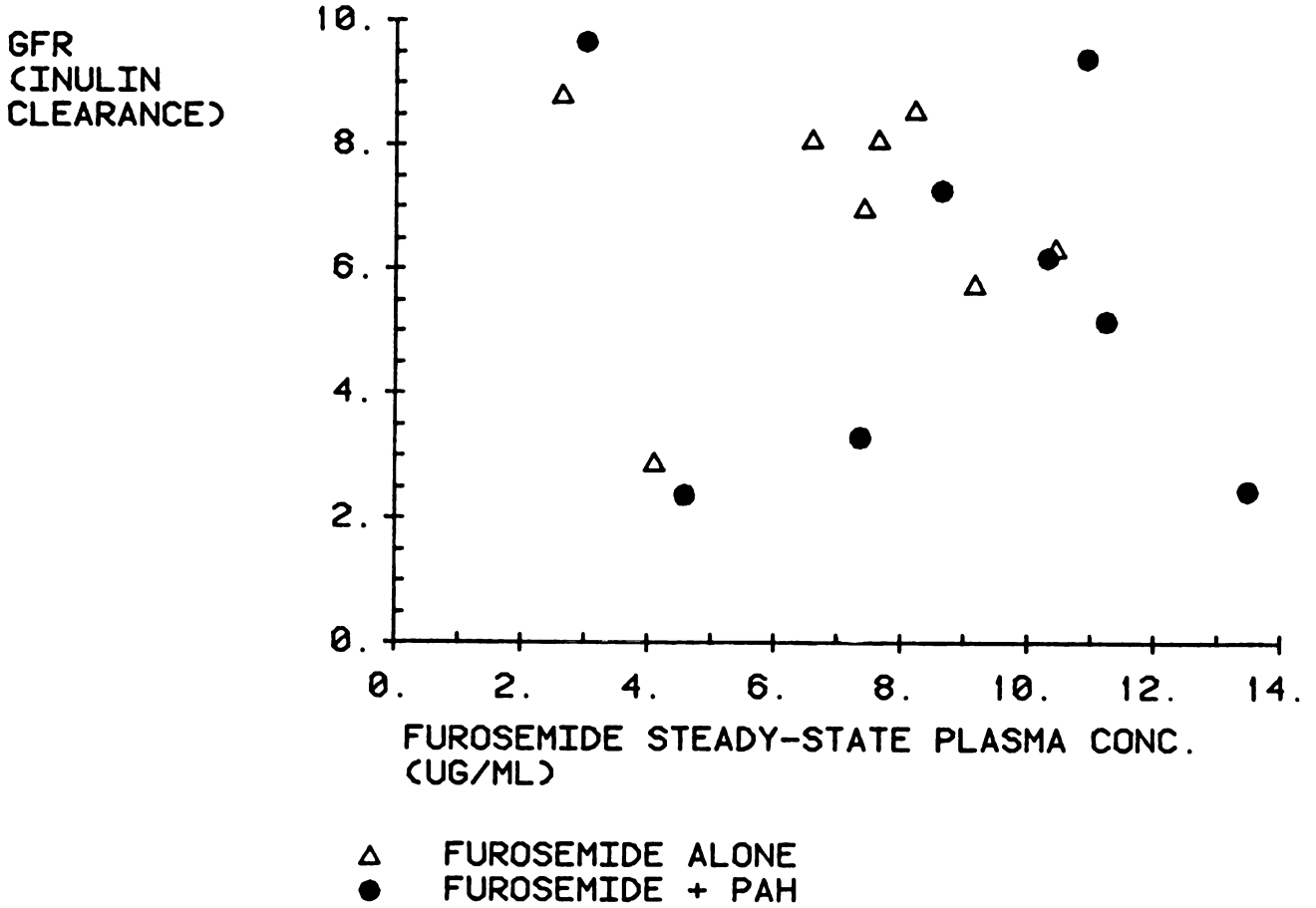

Figure VII-6. Relationship between GFR (measured by inulin clearance) and furosemide steady-state plasma concentration. ($r=-0.1776$, $p>0.1$)

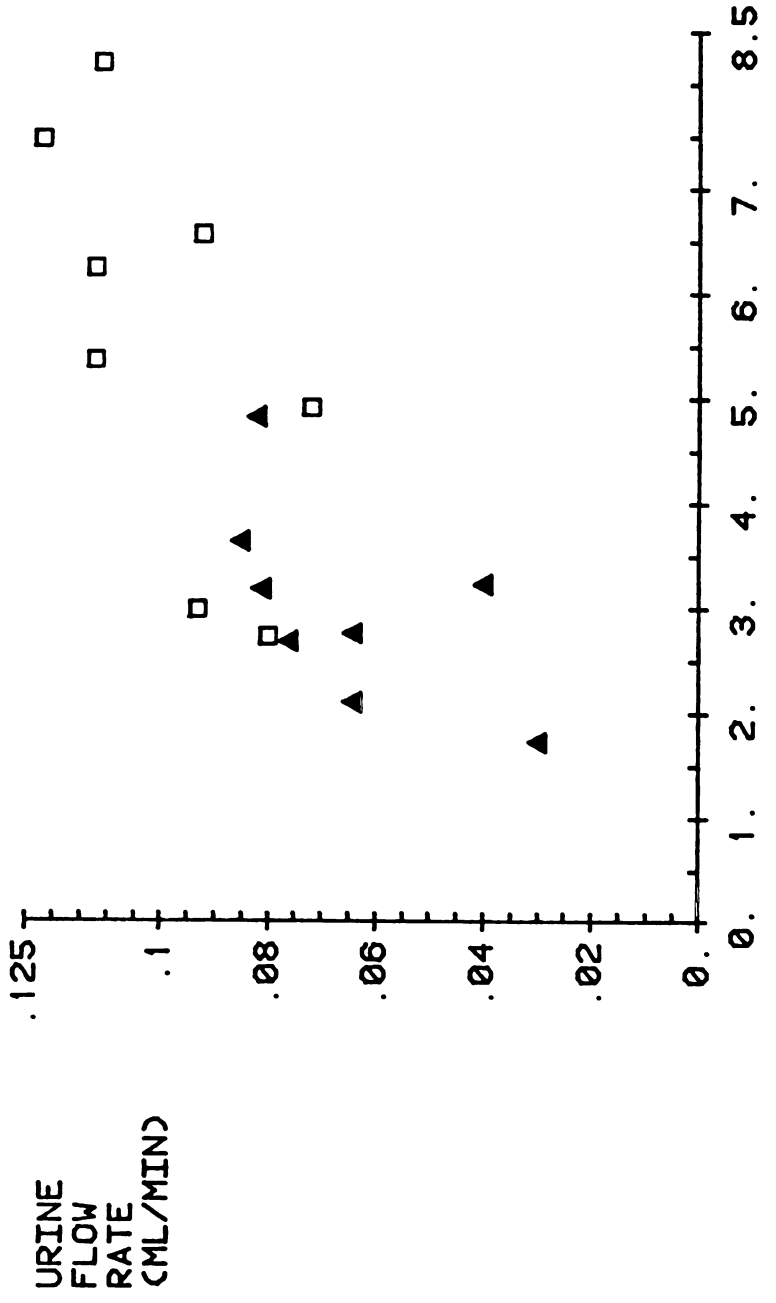

Figure VII-7. Relationship between urine flow rate and furosemide excretion rate. ($r=0.771$, $p<0.001$)

comparing changes in CL_F/CL_{IN} before and after addition of PAH, a decrease in CL_F/CL_{IN} was always seen.

A plot of GFR versus furosemide $C_{p_{ss}}$ (Figure VII-6) shows no significant correlation ($r = -0.1776$, $p>0.1$). Smith and Benet (57) have shown a weak negative correlation for this relationship, and other researchers (223,230-234) have also shown that furosemide can decrease GFR. Still others (235-237) have seen no change in GFR due to furosemide. It appears that GFR is not significantly dependent upon the plasma concentration of furosemide in these experiments.

No significant correlation ($r = -0.3174$, $p>0.1$) for urine flow rate versus $C_{p_{ss}}$ was seen (figure not shown). This agrees with results obtained by Smith and Benet (57), indicating that the diuretic effect of furosemide is not directly related to its plasma concentration. There is, however, a correlation between urine flow rate and urinary excretion rate ($r = 0.7771$, $p<0.001$) (Figure VII-7). This again correlates well with the results obtained by Smith and Benet (57) and lends further evidence to the theory that furosemide exerts its diuretic effect within the lumen of the tubule.

b. Discussion

It has long been known that furosemide is secreted by the kidney (170). More recently, Smith and Benet (57) have shown that furosemide's diuretic response in rats is related to its luminal concentration, rather than its plasma concentration. The data presented here offer further support for that conclusion.

These data also indicate that CL_F/CL_{IN} tends to decrease as the

$C_{p_{ss}}$ of furosemide increases. This suggests that the removal of furosemide by the rat kidney is a saturable process. The data from clearance periods containing no PAH are very similar to results reported by Smith and Benet (57). Results in the presence of PAH, however, generally exhibit smaller CL_F/CL_{IN} ratios at equivalent plasma concentrations. This is most likely due to a decrease in furosemide clearance caused by PAH.

As previously mentioned, conflicting results concerning furosemide's effect on GFR have been reported (57,223,230-237). Although the data here exhibit no significant correlation between GFR and furosemide $C_{p_{ss}}$, there may be a slight downward trend in GFR as $C_{p_{ss}}$ of furosemide increases. Also, the values for GFR tend to be somewhat lower than those to be presented in the next section dealing with furosemide's effect on PAH secretion (Section VII.C.2.).

It is possible that some time-related change is taking place which decreases the clearance of furosemide. In order to test this, several experiments were attempted using a reverse protocol, i.e. furosemide and PAH administered first, followed by furosemide. Unfortunately, the relatively long $t_{1/2_\beta}$ of PAH precludes its complete removal from plasma within a reasonable washout period. This results in excessive lengthening of the experiments, and it becomes extremely difficult to maintain normal bodily functions in the experimental animal. Consequently, all experiments included here were performed with furosemide-alone administration first, followed by infusion of both drugs.

Based on the results presented here, it appears that PAH decreases the secretion of furosemide by the rat kidney. A number of other

compounds are known to affect furosemide's elimination by the kidney. Among these are probenecid (174-178), acetylsalicylic acid (179-182) and indomethacin (183-188). Since there is a definite interaction between PAH and each of these compounds (87,88,158) it is possible that PAH could also affect the transport of furosemide. These results indicate that this interaction probably exists.

In contrast, a 1965 study by Gayer (238) indicated that PAH does not inhibit the transport of furosemide in dogs. However, in the dogs used in his study, the CL_F/CL_{IN} ratio was 2 to 4 at furosemide $C_{p_{ss}}$ values between 5 and 15 µg/ml. For the rat studies presented here, the CL_F/CL_{IN} values cover a range of 0.24 to 0.70 at similar furosemide plasma concentration levels. Obviously, the two species handle furosemide quite differently. Because of this the effects of PAH on furosemide's secretion in these two studies cannot be compared.

2. Effect of furosemide on PAH clearance

a. Results

These studies were designed to examine the other side of the potential interaction between furosemide and PAH. They were performed by infusing PAH alone first, followed by a PAH and furosemide infusion (see Chapter IV). Mannitol (5 gm%) was included in all infusion solutions. This was done to insure that sufficient urine was produced during the first half of the experiment (PAH alone); the mannitol was continued during the second half to avoid confounding the study. Table VII-4 shows the results from these experiments.

TABLE VII-4. RESULTS FROM PAH-FUROSEMIDE INTERACTION[a] STUDY. EFFECT OF FUROSEMIDE ON PAH RENAL CLEARANCE.

Rat #	+ or - Furosemide[b]	Weight (kg)	Urine Flow (ml/min)	ΔAe/Δt (mg/min)	$C_{p_{ss}}$ (μg/ml)	CL_{PAH} (ml/min-kg)	Urinary pH	CL_{IN} (ml/min-kg)	CL_{PAH}/CL_{IN}
1	-	0.369	0.036	0.040	4.12	26.28	—[c]	12.29	2.14
	+		0.062	0.044	7.98	15.02	—[c]	3.71	4.05
2	-	0.350	0.050	0.026	4.48	16.76	6.43	9.97	1.68
	+		0.192	0.044	8.07	16.18	5.28	7.73	2.09
3	-	0.353	0.052	0.030	4.86	17.58	6.08	10.85	1.62
	+		0.084	0.036	10.51	9.59	5.09	6.20	1.55
4	-	0.322	0.041	0.027	4.74	13.79	6.10	11.63	1.19
	+		0.112	0.036	10.30	11.12	5.26	7.20	1.54
5	-	0.480	0.048	0.043	3.00	29.35	6.06	13.46	2.18
	+		0.128	0.063	5.88	23.04	5.12	5.86	3.93
6	-	0.394	0.048	0.039	3.43	28.59	6.28	11.40	2.51
	+		0.117	0.057	5.63	25.98	5.38	4.13	6.29
7	-	0.351	0.045	0.045	3.65	35.08	6.38	11.81	2.97
	+		0.094	0.050	8.49	17.62	5.20	4.32	4.08
8	-	0.370	0.053	0.051	4.42	31.39	6.39	11.67	2.69
	+		0.082	0.048	10.22	13.08	5.42	2.69	4.86

[a]Study was performed by infusion of PAH, 49.6 μg/min, for eighty minutes followed by infusion of PAH, 49.6 μg/min plus furosemide, 30.0 μg/min, for eighty minutes. Mannitol 5 gm% was included in all infusion solutions.

[b]Values are the means for 2 ten-minute clearance periods. PAH-alone clearance periods were between 60 and 80 minutes during the first infusion. PAH-plus-furosemide clearance periods were between 60 and 80 minutes during the second infusion, or 140 to 160 minutes total infusion time.

[c]Urinary pH values not available.

Figure VII-8 shows a plot of CL_{PAH}/CL_{IN} versus PAH $C_{p_{ss}}$. There is no significant correlation between CL_{PAH}/CL_{IN} and $C_{p_{ss}}$ of PAH for either PAH alone ($r = -0.5987$, $p>0.1$) or PAH in the presence of furosemide ($r = -0.6114$, $p>0.1$). This indicates that the transport system is not being saturated by the PAH plasma levels attained in these studies. (Lack of saturation was desired in these experiments.) There was also no significant correlation between urinary excretion rate of PAH and urine flow rate ($r = 0.1877$, $p>0.1$) (figure not shown) during periods when furosemide was present. This indicates that no significant reabsorption of PAH was taking place.

b. Discussion

A number of compounds are known to decrease PAH transport by the kidney. Probenecid (88), indomethacin (158), acetylsalicylic acid (87), bumetanide (90), cinoxacin (89), uric acid (86), cephaloridine (91), and penicillin G (87) are among these compounds. Furosemide has also been shown to inhibit PAH clearance in isolated perfused rabbit kidneys (87). One might, therefore, expect to see a similar effect of furosemide on PAH renal excretion in rats. However, such an interaction is not obvious. Although CL_{PAH} is decreased in the presence of furosemide, the clearance of inulin is decreased to an even greater extent. It is impossible to determine if these decreases are due to a general decrease in renal function over the course of the experiment or are due to some other effect.

One possibility is that furosemide is decreasing GFR significantly. As stated before, a number of researchers (57,223,230-

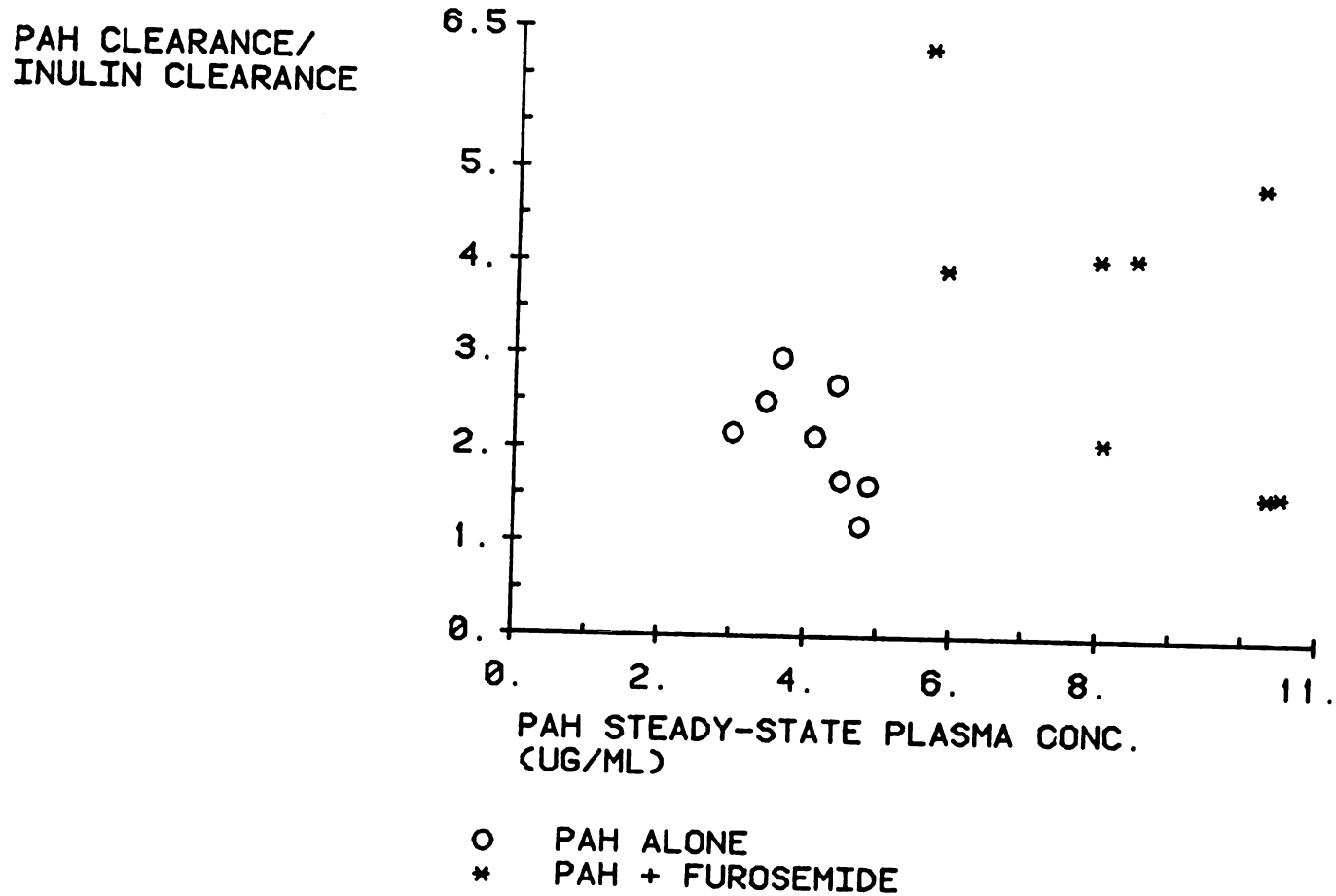

Figure VII-8. Relationship between CL_{PAH}/CL_{IN} and PAH steady-state plasma concentration.

234) have observed a decrease in GFR when furosemide is added to the system. For this set of experiments, GFR was measured in rats administered PAH alone first, while the previous set of experiments (Section VII.C.1.) measured GFR in rats given furosemide alone first. Comparison of these two sets of data shows that the mean GFR for PAH alone is 11.64±1.02 ml/min-kg, whereas mean GFR for rats with furosemide alone is 6.94±1.96 ml/min-kg. These means are significantly different ($p<0.001$) indicating that furosemide decreased the GFR in rats to whom it was given alone first. As a result, furosemide may also significantly decrease GFR in the rats when it is added to the PAH infusion. This effect may then obscure any decrease in CL_{PAH}/CL_{IN} caused by competition with furosemide.

D. Renal failure studies

Effect on PAH and inulin clearances

1. Results

Inulin and PAH renal clearance studies were performed in renally-damaged rats as described in Chapter IV. Results obtained from control rats and rats dosed with 0.3, 1.0 and 3.0 mg/kg uranyl nitrate are shown in Tables VII-5 through VII-8. These data show that there was little inter-rat variability for control rats. There was somewhat more variability, however, within the three groups dosed with uranyl nitrate.

Mean data for CL_{PAH}, CL_{IN} and CL_{PAH}/CL_{IN} for each group are shown in Table VII-9. This table shows that the mean CL_{PAH} for each of the uranyl nitrate-treated groups was statistically different from mean

TABLE VII-5. EFFECT OF RENAL FAILURE ON PAH AND INULIN CLEARANCE. CONTROL RATS[a].

Rat #	Weight (kg)	Urine Flow (ml/min)	ΔAe/Δt (mg/min)	$C_{p_{mid}}$ (μg/ml)	CL_{PAH} (ml/min-kg)	Urinary pH	CL_{IN} (ml/min-kg)	CL_{PAH}/CL_{IN}
1	0.369	0.036	0.040	4.12	26.28	—[c]	12.29	2.14
2	0.480	0.048	0.043	3.00	29.35	6.06	13.46	2.18
3	0.394	0.048	0.039	3.43	28.59	6.28	11.40	2.51
4	0.351	0.045	0.045	3.65	35.08	6.38	11.81	2.97
5	0.370	0.053	0.051	4.42	31.39	6.39	11.67	2.69
6	0.241	0.042	0.017	2.90	25.12	6.33	16.05	1.57

[a]Experiments were performed by infusion of PAH 49.6 μg/min, inulin 1.6 mg/min and mannitol 4 mg/min for eighty minutes. Values are means for 2 ten-minute clearance periods collected during 60 to 80 minutes infusion time.

TABLE VII-6. EFFECT OF RENAL FAILURE ON PAH AND INULIN CLEARANCE. RATS DOSED WITH URANYL NITRATE 0.3 MG/KG BODY WEIGHT[a].

Rat #	Weight (kg)	Urine Flow (ml/min)	$\Delta Ae/\Delta t$ (µg/min)	$C_{P_{mid}}$ (µg/ml)	CL_{PAH} (ml/min-kg)	Urinary pH	CL_{IN} (ml/min-kg)	CL_{PAH}/CL_{IN}
7	0.254	0.101	31.33	4.15	29.76	6.54	14.94	1.99
8	0.305	0.060	19.68	3.83	18.63	6.11	16.99	1.10
9	0.390	0.081	20.82	6.84	7.77	7.34	9.56	0.81
10	0.371	0.088	26.60	5.42	13.37	6.64	16.06	0.83
11	0.245	0.121	39.27	5.91	27.14	6.66	16.51	1.64
12	0.417	0.068	17.27	6.82	6.20	6.92	7.14	0.87

[a]Experiments were performed by infusion of PAH 49.6 µg/min, inulin 1.6 mg/min and mannitol 4.0mg/min for eighty minutes. Values are means for 2 ten-minute clearance periods collected during 60 to 80 minutes infusion time.

TABLE VII-7. EFFECT OF RENAL FAILURE ON PAH AND INULIN CLEARANCE. RATS DOSED WITH URANYL NITRATE 1.0 MG/KG BODY WEIGHT[a].

Rat #	Weight (kg)	Urine Flow (ml/min)	$\Delta Ae/\Delta t$ (µg/min)	$C_{P_{mid}}$ (µg/ml)	CL_{PAH} (ml/min-kg)	Urinary pH	CL_{IN} (ml/min-kg)	CL_{PAH}/CL_{IN}
13	0.388	0.052	20.70	8.90	5.99	5.76	3.56	1.68
14	0.364	0.086	6.77	14.54	1.31	7.20	2.30	0.90
15	0.357	0.070	9.61	12.92	2.08	7.20	2.30	0.90
16	0.357	0.074	16.75	10.30	4.69	7.26	2.27	2.06
17	0.319	0.082	15.54	15.14	3.29	7.02	5.54	0.59
18	0.357	0.064	10.43	11.54	2.61	6.67	5.77	0.45

[a]Experiments were performed by infusion of PAH 49.6 µg/min, inulin 1.6 mg/min and mannitol 4.0 mg min for eighty minutes. Values are means for 2 ten-minute clearance periods collected during 60 to 80 minutes infusion time.

TABLE VII-8. EFFECT OF RENAL FAILURE ON PAH AND INULIN CLEARANCE. RATS DOSED WITH URANYL NITRATE 3.0 MG/KG BODY WEIGHT[a].

Rat #	Weight (kg)	Urine Flow (ml/min)	ΔAe/Δt (μg/min)	$C_{P_{mid}}$ (μg/ml)	CL_{PAH} (ml/min-kg)	Urinary pH	CL_{IN} (ml/min-kg)	CL_{PAH}/CL_{IN}
19	0.268	0.016	1.25	27.88	0.163	—[b]	0.166	0.982
20	0.506	0.025	2.30	17.78	0.285	6.25	0.289	0.986
21	0.305	0.062	6.03	20.15	0.976	6.72	0.732	1.333
22	0.438	0.052	7.44	15.90	1.117	6.51	1.021	1.094
23	0.228	0.095	9.91	22.79	1.906	6.60	2.986	0.638

[a]Experiments were performed by infusion of PAH 49.6 μg/min, inulin 1.6 mg/min and mannitol 4.0 mg/min for eighty minutes. Values are means for 2 ten-minute clearance periods collected during 60 to 80 minutes infusion time.

[b]Urinary pH not available.

TABLE VII-9. EFFECT OF RENAL FAILURE ON PAH AND INULIN CLEARANCE. MEAN DATA[a].

Uranyl Nitrate Dose (mg/kg)	CL_{PAH} (ml/min-kg)	CL_{IN} (ml/min-kg)	CL_{PAH}/CL_{IN}
Control	29.30±3.60	11.59±1.50	2.55±0.34
0.3 mg/kg	17.14±10.09[b]	13.53±4.14	1.21±0.50[c]
1.0 mg/kg	3.33±1.74[c]	3.37±1.98[c]	1.24±0.45[d]
3.0 mg/kg	0.89±0.71[c]	1.04±1.14[c]	1.01±0.25[c]

[a]Values are means±S.D. for 6 rats for each of the first 3 groups, and 5 rats for the 3.0 mg/kg-dosed group.

[b]$p<0.025$ compared to control values.

[c]$p<0.001$.

[d]$p<0.005$.

CL_{PAH} for control rats ($p<0.025$ for the 0.3 mg/kg dose; $p<0.001$ for 1.0 and 3.0 mg/kg doses). For inulin clearance, there was a significant decrease ($p<0.001$) for the 1.0 and 3.0 mg/kg dosed groups when compared to controls. However, there was no significant change in CL_{IN} between control rats and the 0.3 mg/kg-dosed group. Finally, a significant decrease in CL_{PAH}/CL_{IN} was seen for each uranyl nitrate-dosed group when compared to control ($p<0.001$ for 0.3 and 3.0 mg/kg doses; $p<0.005$ for the 1.0 mg/kg dose).

Statistically significant decreases in CL_{PAH} are also seen between uranyl nitrate doses ($p<0.001$ between 0.3 and 1.0 and 0.3 and 3.0, and $p<0.025$ between 1.0 and 3.0 mg/kg doses). In the case of CL_{IN}, $p<0.001$ for the change seen between 0.3 and 1.0 mg/kg and 0.3 and 3.0 mg/kg, and $p<0.05$ for 1.0 and 3.0 mg/kg doses. However, there was no significant change for CL_{PAH}/CL_{IN} at any dose.

2. Discussion

As discussed in Chapter I, administration of uranyl nitrate is one of many methods to induce renal failure. This method was chosen for these experiments because it is known to specifically affect the proximal tubule (130), the site where PAH is secreted. Since the purpose of these experiments was to determine if PAH secretion could be affected so that it would no longer accurately measure renal plasma flow, the use of uranyl nitrate for induction of renal failure seemed particularly appropriate.

Literature values indicate that normal GFR in rats ranges from 5.5 to 17.3 ml/min-kg (223,224,234,235,237,239,240). The values for control

rats and 0.3 mg/kg uranyl nitrate-dosed rats in these studies fall within this range. With higher doses of uranyl nitrate, GFR is significantly decreased.

In the case of CL_{PAH} however, a significant decrease is seen with even the lowest dose of uranyl nitrate. Because of this decrease, the ratio of CL_{PAH}/CL_{IN} is decreased by 50% from control values, bringing it close to a value of 1. If the ratio of CL_{PAH}/CL_{IN} falls to 1, it indicates that virtually no net secretion is taking place and all PAH elimination is due to filtration. Since only about 1/3 to 1/4 of renal plasma flow is filtered in rats (8), such a decrease would indicate that PAH is no longer serving as an effective measure of this parameter.

Haberle et al. (241,242) have examined the effect of GFR on excretion of PAH in the rat and have found a positive correlation, i.e., GFR decreases cause PAH elimination decreases. However, in these studies a decrease in CL_{PAH} but not in GFR was seen at the lowest uranyl nitrate dose. The findings of Haberle et al. cannot explain these results. Brenner et al. (10) have also demonstrated a dependence of GFR on renal plasma flow. Again, these results do not explain the results found here with the 0.3 mg/kg dose of uranyl nitrate, where PAH clearance is decreased significantly but GFR is not. At higher doses concommitant decreases in both CL_{PAH} and GFR are seen.

The results of both Haberle et al. (241,242) and Brenner et al. (10) fit well with the intact nephron hypothesis (17). This hypothesis states that if a portion of a nephron becomes diseased or inoperative, the entire nephron ceases to function. If this theory holds true, no change in CL_{PAH}/CL_{IN} should be seen with increasing renal failure. Our results show that a change in this ratio does occur indicating that the

intact nephron hypothesis does not hold in these studies. Also, the lowest uranyl nitrate dose causes a change in CL_{PAH} but not in CL_{IN}. This provides further evidence that the hypothesis does not hold true for this type of renal failure.

Our results might be explained by saturation of the PAH transport system. If the PAH plasma concentrations seen in the rats dosed with uranyl nitrate were high enough to saturate the system a decrease in CL_{PAH} should be seen and it should approach CL_{IN} in value. However, in these studies the maximum plasma concentration measured was 33.65 µg/ml. Kau et al. (205) used plasma levels of PAH up to 119.4 µg/ml in the rat and considered the transport system to be unsaturated. PAH plasma levels up to 122 µg/ml and 248 µg/ml were used by Haberle et al. (references 241 and 242, respectively) as a nonsaturated system in the rat. These levels are much higher than those attained in the work presented here, indicating that the renal transport system in these studies should not have been saturated. Thus, this potential explanation for the observed decrease in CL_{PAH}/CL_{IN} values is invalid.

A number of researchers have reported that uranium compounds decrease GFR. Nomiyama and Foulkes (130), Meffin et al. (11), and Sudo et al. (12) report GFR decreases in the rabbit, while Szocs et al. (13) and Nizet (14) report GFR decreases in dogs upon administration of uranyl acetate or nitrate. Flamenbaum et al. (15,136), Avasthi et al. (134), Mendelsohn and Smith (135), Haley et al. (16), and Blantz (137) all demonstrate GFR decreases in the rat. The results presented here agree with the decreases in GFR seen in these studies.

It is possible that uranium-containing compounds also decrease renal plasma flow. This could be the reason for the decrease in

CL_{PAH}. Flamenbaum et al. have seen a decrease in renal plasma flow up to 48 hours after administration of 10 mg/kg uranyl nitrate in rats (15), and up to 96 hours after 10 mg/kg uranyl nitrate doses in dogs (136). Nizet (14) has also seen a decrease in renal plasma flow within a few hours after a 2.6 mg/kg uranyl nitrate dose given to dogs. However, Blantz (137) saw no decrease in renal plasma flow a few hours after administering high (15 and 25 mg/kg) uranyl nitrate doses to rats, and Sudo et al. (12) reported increases in renal plasma flow five days after uranyl nitrate doses of 2.0 mg/kg to rabbits. Szocs et al. (13) measured renal plasma flow at various times up to four days after 10mg/kg uranyl nitrate administration to dogs and saw decreases in renal plasma flow at early times, followed by a return to normal flow and a subsequent 36% increase over normal flow on day four.

Obviously, the data are conflicting. However, in all cases with the exception of Flamenbaum et al. (136), decreases in renal plasma flow were measured at early times (<48 hours) after uranyl nitrate administration, while measurements at later times showed normal or increased renal plasma flow. The studies presented here were done on the fifth day after uranyl nitrate administration. Also, it seems unlikely that renal plasma flow has been decreased to 3% of its normal value by this low dose of uranyl nitrate. No other researchers have found this great a decrease in renal plasma flow. The maximum decrease seen was 71%, reported by Flamenbaum et al. (15). A decrease of 97% would be required however, if CL_{PAH} is accurately measuring renal plasma flow in these animals.

It appears that, at the lowest uranyl nitrate dose used here, the compound has a greater effect on CL_{PAH} than on CL_{IN}. This is supported

by similar results in rabbits reported by Nomiyama and Foulkes (130). We conclude that PAH is not being cleared as efficiently by these rats as by untreated rats and consequently PAH clearance is not able to provide an accurate measure of renal plasma flow. Furthermore, it can be concluded that the intact nephron hypothesis is not valid in this particular type of renal failure.

E. Conclusions

The results presented here have shown the following: 1) PAH decreases CL_F and CL_F/CL_{IN} in the rat. This suggests competition of furosemide and PAH for secretion transport sites. 2) Furosemide significantly decreased the secretion of PAH in the rat. However, a significant increase in CL_{PAH}/CL_{IN} was seen in the presence of furosemide. This is thought to be due to a large decrease in GFR caused by the addition of furosemide. This decrease obscures any decrease in CL_{PAH}/CL_{IN} that would be caused by competition for secretory sites. 3) CL_{PAH} and CL_{PAH}/CL_{IN} were decreased significantly with all doses of uranyl nitrate used. However, CL_{IN} was only decreased at the two higher doses of uranyl nitrate. Two conclusions may be drawn from these results. The first is that CL_{PAH} is probably not a good measure of renal plasma flow in this type of renal failure since secretion seems to be preferentially decreased at the low uranyl nitrate dose. The second is that the intact nephron hypothesis does not appear to hold true for this type of renal failure.

Competition studies in whole animals and in renal proximal tubule vesicles indicate that furosemide and PAH are able to inhibit the

transport of each other. Based on these results and those observed in the renal failure studies, we conclude that either the presence of another organic anion which is secreted or the presence of renal failure may alter the renal clearance of PAH and thus make its measurement of renal plasma flow inaccurate. The effect of PAH on furosemide renal clearance might adversely affect furosemide's pharmacokinetics. Further studies should delineate the extent to which these effects alter clinical results.

BIBLIOGRAPHY

1. Tisher, C., Anatomy of the kidney. In: The Kidney, B.M. Brenner, F.C. Rector, Jr., Eds., W.B. Saunders Company, Philadelphia, Pa., 1976, Volume I, p.3-64.

2. Pitts, R.F., Physiology of the Kidney and Body Fluids, Third Edition, Year Book Medical Publishers, Inc., Chicago, Ill., 1974.

3. Valtin, H., Renal Function: Mechanisms Preserving Fluid and Solute Balance in Health, Little, Brown and Company, Boston, 1973.

4. Latta, H., Ultrastructure of the glomerulus and juxtaglomerular apparatus. In: Handbook of Physiology, Sec. 8: Renal Physiology, J. Orloff, R.W. Berliner, S.R. Geiger, Eds., Am. Physiol. Soc., Washington, D.C., 1973, p.1-30.

5. Maunsbach, A.B., Ultrastructure of the proximal tubule. In: Handbook of Physiology, Sec. 8: Renal Physiology, J. Orloff, R.W. Berliner, S.R. Geiger, Eds., Am. Physiol. Soc., Washington, D.C., 1973, p.31-80.

6. Osvaldo-Decima, L., Ultrastructure of the lower nephron. In: Handbook of Physiology, Sec. 8: Renal Physiology, J. Orloff, R.W. Berliner, S.R. Geiger, Eds., Am. Physiol. Soc., Washington, D.C., 1973, p.81-102.

7. Anders, M.W. Metabolism of drugs by the kidney. Kidney Int. 18: 636-647, 1980.

8. Altman, P.L. and Dittmer, D.S., Eds., Blood and Other Body Fluids, Fed. Am. Soc. Exp. Biol., Bethesda, Md., 1961.

9. Renkin, E.M. and Gilmore, J.P., Glomerular filtration. In: Handbook of Physiology, Sec. 8: Renal Physiology, J. Orloff, R.W. Berliner, S.R. Geiger, Eds., Am. Physiol. Soc., Washington, D.C., 1973, p.185-248.

10. Brenner, B.M., Troy, J.L., Daugherty, T.M., Deen, W.M. and Robertson, C.R. Dynamics of glomerular ultrafiltration in the rat. II. Plasma-flow dependence of GFR. Am. J. Physiol. 223: 1184-1190, 1972.

11. Meffin, P.J., Zilm, D.M. and Veenendaal, J.R. Reduced clofibric acid clearance in renal dysfunction is due to a futile cycle. J. Pharmacol. Exp. Ther. 227:732-738, 1983.

12. Sudo, M., Honda, N., Hishida, A. and Nagase, M. Renal hemodynamics in oliguric and nonoliguric acute renal failure of rabbits. Nephron 25:144-150, 1980.

13. Szocs, E., Zahajszky, T., Juszko, J. and Balint, P. Intrarenal haemodynamics in uranyl nitrate-induced acute renal failure. Acta Physiol. Acad. Scient. Hung. 54:51-68, 1979.

14. Nizet, A. Influence of uranyl nitrate upon tubular reabsorption and glomerular filtration in blood perfused isolated dog kidneys. Pflugers Archiv. 391.296-300, 1981.

15. Flamenbaum, W., Huddleston, M.L., McNeil, J.S. and Hamburger, R.J. Uranyl nitrate-induced acute renal failure in the rat: micropuncture and renal hemodynamic studies. Kidney Int. 6:408-418, 1974.

16. Haley, D.P., Bulger, R.E. and Dobyan, D.C. The long-term effects of uranyl nitrate on the structure and function of the rat kidney. Virchows Arch. [Cell Pathol.] 41:181-192, 1982.

17. Bricker, N.S., Klahr, S., Lubowitz, H. and Slatopolsky, E. The pathophysiology of renal insufficiency. On the functional transformations in the residual nephrons with advancing disease. Ped. Clin. N.A. 18:595-611, 1971.

18. Knepper, M. and Burg, M. Organization of nephron function. Am. J. Physiol. 244:F579-F589, 1983.

19. Lombard, W.E., Kokko, J.P. and Jacobsen, H.R. Bicarbonate transport in cortical and outer medullary collecting tubules. Am. J. Physiol. 244:F289-F296, 1983.

20. Rector, F.C., Jr. Sodium, bicarbonate, and chloride absorption by the proximal tubule. Am. J. Physiol. 244:F461-F471, 1983.

21. McKinney, T.D. and Burg, M.B. Bicarbonate and fluid absorption by renal proximal straight tubules. Kidney Int. 12:1-8, 1977.

22. Karlmark, B. and Danielson, B.G. Titratable acid, P_{CO_2}, bicarbonate and ammonium ions along the rat proximal tubule. Acta Physiol. Scand. 91:243-258, 1974.

23. Rector, F.C., Jr., Carter, N.W. and Seldin, D.W. The mechanism of bicarbonate reabsorption in the proximal and distal tubules of the kidney. J. Clin. Invest. 44:278-290, 1965.

24. Jacobsen, H.R. Functional segmentation of the mammalian nephron. Am. J. Physiol. 241:F203-F218, 1981.

25. Herbert, S.C. and Andreoli, T.E. Control of NaCl transport in the thick ascending limb. Am. J. Physiol. 246:F745-F756, 1984.

26. DeWardener, H.E., The control of sodium excretion. In: Handbook of Physiology, Sec. 8: Renal Physiology, J. Orloff, R.W. Berliner, S.R. Geiger, Eds., Am. Physiol. Soc., Washington, D.C., 1973, p. 677-720.

27. Neumann, K.H. and Rector, F.C., Jr. Mechanism of NaCl and water reabsorption in the proximal convoluted tubule of rat kidney. Role of chloride concentration gradients. J. Clin. Invest. 58: 1110-1118, 1976.

28. Marsh, D.J. and Azen, S.P. Mechanism of NaCl reabsorption by hamster thin ascending limbs of Henle's loop. Am. J. Physiol. 228:71-79, 1975.

29. Sachs, G. Ion pumps in the renal tubule. Am. J. Physiol. 233: F359-F365, 1977.

30. Kaufman, J.S. and Hamburger, R.J. Potassium transport in the isolated proximal convoluted tubule. Am. J. Physiol. 244:F409-F417, 1983.

31. Wright, F.S. Sites and mechanisms of potassium transport along the renal tubule. Kidney Int. 11:415-432, 1977.

32. Giebisch, G. Some reflections on the mechanism of renal tubular potassium transport. Yale J. Biol. Med. 48:315-336, 1975.

33. Grantham, J.J., Burg, M.B. and Orloff, J. The nature of transtubular Na and K transport in isolated rabbit renal collecting tubules. J. Clin. Invest. 49:1815-1826, 1970.

34. Hall, S. and Rowland, M. Relationship between renal clearance, protein binding and urine flow for digitoxin, a compound of low clearance in the isolated perfused kidney. J. Pharmacol. Exp. Ther. 227:174-179, 1983.

35. Ferrier, B., Martin, M. and Roch-Ramel, F. Effects of p-aminohippurate and pyrazinoate on the renal excretion of salicylate in the rat: a micropuncture study. J. Pharmacol. Exp. Ther. 224:451-458, 1983.

36. Weiner, I.M., Washington, J.A., II and Mudge, G.H. Studies on the renal excretion of salicylate in the dog. Bull. Johns Hopkins Hosp. 105:284-297, 1959.

37. Kinne, R., Murer, H., Kinne-Safran, E., Thees, M. and Sachs, G. Sugar transport by renal plasma membrane vesicles. Characterization of the systems in the brush-border microvilli and basal-lateral plasma membranes. J. Membr. Biol. 21:375-395, 1975.

38. Turner, R.J. and Silverman, M. Interaction of phlorizin and sodium with the renal brush-border membrane D-glucose transporter: stoichiometry and order of binding. J. Membr. Biol. 58:43-55, 1981.

39. Thierry, J., Poujeol, P. and Ripoche, P. Interactions between Na^+-dependent uptake of D-glucose, phosphate and L-alanine in rat renal brush border membrane vesicles. Biochim. Biophys. Acta, 647:203-210, 1981.

40. Aronson, P.S. and Sacktor, B. The Na^+ gradient-dependent transport of D-glucose in renal brush border membranes. J. Biol. Chem. 250:6032-6039, 1975.

41. Hammerman, M. and Sacktor, B. Transport of -alanine in renal brush border membrane vesicles. Biochim. Biophys. Acta 509:338-347, 1978.

42. Busse, D. Transport of L-arginine in brush border vesicles derived from rabbit kidney cortex. Arch. Biochem. Biophys. 191: 551-560, 1978.

43. Schneider, E.G., Hammerman, M.R. and Sacktor, B. Sodium gradient-dependent L-glutamate transport in renal brush-border membrane vesicles. Evidence for an electroneutral mechanism. J. Biol. Chem. 255:7650-7656, 1980.

44. Arvidsson, A., Borga, O. and Alvan, G. Renal excretion of cephapirin and cephaloridine: evidence for saturable tubular reabsorption. Clin. Pharmacol. Ther. 25:870-876, 1979.

45. Shideman, J.R., Zmuda, M.J. and Quebbemann, A.J. The acute effects of furosemide, ethacrynic acid and chlorothiazide on the renal tubular handling of uric acid in the chicken. J. Pharmacol. Exp. Ther. 216:441-446, 1981.

46. Roch-Ramal, F. Renal excretion of uric acid in mammals. Clin. Nephrol. 12:1-6, 1979.

47. Weinman, E.J., Steplock, D., Suki, W.N. and Eknoyan, G. Urate reabsorption in the proximal convoluted tubule of the rat kidney. Am. J. Physiol. 231:509-515, 1976.

48. Weiner, I.M. Urate transport in the nephron. Am. J. Physiol. 237:F85-F92, 1979.

49. Weinman, E.J., Senekjian, H.O., Sansom, S.C., Steplock, D., Sheth, A. and Knight, T.F. Evidence for active and passive urate transport in the rat proximal tubule. Am. J. Physiol. 240:F90-F93, 1981.

50. Weinman, E.J., Sansom, S.C., Bennett, S. and Kahn, A.M. Effect of anion exchange inhibitors and para-aminohippurate on the transport of urate in the rat proximal tubule. Kidney Int. 23:832-837, 1983.

51. Peterson, L.N. and Wright, F.S. Effect of sodium intake on renal potassium excretion. Am J. Physiol. 233:F225-F234, 1977.

52. Good, D.W. and Wright, F.S. Luminal influences on potassium secretion: sodium concentration and fluid flow rate. Am. J. Physiol. 236:F192-F205, 1979.

53. Warnock, D.G. and Rector, F.C., Jr. Proton secretion by the kidney. Ann. Rev. Physiol. 41:197-210, 1979.

54. Al-Awqati, Q. H^+ transport in urinary epithelia. Am. J. Physiol. 235:F77-F88, 1978.

55. Weiner, I.M. Mechanisms of drug absorption and excretion. The renal excretion of drugs and related compounds. Ann. Rev. Pharmacol. 7:39-56, 1967.

56. Forster, R.P. Renal transport mechanisms. Fed. Proc. 26:1008-1019, 1967.

57. Smith, D.E. and Benet, L.Z. Relationship between urinary excretion rate, steady state plasma levels and diuretic response of furosemide in the rat. Pharmacology 19:301-306, 1979.

58. Cohen, J.J. Is the function of the renal papilla coupled exclusively to an anaerobic pattern of metabolism? Am. J. Physiol. 236:F423-F433, 1979.

59. Gullans, S.R., Brazy, P.C., Soltoff, S.R., Dennis, V.W. and Mandel, L.J. Metabolic inhibitors: effects on metabolism and transport in the proximal tubule. Am. J. Physiol. 243:F133-F140, 1982.

60. Simpson, D.P. Citrate excretion: a window on renal metabolism. Am. J. Physiol. 244:F223-F234, 1983.

61. Kluwe, W.M. and Hook, J.B. Effects of environmental chemicals on kidney metabolism and function. Kidney Int. 18:648-655, 1980.

62. Diamond, G.L. and Quebbemann, A.J. In vivo quantification of glucuronide and sulfate conjugation in the rat kidney. Pharmacologist 21:193, 1979.

63. Rennick, B., Ziemniak, J., Smith, I., Taylor, M. and Acara, M. Tubular transport and metabolism of cimetidine in chicken kidneys. J. Pharmacol. Exp. Ther. 228:387-392, 1984.

64. Øie, S. and Benet, L.Z., Altered drug disposition in disease states. In: Ann. Rep. Med. Chem., H.-J. Hess, Ed., Academic Press, New York, N.Y., 1980, Vol. 15, p. 277-287.

65. Benet, L.Z. and Sheiner, L.B., Design and optimization of dosage regimens; pharmacokinetic data. In: Goodman and Gilman's The Pharmacological Basis of Therapeutics, Sixth Edition, A.G. Gilman, L.S. Goodman, A.Gilman, Eds., Macmillan Publishing Company, New York, N.Y., 1980, p. 1675-1737.

66. Tang-Liu, D.D.-S., Tozer, T.N. and Riegelman, S. Dependence of renal clearance on urine flow: a mathematical model and its application. J. Pharm. Sci. 72:154-158, 1983.

67. Weiner, I.M., Transport of weak acids and bases. In: Handbook of Physiology, Sec. 8: Renal Physiology, J. Orloff, R.W. Berliner, S.R. Geiger, Eds., Am. Physiol. Soc., Washington, D.C., 1973, p. 521-554.

68. Irish, J.M., III and Grantham, J.J. Renal handling of organic anions and cation. In: The Kidney, B.M. Brenner, F.C. Rector, Jr., Eds., W.B. Saunders Company, Philadelphia, Pa., 1981, Vol. I, p. 619-649.

69. Tune, B.M., Burg, M.B. and Patlak, C.S. Characteristics of p-aminohippurate transport in proximal renal tubules. Am. J. Physiol. 217:1057-1063, 1969.

70. Ross, C.R., Pessah, N.I. and Farah, A. Studies of uptake and runout of p-aminohippurate and N-methylmicotinamide in dog renal slices. J. Pharmacol. Exp. Ther. 160:381-386, 1968.

71. Shimomura, A., Chonko, A.M. and Grantham, J.J. Basis for heterogeneity of para-aminohippurate secretion in rabbit proximal tubules, Am. J. Physiol. 240:F430-F436, 1981.

72. Weinnam, E.J., Frankfurt, S.J., Ince, A. and Sansom, S. Renal tubular transport of organic acids. Studies with oxalate and para-aminohippurate in the rat. J. Clin. Invest. 61:801-806, 1978.

73. Roch-Ramel, F., White, F., Vowles, L., Simmonds, H.A. and Cameron, J.S. Micropuncture study of tubular transport of urate and PAH in the pig kidney. Am. J. Physiol. 239:F107-F112, 1980.

74. Dantzler, W.H. PAH transport by snake proximal renal tubules: differences from urate transport. Am. J. Physiol. 226:634-641, 1974.

75. Dantzler, W.H. Characteristics of urate transport by isolated perfused snake proximal renal tubules. Am. J. Physiol. 224:445-453, 1973.

76. Shimomura, A. Chonko, A.A., Tanner, R., Edwards, R. and Grantham, J. Nature of urate transport in isolated rabbit proximal tubules. Am. J. Physiol 241:F565-F578, 1981.

77. Chung, S.T., Park, Y.S. and Hong, S.K. Effect of cations on transport of weak organic acids in rabbit kidney slices. Am. J. Physiol. 219:30-33, 1970.

78. Tune, B.M. and Fernholt, M. Relationship between cephaloridine and p-aminohippurate transport in the kidney. Am. J. Physiol. 225:1114-1117, 1973.

79. Willliams, W.M. and Huang, K.C. Renal tubular transport of folic acid and methotrexate in the monkey. Am. J. Physiol. 242:F484-F490, 1982.

80. Meisel, A.D. and Diamond, H.S. Inhibition of probenecid uricosuria by pyrazinamide and para-aminohippurate. Am. J. Physiol 232:F222-F226, 1977.

81. Berner, W. and Kinne, R. Transport of p-aminohippuric acid by plasma membrane vesicles isolated from rat kidney cortex. Pflugers Arch. 361:269-277, 1976.

82. Kinsella, J.L., Holohan, P.D., Pessah, N.I. and Ross, C.R. Transport of organic ions in renal cortical luminal and antiluminal membrane vesicles. J. Pharmacol. Exp. Ther. 209:443-450, 1979.

83. Dantzler, W.H. and Bentley, S.K. Effects of inhibitors in lumen on PAH and urate transport by isolated renal tubules. Am. J. Physiol. 236:F379-F386, 1979.

84. Kahn, A.M., Branham, S. and Weinman, E.J. Mechanism of urate and p-aminohippurate transport in rat renal microvillus membrane vesicles. Am. J. Physiol. 245:F151-F158, 1983.

85. Blomstedt, J.W. and Aronson, P.S. pH Gradient-stimulated transport of urate and p-aminohippurate in dog renal microvillus membrane vesicles. J. Clin. Invest. 65:931-934, 1980.

86. Steele, T.H., Stromberg, B.A. and Underwood, J.L. Inhibitory action of urate on p-aminohippurate secretion by the isolated rat kidney. Nephron 31:266-269, 1982.

87. Bito, L.Z. and Baroody, R.A. Comparison of renal prostaglandin and p-aminohippuric acid transport processes. Am. J. Physiol. 234:F80-F88, 1978.

88. Moller, J.V. The renal accumulation of urate and p-aminohippurate in the rabbit. J. Physiol. 192:519-527, 1967.

89. Gemba, M., Komamura, T., Matsushima, Y., Itoh, T., Miyata, K. and Nakamura, M. Cinoxacin: competitive inhibitory effect on p-aminohippurate transport and its uptake in renal cortical slices. Arch. int. Pharmacodyn. 261:308-315, 1983.

90. Gemba, M., Taniguchi, M. and Matsushima, Y. Effect of bumetanide on p-aminohippurate transport in renal cortical slices. J. Pharmacobiodyn. 4:162-166, 1981.

91. Kasher, J.S., Holohan, P.D. and Ross, C.R. Effect of cephaloridine on the transport of organic ions in dog kidney plasma membrane vesicles. J. Pharmacol. Exp. Ther. 225:606-610, 1983.

92. Kasher, J.S., Holohan, P.D. and Ross, C.R. Na^+-gradient-dependent p-aminohippurate (PAH) transport in rat basolateral membrane vesicles. J. Pharmacol. Exp. Ther. 227:122-129, 1983.

93. Tse, S.S., Bildstein, C.L., Liu, D. and Mamelok, R.D. Effects of divalent cations and sulfhydryl reagents on the p-aminohippurate (PAH) transporter of renal basal-lateral membranes. J. Pharmacol. Exp. Ther. 226:19-26, 1983.

94. Mamelok, R.D., Tse, S.S., Newcomb, K., Bildstein, C.L. and Liu, D. Basal-lateral membranes from rabbit renal cortex prepared on a large scale in a zonal rotor. Biochim. Biophys. Acta 692:115-125, 1982.

95. Eveloff, J., Kinne, R. and Kinter, W.B. p-Aminohippuric acid transport into brush border vesicles isolated from flounder kidney. Am. J. Physiol. 237:F291-F298, 1979.

96. Miller, D.S. Heavy metal inhibition of p-aminohippurate transport in flounder renal tissue: sites of $HgCl_2$ action. J. Pharmacol. Exp. Ther. 219:428-434, 1981.

97. Hori, R., Takano, M., Okano, T., Kitazawa, S. and Inui, K.-I. Mechanisms of p-aminohippurate transport by brush-border and basolateral membrane vesicles isolated from rat kidney cortex. Biochim. Biophys. Acta 692:97-100, 1982.

98. Kippen, I., Hirayama, B., Klinenberg, J.R. and Wright, E.M. Transport of p-aminohippuric acid, uric acid and glucose in highly purified rabbit renal brush border membranes. Biochim. Biophys. Acta 556:161-174, 1979.

99. Dantzler, W.H. and Bentley, S.K. Low Na^+ effects on PAH transport and permeabilities in isolated snake renal tubules. Am. J. Physiol. 230:256-262, 1976.

100. Gerencser, G.A. and Chaisetseree, C. Comparative p-aminohippurate transport characteristics in human kidney. Comp. Biochem. Physiol. 74A:697-700, 1983.

101. Hayashi, H. and Hoshi, T. Sodium-dependence of p-aminohippurate transport by rat kidney cortex slices. Arch. int. Pharmacodyn. 240:103-115, 1979.

102. Kikuta, Y. and Hoshi, T. Role of sodium ions in p-aminohippurate transport by newt kidney. Biochim. Biophys. Acta 553:404-416, 1979.

103. Maxild, J., Moller, J.V. and Sheikh, M.I. Kinetics of p-aminohippurate transport in rabbit kidney slices. Role of Na^+. Biochim. Biophys. Acta 601: 490-499, 1980.

104. Podevin, R.A. and Boumendil-Podevin, E.F. Monovalent cation and ouabain effects on PAH uptake by rabbit kidney slices. Am. J. Physiol. 232:F239-F247, 1977.

105. Maxild, J., Moller, J.V. and Sheikh, M.I. Involvement of Na^+-K^+-ATPase in p-aminohippurate transport by rabbit kidney tissue. J. Physiol. 315:189-201, 1981.

106. Spencer, A.M., Sach, J. and Hong, S.K. Relationship between PAH transport and Na-K-ATPase activity in the rabbit kidney. Am. J. Physiol. 236:F126-F130, 1979.

107. Kliger, A.S., Resing, J.A., Eastman, A.H., Eastman, S.T. and Preuss, H. Effects of medium pH on p-aminohippurate transport in rat kidney fragments. Nephron 20:32-39, 1978.

108. Lee, S.H., Stokols, M., Gerencser, G.A. and Hong, S.K. Effects of buffer and temperature on pH dependence of p-aminohippurate transport in rabbit kidney slices. Proc. Soc. Exp. Biol. Med. 158:509-512, 1978.

109. Park, Y.S. and Solomon, S. pH-temperature dependence of organic acid transport in rat kidney slices. Am. J. Physiol. 233:F382-F387, 1977.

110. Guggins, S.E., Martin, G.J. and Aronson, P.S. Specificity and modes of the anion exchanger in dog renal microvillus membranes. Am. J. Physiol. 244:F612-F621, 1983.

111. Dantzler, W.H. and Brokl, O.H. Effects of low $[Ca^{2+}]$ and La^{3+} on PAH transport by isolated perfused renal tubules. Am. J. Physiol. 246:F175-F187, 1984.

112. Baker, J.T. Dependence of p-aminohippurate transport on calcium in canine renal cortical slices. J. Physiol. 288:425-435, 1979.

113. Matsushima, Y. and Gemba, M. Stimulatory effect of calcium ions on p-aminohippurate accumulation by rat kidney cortical slices. Renal Physiol. 4:191-198, 1981.

114. Dantzler, W.H. and Bentley, S.K. Effects of chloride substitutes on PAH transport by isolated perfused renal tubules. Am. J. Physiol. 241:F632-F644, 1981.

115. Goldinger, J.M., Eramus, B.D., Song, Y.K., Koschier, F.J. and Hong, S.K. Effects of SCN^- and NO_3^- on organic anion transport in rabbit kidney cortical slices. Biochim. Biophys. Acta 598:357-365, 1980.

116. Dantzler, W.H., Comparison of uric acid and PAH transport by isolated perfused snake renal tubules. In: Amino Acid Transport and Uric Acid Transport, S. Silbernagel, F. Lang and R. Greger, Eds., Thieme, Stuttgart, 1976, p. 169-180.

117. Rosenthall, L., Tyler, J.L. and Arzoumanian, A. A crossover study comparing delayed radiohippurate images with furosemide renograms. Diagn. Imaging 52:267-275, 1983.

118. Rennick, B.A. Renal tubule transport of organic cations. Am. J. Physiol. 240:F83-F89, 1981.

119. Till, A.E. and Benet, L.Z. Renal excretion of pseudoephedrine in the rat. J. Pharmacol. Exp. Ther. 211:555-560, 1979.

120. Holohan, P.D. and Ross, C.R. Mechanisms of organic cation transport in kidney plasma membrane vesicles: 2. pH studies. J. Pharmacol. Exp. Ther. 216:294-298, 1981.

121. Holohan, P.D. and Ross, C.R. Mechanisms of organic cation transport in kidney plasma membrane vesicles: 1. Countertransport studies. J. Pharmacol. Exp. Ther. 215:191-197, 1980.

122. Basseghir, K., Pearce, B. and Rennick, B. Renal tubular transport and metabolism of organic cations by the rabbit. Am. J. Physiol. 241:F308-F314, 1981.

123. Levinsky, N.G. and Levy, M., Clearance techniques. In: Handbook of Physiology, Sec 8: Renal Physiology, J. Orloff, R.W. Berliner, S.R. Geiger, Eds., Am. Physiol. Soc., Washington, D.C., 1973, p. 103-117.

124. Wiater, L.A. and Dunham, P.B. Passive transport of K^+ and Na^+ in human red blood cells: sulfhydryl binding agents and furosemide. Am. J. Physiol. 245:C348-C356, 1983.

125. Murer, H. and Kinne, R. The use of isolated membrane vesicles to study epithelial transport processes. J. Membr. Biol. 55:81-95, 1980.

126. Heidrich, H.-G., Kinne, R., Kinne-Safran, E. and Hannig, K. The polarity of the proximal tubule cell in rat kidney: Different surface charges for the brush-border microvilli and plasma membranes from the basal infoldings. J. Cell Biol. 54:232-245, 1972.

127. Kirk, G. and Prusiner, S.B. Comparative studies on membranes from bovine choroid plexus and rat kidney cortex. Life Sci. 21:833-840, 1977.

128. Kinsella, J.L., Holohan, P.D., Pessah, N.I. and Ross, C.R. Isolation of luminal and antiluminal membranes from dog kidney cortex. Biochim. Biophys. Acta 552:468-477, 1979.

129. Curtis, J.R. Drug-induced renal disease. Drugs 18:377-391, 1979.

130. Nomiyama, K. and Foulkes, E.C. Some effects of uranyl acetate on proximal tubular function in rabbit kidney. Toxicol. Appl. Pharmacol. 13:89-98, 1968.

131. Ting-Beall, H.P. Interactions of uranyl ions with lipid bilayer membranes. J. Microsc. 188:221-227, 1980.

132. Haley, D.P. Morphologic changes in uranyl nitrate-induced acute renal failure in saline- and water-drinking rats. Lab. Invest. 46: 196-208, 1982.

133. Goel, K.A., Garg, U.K. and Garg, V. Histopathology of kidney of albino rat poisoned with uranyl nitrate. Bull. Environm. Contam. Toxicol. 24:9-12, 1980.

134. Avasthi, P.S., Evan, A.P. and Hay, D. Glomerular endothelial cells in uranyl nitrate-induced acute renal failure in rats. J. Clin. Invest. 65:121-127, 1980.

135. Mendelsohn, F.A.O. and Smith, E.A. Intrarenal renin, angiotensin II and plasma renin in rats with uranyl nitrate-induced and glycerol-induced acute renal failure. Kidney Int. 17:465-472, 1980.

136. Flamenbaum, W., Hamburger, R.J., Huddleston, M.L., Kaufman, J., McNeil, J.S., Schwartz, J.H. and Nagle, R. The initiation phase of experimental acute renal failure: an evaluation of uranyl nitrate-induced acute renal failure in the rat. Kidney Int. 10:S115-S122, 1976.

137. Blantz, R.C. The mechanism of acute renal failure after uranyl nitrate. J. Clin. Invest. 55:621-635, 1975.

138. Flamenbaum, W., McNeil, J.S., Kotchen, T.A. and Saladino, A.J. Experimental acute renal failure induced by uranyl nitrate in the dog. Circ. Res. 31:682-698, 1972.

139. Windholz, M., Ed., The Merck Index, Ninth Edition, Merck & Co, Inc. Rahway, N.J., 1976.

140. Smith, R.L. The Excretory Function of Bile. The Elimination of Drugs and Toxic Substances in Bile, Chapman and Hall, Ltd., London, 1973, p. 125.

141. Aurell, M., Fritjofsson, A., Granerus, G. and Grimby, G. Renal extraction of p-aminohippurate: physiological and clinical observations. Contrib. Nephrol. 11:14-18, 1978.

142. Schnurr, E., Lahme, W. and Kuppers, H. Measurement of renal clearance of inulin and PAH in the steady state without urine collection. Clin. Nephrol. 13:26-29, 1980.

143. Favre, H. Critical study of the value of renal clearances measured by the simple shot technique. Contrib. Nephrol. 11:19-21, 1978.

144. Smith, H.W., Finkelstein, N., Aliminosa, L., Crawford, B. and Graber, M. The renal clearances of substituted hippuric acid derivatives and other aromatic acids in dog and man. J. Clin. Invest. 24:388-404, 1945.

145. Cortney, M.A., Mylle, M., Lassiter, W.E. and Gottschalk, C.W. Renal tubular transport of water, solute, and PAH in rats loaded with isotonic saline. Am. J. Physiol. 209:1199-1205, 1965.

146. Tanner, G.A. and Isenberg, M.T. Secretion of p-aminohippurate by rat kidney proximal tubules. Am. J. Physiol. 219:889-892, 1970.

147. Aukland, K. and Loyning, E.W. Intra-renal blood flow and para-amino-hippurate (PAH) extraction. Acta Physiol. Scand. 79:95-108, 1970.

148. Friedman, M. The creatinine, inulin and hippurate clearance in the rat. Am. J. Physiol. 148:387-391, 1947.

149. Lippman, R.W. Clearances as a measure of renal function in the rat. Am. J. Physiol. 152:27-35, 1948.

150. Corcoran, A.C., Masson, G., Reuting, R. and Page, I.H. Measurement of renal functions in rats. Am. J. Physiol. 154:170-173, 1948.

151. Wedeen, R.P., Batuman, V. and Sobel, H. Effect of antitubular basement membrane and brush border antibodies on p-aminohippurate transport in kidney. Nephron 29:258-264, 1981.

152. Biber, T.U.L., Mylle, M., Lassiter, W.E. and Gottschalk, C.W. Micropuncture study of water reabsorption and PAH secretion in urea diuresis in rats. Proc. Soc. Exp. Biol. Med. 119:871-876, 1965.

153. Koshi, K., Shirai, Y., Katayama, K., Kakemi, M., Ueda, M. and Koizumi, T. A note on saturable and inhibitory kinetics of p-aminohippurate renal transport in rabbits. J. Pharmacobiodyn. 6:161-169, 1983.

154. Foulkes, E.C. Kinetics of p-aminohippurate secretion in the rabbit. Am. J. Physiol. 205:1019-1024, 1963.

155. Malyusz, M., Girndt, J., Malyusz, G. and Ochwadt, B. The metabolism of p-aminohippurate in the kidney of normal rats and rats with experimental Goldblatt-Hypertension. Pflugers Archiv. 333:156-165, 1972.

156. Carpenter, H.M. and Mudge, G.H. Uptake and acetylation of p-aminohippurate by slices of mouse kidney cortex. J. Pharmacol. Ther. 213:350-354, 1980.

157. Franke, H., Malyusz, M. and Runge, D. Improved sodium and PAH transport in the isolated fluorocarbon-perfused rat kidney. Nephron 22:423-431, 1978.

158. Bartha, J. and Hably, C. In vitro and in vivo analysis of para-aminohippuric acid (PAH) transport: effect of indomethacin. Acta Physiol. Acad. Scient. Hung. 58:131-140, 1981.

159. Riley, T.N., Ed., A Pocket Guide to Organic Medicinal Structures, B.J. & F.W. Taylor, Camden, Me., 1979.

160. Stason, W.B., Cannon, P.J., Heinemann, H.O. and Laragh, J.H. Furosemide: a clinical evaluation of its diuretic action. Circulation 34:910-920, 1966.

161. Kirkendall, W.M. and Stein, J.H. Clinical pharmacology of furosemide and ethacrynic acid. Am. J. Physiol. 22:162-167, 1968.

162. Kim, K.E., Onesti, G., Moyer, J.H. and Swartz, C. Ethacrynic acid and furosemide: diuretic and hemodynamic effects and clinical uses. Am. J. Cardiol. 27:407-415, 1971.

163. Allison, M.E. and Kennedy, A.C. Diuretics in chronic renal disease: a study of high dosage furosemide. Clin. Sci. 41:171-187, 1971.

164. Levin, N.W. Furosemide and ethacrynic acid in renal insufficiency. Med. Clin. N. A. 55:107-120, 1971.

165. Seely, J.F. and Dirks, J.H. Site of action of diuretic drugs. Kidney Int. 11:1-8, 1977.

166. McGiff, J.C. Crowshaw, K. and Itskovitz, H.D. Protaglandins and renal function. Fed. Proc. 33:39-47, 1974.

167. Stone, K.J. and Hart, M. Inhibition of renal PGE_2-9-ketoreductase by diuretics. Prostaglandins 12:197-207, 1976.

168. Paulsrud, J.R. and Miller, O.N. Inhibition of 15-OH prostaglandin dehydrogenase by several diuretic drugs. Fed. Proc. 33:590, 1974.

169. Weber, P.C., Scherer, B. and Larsson, C. Increase of free arachidonic acid by furosemide in man as the cause of prostaglandin and renin release. Eur. J. Pharmacol. 41:329-332, 1977.

170. Benet, L.Z. Pharmacokinetics/pharmacodynamics of furosemide in man: a review. J. Pharmacokin. Biopharm. 7:1-27, 1979.

171. Smith, D.E., Lin, E.T. and Benet, L.Z. Absorption and disposition of furosemide in healthy volunteers, measured with a metabolite specific assay. Drug Metab. Dispos. 8:337-372, 1980.

172. Bowman, R.H. Renal secretion of [^{35}S] furosemide and its depression by albumin binding. Am. J. Physiol. 229:93-97, 1975.

173. Hammarlund, M.M. and Paalzow, L.K. Dose-dependent pharmacokinetics of furosemide in the rat. Biopharm. Drug Disp. 3:345-359, 1982.

174. Smith, D.E., Gee, W.L., Brater, D.C., Lin, E.T. and Benet, L.Z. Preliminary evaluation of furosemide-probenecid interaction in humans. J. Pharm. Sci. 69:571-575, 1980.

175. Chennavasin, P., Seiwell, R., Brater, D.C. and Liang, W.M.M. Pharmacodynamic analysis of the furosemide-probenecid interaction in man. Kidney Int. 16:187-195, 1979.

176. Homeida, M., Roberts, C. and Branch, R.A. Influence of probenecid and spironolactone on furosemide kinetics and dynamics in man. Clin. Pharmacol. Ther. 22:402-409, 1977.

177. Honari, J., Blair, A.D. and Cutler, R.E. Effects of probenecid on furosemide kinetics and natriuresis in man. Clin. Pharmacol. Ther. 22:395-401, 1977.

178. Andreasen, F., Sigurd, B. and Steiness, E. Effect of probenecid on excretion and natriuretic action of furosemide. Eur. J. Clin. Pharmacol. 18:489-495, 1980.

179. Planas, R., Arroyo, V., Rimola, A., Perez-Ayuso, R.M. and Rodes, J. Acetylsalicylic acid suppresses the renal hemodynamic effect and reduces the diuretic action of furosemide in cirrhosis with ascites. Gastroenterology 84:247-252, 1983.

180. Berg, K.J. and Loew, D. Inhibition of furosemide-induced natruiresis by acetylsalicylic acid in dogs. Scand. J. Clin. Invest. 37:125-131, 1977.

181. Giugliano, D., Torella, R., Sgambato, S. and D'Onofrio, F. Acetylsalicylic acid restores acid insulin response reduced by furosemide in man. Diabetes 28:841-845, 1979.

182. Bartoli, E., Arras, S., Faedda, R., Soggia, G., Satta, A. and Olmeo, N.A. Blunting of furosemide diuresis in man. J. Clin. Pharmacol. 20:452-458, 1980.

183. Smith, D.E., Brater, D.C., Lin, E.T. and Benet, L.Z. Attenuation of furosemide's diuretic effect by indomethacin: pharmacokinetic evaluation. J. Pharmacokin. Biopharm. 7:265-274, 1979.

184. Chennavasin, P., Seiwell, R. and Brater, D.C. Pharmacokinetic-dynamic analysis of the indomethacin-furosemide interaction in man. J. Pharmacol. Exp. Ther. 215:77-81, 1980.

185. Poe, T.E., Scott, R.B. and Keith, J.F., Jr. Interaction of indomethacin with furosemide. J. Fam. Pract. 16:610-616, 1983.

186. Nies, A.S., Gal, J., Fadul, S. and Gerber, J.G. Indomethacin-furosemide interaction: the importance of renal blood flow. J. Pharmacol. Exp. Ther. 226:27-32, 1983.

187. Kover, G. and Tost, H. The effect of indomethacin on kidney function: indomethacin and furosemide antagonism. Pflugers Archiv. 372:215-220, 1977.

188. Data, J.L., Rane, A., Gerkens, J., Wilkinson, G.R., Nies, A.S. and Branch, R.A. The influence of indomethacin on the pharmacokinetics, diuretic response and hemodynamics of furosemide in the dog. J. Pharmacol. Exp. Ther. 206:431-438, 1978.

189. Sacktor, B., Rosenbloom, I.L., Liang, C.T. and Cheng, L. Sodium gradient- and sodium plus potassium gradient-dependent l-glutamate uptake in renal basolateral membrane vesicles. J. Membr. Biol. 60: 63-71, 1981.

190. Liang, C.T. and Sacktor, B. Preparation of renal cortex basal-lateral and brush border membranes: localization of adenylate cyclase and guanylate cyclase activities. Biochim. Biophys. Acta 466:474-487, 1977.

191. Reynolds, R.A., Wald, H., McNamara, P.D. and Segal, S. An improved method for isolation of basolateral membranes from rat kidney. Biochim. Biophys. Acta 601:92-100, 1980.

192. Ichui, K.-I., Okano, T., Takano, M., Kitazawa, S. and Hori, R. A simple method for the isolation of basolateral plasma membrane vesicles from rat kidney cortex: enzyme activities and some properties of glucose transport. Biochim. Biophys. Acta 647:150-154, 1981.

193. Biber, J., Stieger, B., Haase, W. and Murer, H. A high yield preparation for rat kidney brush border membranes: different behaviour of lysosomal markers. Biochim. Biophys. Acta 647:169-176, 1981.

194. Beck, J.C. and Sacktor, B. The sodium electrochemical potential-mediated uphill transport of D-glucose in renal brush border membrane vesicles. J. Biol. Chem. 253:5531-5535, 1978.

195. Warnock, D.G. and Yee, V.J. Chloride uptake by brush border membrane vesicles isolated from rabbit renal cortex: coupling to proton gradients and K^+ diffusion potentials. J. Clin. Invest. 67:103-115, 1981.

196. Booth, A.G. and Kenny, A.J. A rapid method for the preparation of microvilli from rabbit kidney. Biochem. J. 142:575-581, 1974.

197. Berger, S.J. and Sacktor, B. Isolation and biochemical characterization of brush borders from rabbit kidney. J. Cell Biol. 47: 637-645, 1970.

198. Vannier, C., Louward, D., Maroux, S. and Desnuelle, P. Structural and topological homology between porcine intestinal and renal brush border aminopeptidases. Biochim. Biophys. Acta 455:185-199, 1976.

199. Scalera, V., Huang, Y.-K., Hildmann, B. and Murer, H. A simple isolation method for basal-lateral plasma membranes from rat kidney cortex. Membr. Biochem. 4:49-61, 1981.

200. Mamelok, R.D., Groth, D.F. and Prusiner, S.B. Separation of membrane-bound -glutamyl transpeptidase from brush border transport and enzyme activities. Biochemistry 19:2367-2373, 1980.

201. Gornall, A.G., Bardawill, C. and David, M.M. Determination of serum proteins by means of the biuret reaction. J. Biol. Chem. 177:751-766, 1949.

202. Bradford, M.M. A rapid and sensitive method for the quantitation of microgram quantities of protein utilizing the principle of protein-dye binding. Anal. Biochem. 72:248-254, 1976.

203. Ross, C.R., Diezi-Chometry, F. and Roch-Ramel, F. Renal excretion of N'-methylnicotinamide in the rat. Am. J. Physiol. 228:1641-1645, 1975.

204. Harvey, A.M. and Malvin, R.L. Comparison of creatinine and inulin clearances in male and female rats. Am. J. Physiol. 209:849-852, 1965.

205. Kau, S.T., Sastry, B.V.R. and Michelakis, A.M. Ketamine as a suitable anesthetic agent for the measurement of renal clearance in the rat. Arch. int. Pharmacodyn. 211:115-122, 1974.

206. Till, A.E. Renal Excretion of Pseudoephedrine in the Rat. Dissertation for Doctor of Philosophy in Pharmaceutical Chemistry, University of California, San Francisco, 1979, pg. 26.

207. Bratton, A.C. and Marshall, E.K., Jr. A new coupling component for sulfanilamide determination. J. Biol. Chem. 128:537-550, 1939.

208. Marshall, E.K., Jr. and Cutting, W.C. Absorption and excretion of sulfanilamide in the mouse and rat. Bull. Johns Hopk. Hosp. 63: 328-336, 1938.

209. Libeer, J.-C., Scharpe, S.L., Verkerk, R.M., Deprettere, A.J. and Schepens, P.J. Simultaneous determination of p-aminobenzoic acid, acetyl-p-aminobenzoic acid and p-aminohippuric acid in serum and urine by capillary gas chromatography with use of a nitrogen-phosphorus detector. Clin. Chim. Acta 115:119-123, 1981.

210. Brown, N.D., Lofberg, R.T. and Gibson, T.P. High-performance liquid chromatographic method for the determination of p-aminobenzoic acid and some of its metabolites. J. Chromatogr. 99:635-641, 1974.

211. Shoup, R.E. and Kissinger, P.T. A simple liquid chromatography procedure for p-aminohippuric acid in blood serum and urine. Biochem. Med. 14:317-323, 1975.

212. Ito, S., Maruta, K., Imai, Y., Kato, T., Ito, M., Nakajima, S., Fujita, K. and Kurahashi, T. Urinary p-aminobenzoic acid determined in the pancreatic function test by liquid chromatography, with electrochemical detection. Clin. Chem. 28:323-326, 1982.

213. Prueksaritanont, T., Chen, M.-L. and Chiou, W.L. Simple and micro high-performance liquid chromatographic method for simultaneous determination of p-aminohippuric acid and iothalamate in biological fluids. J. Chromatogr. 306:89-97, 1984.

214. Smith, D.E. The Pharmacokinetics of Furosemide. Dissertation for Doctor of Philosophy in Pharmaceutical Chemistry, University of California, San Francisco, 1981, pp. 35-39.

215. Sheikh, M.I. and Moller, J.V. Na^+-gradient-dependent stimulation of renal transport of p-aminohippurate. Biochem. J. 208:243-246, 1982.

216. Miller, J.H. and Morris, L.L. Mechanisms of organic acid and monosaccharide transport in kidney of the brush-tailed possum, Trichosurus vulpecula. Aust. J. Biol. Sci. 35:363-72, 1982.

217. Braunlich, H. Renal pharmacokinetics of furosemide in young and adult rats. Arch. int. Pharmacodyn. 246:4-12, 1980.

218. Hori, R., Ishikawa, Y., Takano, M., Okano, T., Kitazawa, S. and Inui, K.-I. The interaction of cephalosporin antibiotics with renal cortex of rats: accumulation to cortical slices and binding to purified plasma membranes. Biochem. Pharmacol. 31:2267-2272, 1982.

219. Miller, J.H. and Wisniewski, J.W. Limitations of standard filtration techniques in measuring specific binding of transported substrates to renal plasma membranes. Aust. J. Exp. Biol. Med. Sci. 61:339-343, 1983.

220. Berner, W., Kinne, R. and Murer, H. Phosphate transport into brush-border membrane vesicles isolated from rat small intestine. Biochem. J. 160:467-474, 1976.

221. Smith, D.E. and Benet, L.Z. Plasma protein binding of furosemide in kidney transplant patients. J. Pharmacokin. Biopharm. 10:663-674, 1982.

222. Sugita, M., Sugita, K., Furukawa, T. and Abe, H. Studies on the transport mechanism of sulfonamide compounds in renal tubules. Stop flow analysis applied to the excretion of sulfonamide compounds. Jap. Circ. J. 31:423-433, 1967.

223. Brennan, F.T., Sosnowski, G.F., Mann, W.A., Sulat, L. and Wiebelhaus, V.D. Renal clearance procedure for the rat: effect of dopamine and standard diuretics. J. Pharm. Pharmacol. 29:744-747, 1977.

224. Guignard, J.P. and Peters, G. Effects of triamtereme and amiloride on urinary acidification and potassium excretion in the rat. Eur. J. Pharmacol. 10:255-267, 1970.

225. Dev, B., Haberle, D., Schnerman, J. and Wunderlich, P. Effect of barbiturates on GFR and fluid reabsorption along proximal convoluted tubules and loops of Henle in rats. Pflugers Archiv. 344:21-32, 1973.

226. Leenen, F.H.H. Diuretic and cardiovascular effects of furosemide in rats. Can. J. Physiol. Pharmacol. 59:1002-1007, 1981.

227. Chakrabarti, S.K. and Brodeur, J. Effects of fasting on the diuretic response and disposition of furosemide in rats. Can. J. Physiol. Pharmacol. 58:205-211, 1980.

228. Prandota, J. and Wilimowski, M. Simplified pharmacokinetic calculations in an open compartment model as exemplified by furosemide. Polski Tyg. Lek. 31:9-12, 1976.

229. Lee, M.G., Chen, M.-L. and Chiou, W.L. Pharmacokinetics of drugs in blood II. Unusual distribution and storage effect of furosemide. Res. Comm. Chem. Path. Pharmacol. 34:17-28, 1981.

230. Carbon, C., Contrepois, A., Vigneron, A.M. and Lamotte-Barrillon, S. Effects of furosemide on extravascular diffusion protein binding and urinary excretion of cephalosporins and aminoglycosides in rabbits. J. Pharmacol. Exp. Ther. 213:600-606, 1980.

231. Yasuda, M., Fujita, T., Higashio, T., Okahara, T., Abe, Y. and Yamamoto, K. Effects of 4-pentenoic acid and furosemide on renal functions and renal uptake of individual free fatty acids. Pflugers Archiv. 385:111-116, 1980.

232. Tilstone, W.A., Semple, P.F., Lawson, D.H. and Boyle, J.A. Effects of furosemide on glomerular filtration rate and clearance of practolol, digoxin, cephaloridine, and gentamicin. Clin. Pharmacol. Ther. 22:389-394, 1977.

233. First, M. R., Bramlage, R.J., Pesce, A.J. and Pollak, V.E. Albumin excretion by the kidney: the effects of furosemide diuresis. Proc. Soc. Exp. Biol. Med. 158:550-553, 1978.

234. Chiu, P.S. and Long, J.F. Effects of hydration on gentamicin excretion and renal accumulation in furosemide-treated rats. Antimicrob. Agents Chemother. 14:214-217, 1978.

235. Burke, T.J. and Duchin, K.L. Glomerular filtration during furosemide diuresis in the dog. Kidney Int. 16:672-680, 1979.

236. Zager, R.A. Glomerular filtration rate and brush border debris excretion after mercuric chloride and ischemic acute renal failure: mannitol versus furosemide diuresis. Nephron 33:196-201, 1983.

237. Devane, J. and Ryan, M.P. Dose-dependent reduction in renal magnesium clearance by amiloride during frusemide induced diuresis in rats. Br. J. Pharmacol. 80:421-428, 1983.

238. Gayer, J. Die renale exkretion des neuen diureticum furosemid. Klin. Wochenschr. 43:898-902, 1965.

239. Gellai, M. and Valtin, H. Chronic vascular constrictions and measurements of renal function in conscious rats. Kidney Int. 15: 419-426, 1979.

240. Sadjak, A., Leimuller, A., Vogel, G., Leng, E. and George, I. A new method for determining inulin and PAH clearances in the conscious rat- fundamentals of the method (Part 1) with examples of its application in artifically induced renal damage (Part 2). Agents Actions 9:589-599, 1979.

241. Haberle, D. Influence of glomerular filtration rate on the rate of paraminohippurate secretion by the rat kidney: micropuncture and clearance studies. Kidney Int. 7:385-396, 1975.

242. Haberle, D.A., Ruhland, G., Lausser, A., Moore, L. and Neiss, A. Influence of glomeruler filtration rate on renal PAH secretion rate in the rat kidney. Pflugers Archiv. 375:131-139, 1978.

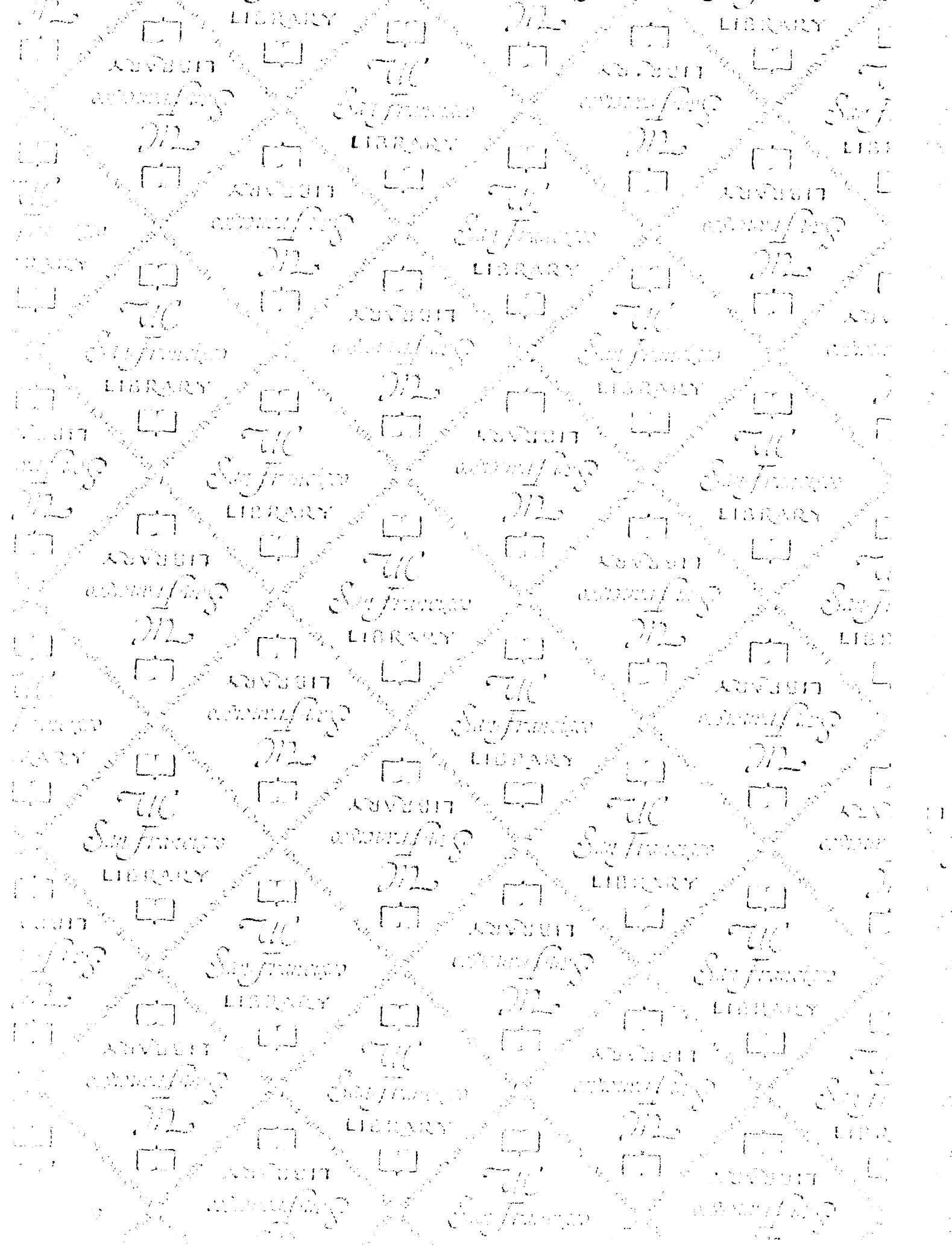
THE
San Francisco
LIBRARY